Dynamics of Some Monohydric Alcohols, and The effect of 2,2,2-Trifluoroethanol on structure and folding of Globular and Intrinsically Disordered Proteins

A Thesis Submitted for the Degree of DOCTOR OF PHILOSOPHY

By Mujahid Hossain 17CHPH21



School of Chemistry
University of Hyderabad
Hyderabad 500046
INDIA

JULY 2023

Dedicated to

My Parents

CONTENTS

STATEMENT	I
DECLARATION	II
CERTIFICATE	III
ACKNOWLEDGEMENT	\mathbf{V}
List of Abbreviations and Symbols	II III V VII 1 1 5 8 vdric aliphatic alcohols 13 13 15 16 28 ss for reversible protes 36 37
Chapter 1 Introduction	
1.1 Overview	1
1.2 Ternary to binary system	1
1.3 Effect of 2,2,2-trifluoroethanol (TFE) on protein	5
1.4 References	8
Chapter 2 Aggregation and diffusive dynamics of some monohydr	ric aliphatic alcohols
Abstract	13
2.1 Introduction	13
2.2 Experimental Section	15
2.3 Results and Discussions	16
2.4 References	28
Chapter 3 A surprisingly simple three-state generic process	for reversible protein
denaturation by trifluoroethanol	
Abstract	36
3.1 Introduction	37
3.2 Materials and Methods	39
3.3 Results	40
3.4 Discussions	58
3.5 Conclusion and Future Prospects	62
3.6 References	63

 $\label{lem:chapter 4} \begin{tabular}{ll} A three-state mechanism for trifluoroethanol denaturation of an intrinsically disordered protein (IDP) \end{tabular}$

	Abstract	72
	4.1 Introduction	73
	4.2 Materials and Methods	75
	4.3 Results	76
	4.4 Discussions	91
	4.5 References	94
Publications		102
Plagi	arism report	103



STATEMENT

I hereby declare that the matter embodied in this thesis is the result of investigations carried out by me in the School of Chemistry, University of Hyderabad, Hyderabad, under the supervision of **Prof. Abani K. Bhuyan**.

In keeping with the general practice of reporting scientific observations, due acknowledgments have been made whenever the work described is based on the finding of other investigators. Any omission which might have occurred by oversight or error is regretted.

Hyderabad

July 2023

Mujahid Hossain

(17CHPH21)

Prof. Abani K. Bhuyan Phone: +91 40 23134810 (O) Phone: +91 40 23134810 (O) Fax: +91-40-23012460

Email: akbsc@uohyd.ac.in

DECLARATION

I, Mujahid Hossain, hereby declare that this thesis entitled "Dynamics of Some Monohydric Alcohols, and The Effect of 2,2,2-Trifluoroethanol on Structure and Folding of Globular and Intrinsically Disorderd proteins" submitted by me under the guidance and supervision of Prof. Abani K. Bhuyan, is a bonafide research work which is also free from plagiarism. I also declare that it has not been submitted previously in part or in full to this university or any other university or institution for the award of any degree or diploma. I hereby agree that my thesis can be deposited in Shodhganga/INFLIBNET.

A report on plagiarism statistics from the University Librarian is enclosed.

Date: 26/07/2023

Name: Mujahid Hossain

Reg. No.: 17CHPH21

National Signature of the student

Signature of the Supervisor

26/07/2023 J.

ABANI K. BHUYAN, Ph.D. Professor

University of Hyderabad School of Chemistry Hyderabad - 500 046. Prof. Abani K. Bhuyan School of Chemistry University of Hyderabad Hyderabad – 500 046, India



Phone: +91 40 23134810 (O) Fax: +91-40-23012460 Email: akbsc@uohyd.ac.in

CERTIFICATE

This is to certify that the thesis entitled "Dynamics of some monohydric alcohols, and The Effect of 2,2,2-Trifluoroethanol on Structure and Folding of Globular and Intrinsically Disorderd proteins" submitted by Mujahid Hossain bearing registration number 17CHPH21 in partial fulfillment of the requirements for the award of Doctor of Philosophy (Ph. D.) is a bonafide work carried out by him under my supervision and guidance in School of Chemistry, University of Hyderabad. This thesis is free from plagiarism and has not been submitted previously in part or in full to this or any other University or Institution for the award of any degree or diploma. Further, the student has four publications before submission of the thesis for adjudication and has produced shreds of evidence for the same in the form of reprints.

Parts of this thesis have been published as the following articles:

- 1. **M. Hossain**, N. Huda, A. K. Bhuyan, *Biophys. Chem.* **2022**, 291, 106895 (*Chapter 3*).
- 2. M. Hossain, N. Huda, A. K. Bhuyan. J. Biochem. 2023 (accepted for publication). (Chapter 4).

He has also made presentations in the following conferences and attended workshops:

- 1. School: "Winter School on Synchroton Techniques in Materials Science" at S.N, Bose National Centre for Basic Sciences, Kolkata, India 2018.
- 2. Poster: "Effect of 2,2,2-Trifluoroethanol on Protein at different pH" in *Chemfest* 2019 (In-house symposium) at University of Hyderabad.
- 3. **Oral and Poster: "Clustering of Aliphatic alcohols"** in *Chemfest 2022* (In-house symposium) at University of Hyderabad.

Further the student has passed the following courses towards the fulfilment of coursework requirement for Ph. D.

Sl. No.	Course No.	Title of the Course	No. of Credits	Result
1.	CY801	Research Proposal	4	Pass
2.	CY805	Instrumental Methods-A	4	Pass
3.	CY806	Instrumental Methods-B	4	Pass

A bani Woy.

Prof. Abani K. Bhuyan

(Thesis Supervisor)

ABANI K. BHUYAN, Ph.D. Professor University of Hyderabad School of Chemistry Hyderabad - 500 046. Dean

School of Chemistry

University of Hyderabad

Dean SCHOOL OF CHEMISTRY

University of Hyderabad Hyderabad-500 046.

Acknowledgement

I would like to express my deepest gratitude and heartfelt appreciation to the following individuals and groups, without whom the completion of this thesis would not have been possible:

Foremost, I would like to express my sincere gratitude to my advisor Prof. Abani K. Bhuyan for the continuous support, of my PhD study and research, for his patince, motivation, enthusiasm, and immense knowledge. His guidance helped me a lot not only in my academic life but also in my personal life. I thank him for helping me in grooming to a better version of me.

I would like to extend my heartfelt gratitude to the members of my doctoral committee, Prof. Tushar Jana and Dr. Murali Banavoth. Their insightful suggestions, criticism and intellectual engagement have immensely enriched the quality of this work.

I want to thank present and former deans, School of Chemistry, University of Hyderabad, and all the faculty members of the School of chemistry for their help and support on various occasions.

I want to acknowledge UGC for Maulana Azad Fellowship for financial support during my Ph.D. research tenure.

My heartfelt appreciation extends to Mr. Durgesh and Mr. Mahender (NMR, School of Chemistry), Mr. Durgaprasad (AFM and FESEM, School of Chemistry) Mr. Sunil (SEM, School of Chemistry), Mr. Rajesh (TEM, School of Chemistry) Mr. Anand (IR, School of Chemistry) and Mr. Abraham for his help in official work (School Office). Their constant support, from administrative assistance to technical expertise, has been crucial throughout my academic journey. I am grateful for their tireless efforts behind the scenes, which have made the pursuit of knowledge a seamless and enriching experience.

I would also like to thank my lab senior, Dr. P. Sashi and Dr. D. Santi Swarupini for their constructive comments and helpful discussions and in addition thankful to Shanti for introducing me towards the biology part of my research work. I am very grateful to all my colleagues, Noorul, Kirthi, and Ramesh for their help and creating a pleasant research

environment, making it a memorable and enjoyable journey. In particular, I want to thank

Noorul who has supported and helped me a lot in need not only in academic but also in

personal life. Also I admire his technical interest and the updating skills of one with time. I

thank to Kirthi who motivate to think critically and keen to go deeper in any discussion and

also for her helping nature. I extend my gratitude to all the project students who have worked

with me, Belal and Trupti.

I am thankful to my buddies, Isha, Ishfaq and Noorul not only for their unwavering support,

understanding, and encouragement that have been a constant source of motivation but also for

making HCU as my second home. I would also like to thanks my friends Asif, Navneeta, Dr.

Bilal who made my stay in campus a memorable one. Also thanks to my friend Nazir with

whom a memorable journey was made since the initial day of my PhD.

I would also like to thanks my senior at School of Chemistry Alim da, Saddam da, Tanmay

da, Subham da and Soutrick da who help me in neded.

Last but not the least; I would like to thank my family: my father Mr. Mobarak Hossain,

Mother Anjuyara Khatun and Sister Nazma for their inseparable support. With their love,

sacrifice and prayers only this could be possible.

Above all I thank Almighty for sending me at the right place at the right time and making this

happen.

Mujahid Hossain

July,2023

_

VI

List of abbreviations and symbols

H-bond Hydrogen Bond

DLS Dynamic Light Scattering

MD Molecular Dynamics

IR Infrared

NMR Nuclear Magnetic Resonance

TFE 2,2,2-Trifluoroethanol

3D Three Dimensional

IDPs Intrinsically Disordered Proteins

Lys Lysozyme

β-LG Beta-lactoglobulin

MRD Magnetic Relaxation Dispersion

AtPP16 1 Arabidopsis thaliana phloem protein 16 1

MeCP2 Methyl CpG binding protein 2

kDa Kilo Daltons

CD Circular Dichroism

CHAPTER 1

Introduction

1.1. Overview

The complexity of protein structure is a fundamental problem. The difficulty arises from a variety of interactions not only between the protein atoms, but also between those of the protein and the solvent. Although it is the aqueous environment which is relevant in vivo, a key approach to understand structure, conformation, and dynamics of proteins is to examine the influence of mixed solvents where the nonaqueous component could be a solid or another solvent. This is effectively a ternary system comprising water, protein, and the added solvent. The physical properties and the structure of the protein are then examined by varying the mole fraction of the solvent. The idea is to find out how the added solvent affects structure and conformation by either directly interacting with the protein or interfacing with water or both. Some inconclusive studies of proteins in binary solvent system including alcohol-water, SDS-water, and glycerol-water have been reported.

Among these three, the alcohol-water system with the added protein has been one of the most attractive topic for the last 60 years. Although Monohydric alcohols are not considered classic denaturants in contrast to well-known denaturants like urea and compounds containing guanidinium, they have been found to have mixed denaturing and stabilising effects on protein structure. Alcohols including the fluorinated ones are known to act by perturbing the tertiary structure and enhancing the helical structure. These two kinds of effect may lead to the formation of partially folded intermediate states. But recent study reveals that the hydrophobic interaction is also one of the factors that perturb protein structure even at pH 13.

1.2. Ternary to binary system

There are numerous studies of solvent-protein^{1–10} interaction, but very few have highlighted the solvent-water interaction (or better described as co-solvent interaction). Alongside the primary focus on the ternary system, there is an overlooked facet involving alcohol and water

chemistry. It is important to recognize that the influence on the structure, folding, and dynamics of proteins is not solely attributed to the solvent itself, but rather to the combined effect of the solvent and water in the ternary mixture of water, alcohol, and protein. Chapter 2 of this thesis emphasizes on the physical aspects of water and alcohol, their unique characteristics such as simple chemical structures, hydrophobic properties with chain length, and high solubility of alcohol in water. Notably, alcohols are widely used as solutes in studying hydrophobic effects due to their well-established properties.¹⁴

1.2.1. Thermodynamics aspects and molecular origin of aggregation (or clustering) of alcohol in water

Alcohols are used widely as solvent to study the protein stability due to its hydrophobic nature. Aggregation of alcohol process involves the mixing of alcohol and water. For an ideal solution of binary mixture of liquids A and B consisting of n_A and n_B moles respectively, the chemical potential μ_i of each component can be given as

$$\mu_i = \mu_i^0 + RT ln x_i \tag{i}$$

where μ_i^0 is the chemical potential of the species A and B at its pure state. Equation 1 also possess the Raoult's law given by

$$p_i = p_i^0 \times x_i \tag{ii}$$

Where p_i and p_i^0 are the partial pressure of i^{th} species.

Now the Gibbs free energy of the solution before mixing is given as

$$G_i = n_A \mu_A^0 + n_B \mu_B^0 \tag{iii}$$

After the mixing, the chemical potential of each component can be designated as μ_A . So the total Gibbs free energy becomes

$$G_f = n_A(\mu_A^0 + RT \ln x_A) + n_B(\mu_B^0 + RT \ln x_B). \tag{iv}$$

Gibbs energy of mixing can now be obtained by subtracting equation (iii) from the equation (iv), obtained as

$$\Delta_{mix}G = nRT(x_A lnx_A + x_B lnx_B) \tag{v}$$

where n=total numbers of moles = $n_A + n_B$

The ideal entropy of mixing is given as

$$\Delta_{mix}S = -nR(x_A ln x_A + x_B ln x_B), \tag{vi}$$

because $\Delta_{mix}H=\Delta_{mix}G+T\Delta_{mix}S=0$ for an ideal mixing i.e. the enthalpy of mixing is zero for the ideal mixing.

The change in volume of ideal mixing also equals zero, so that

$$\Delta_{mix}V = \left(\frac{\partial \Delta_{mix}G}{\partial P}\right)_{P} \tag{Vii}$$

Because $\Delta_{mix}G$ is independent of pressure, the derivative with respect to pressure would be zero.

The above changes in thermodynamic parameters ΔG_{mix} and ΔS_{mix} are negative and positive respectively whereas ΔH_{mix} and ΔV_{mix} are zero for this case which obeys ideal law in which the interactions between A-A, B-B and A-B are equal while mixing between two liquid A and B otherwise leads to deviation from ideality. But in the world of solution chemistry this doesn't occur due to the interaction between A and B. As a consequence the solution shows non-ideal behaviour. In the non-ideal case ΔH_{mix} and ΔV_{mix} have define values, indicating intra and intermolecular association.

This can be attributed due to not only the changing in volume and enthalpy but also the some other contributions also there which add to the entropy. The other contributions may arise due to the interactions between the molecules of two liquids which may indicate some association or aggregation of the molecules of the same kind or the association between different kinds of molecules like below.^{15, 16}

$$R(H_2O)_{n-1} + H_2O \rightarrow R(H_2O)_n$$
 (viii)

where R denotes alcohol.

This aggregation leads to nonlinearity or anomalies in physicochemical properties of alcohol-water solution like viscosity, density and refractive index of the aqueous solution of lower aliphatic alcohols.¹⁷

1.2.2. Structural features of alcohol-water clusters

In the case of alcohol and water mixture, the alcohol molecule being amphiphilic having both hydrophilic and hydrophobic groups can have opposing effects on water. Strong H-bonds can form between the hydrophilic groups and water, but the hydrophobic groups may cause cooperative ordering in the system through hydrophobic hydration effects. These two factors in their binary mixtures combine together reforming the large H-bond network of water which makes the system behave non-ideally. Such dual roles generally referred to as the "Janus effect" after the name of the Greek god Janus, who has two faces: one facing forward and the other in the opposite direction. As a result of such opposing effect, the formation of self-organized solute takes place in the system. Hydrophobic assemblies can also drastically alter the system's characteristics. The fluctuations in local composition is also play a key role for non-ideal behavior of binary mixtures.

It is proposed that the nonpolar groups of alcohol molecules, which form the first hydration shell and have strong H-bonds, enhance the low entropy water-caging anddevelops an open water network structure(as in ice or in low temperature water). The solute then enters the open network structure of bulk water, resulting in a decrease in the overall volume needed. This is known as "iceberg model" which is supported by several studies. ²²Solutions of the primary aliphatic alcohols have been studied engaging a number of techniques including self-diffusion coefficient ²³, molecular dynamic (MD) simulations, ²⁴ dynamic light scattering (DLS), ²⁵ infrared spectroscopy (IR), ²⁶ dielectric relaxation, ²⁷ and viscosity. ²⁸ Self diffusion coefficient which is a measure of translational motion of molecules can provide useful information like molecular size and intermolecular interactions useful to study the structural changes in solutions. Along with NMR relaxation measurements, ²⁹ the chemical shift measurements ³⁰ also is a good probe to monitor the changes at molecular level.

1.3. Effect of 2,2,2-trifluoroethanol (TFE) on protein

1.3.1. Some general aspects

TFE has marked effect on proteins and peptides due to its special physicochemical and structural properties. Protein-solvent interaction is a fascinating phenomenon; how a solvent affects protein structure and provides elementary conditions to reconstruct and reorganize the secondary structure of the protein is little understood. Various polar and apolar solvents interact differently with proteins depending on the net positive charge on them and the extent of van der Waal interactions. TFE is one among them that can be used as a denaturant for protein folding studies. Several models of proteins with TFE have been studied till now.

1.3.2. Effect of TFE on protein

Depending on structure and compactness, proteins can be globular or intrinsically disordered (ID). The salient features of globular proteins being soluble in water and having well defined (or organised) 3D structure. Electron-transfer proteins, oxygen transporter and storage proteins, and native functional enzymes all are the examples of ordered globular proteins. On the other hand, an amino acid sequence comprising polypeptide segments that have the ability to collapse but not fold into a specific compact structure results in an ensemble of conformers with unstructured or disordered sections. Proteins having such structural disorder are known as intrinsically disordered proteins (IDPs), as these disordered sections are inherent or intrinsic and clearly result from the mix of amino acids that can unfold.

Major portion of this thesis contains a detailed investigation of protein structure and conformation in water-TFE system. TFE has been used in two mutually exclusive ways; one, to denature proteins, and two, to stabilize structures in peptides.³¹Usually TFE is used to enhance the helicity of peptides³². There are two opposing theories about how TFE and peptides interact, according to which TFE either directly interacts with folded peptide chains³³⁻³⁶ or affects the stability of the peptide's unstructured form.³⁷

The general principle of TFE-induced changes in proteins can be described by three reasons. Firstly, it alters the H-bonding by interacting with the H-bonds between the carbonyl and amide groups. Secondly, it can penetrate into the interior of the hydrophobic core and interact with hydrophobic groups belonging to the protein. Thirdly, it affects the solvent structure through hydrophobic interactions, employing its –CF₃ group. It is this characteristic

that sets it apart from other aliphatic alcohols. This general theme of TFE-protein interaction can be attributed to the physical properties of TFE.³⁸ TFE acts as a better proton donor than water but a poor acceptor.³⁹The structure of TFE is given below.

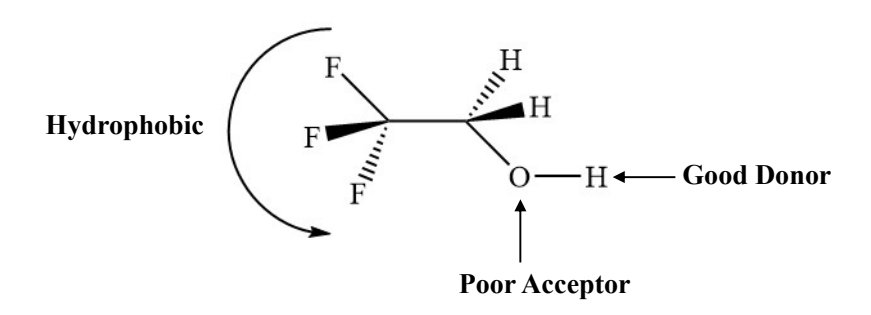


Figure 1. TFE molecule with the three distinct sections with the given qualities. Here, donor and acceptor capacity is compared with water.

It is proposed that TFE specifically binds to carbonyl oxygen group (which can take upto two H-bonds) to increase the strength of intrachain H-bond, because TFE is a better H-bond donor as compared to water. Due to the fact that TFE is nine times larger than water in size, this interaction causes water molecules to be expelled from the mainchain, reducing the exposure of the amide group to solvent, resulting in development of intra-chain hydrogen boundaries. Another recent study has shown that the non-native helix induction and amyloid formation can be due to the alteration in the dielectric constant value.

1.3.3. Effect of TFE on Globular protein

Many studies have been done on the structure, dynamics, and folding pathway of hen lysozyme (lys), which consists of 129 residues. Lys contains two types of helical structure— α and 3_{10} along with an antiparallel β -sheet. TFE turns the native state of lysozyme to a partially unfolded one. The 2D and 3D NMR study at 70% TFE revealed the presence of all native α helices more than their native limits. Moreover the c-terminal of 3_{10} helix and the c-terminal area of β -sheet is transformed to helical structure. It is held that TFE mainly perturb the tertiary structure and enhances the secondary.

Beta-lactoglobulin (β -LG) having 162 amino acids has one α -helix and 9 β -sheet strands. Usually TFE action on β -LG has been $\alpha \to \beta$ transition in a cooperative manner. To understand the underlying molecular mechanism of this cooperative

transition, magnetic relaxation dispersion (MRD) of 19 F was used to study TFE and 2 H and 17 O resonance were used to study the hydration. MRD data clarifies that β -LG maintained its native structure even at 16% TFE, but 30% TFE transformed it to a non-native structure which is mainly caused by the penetration of TFE into the interior of β -LG. 49

1.3.4. Atpp16-1, an IDP

Arabidopsis thaliana phloem protein 16-1 (AtPP16-1) whose NMR solution structure was solved in this laboratory,⁵⁰ consists of several disordered regions among which the longest one is the stretch of residues 10–55 that connects strands β I and β II(Figure 2).

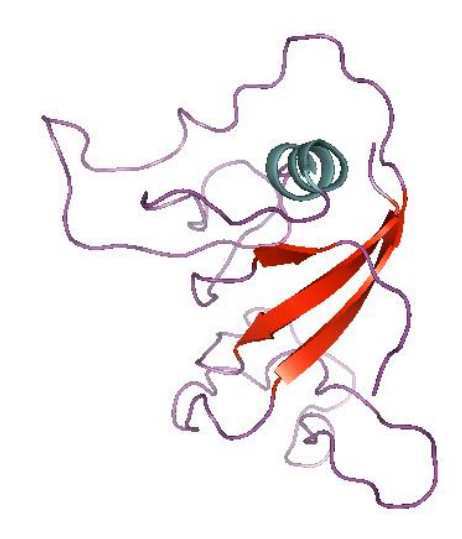


Figure 2. Ribbon diagram of *At*PP16-1 showing many disordered regions.

1.3.5. Effect of TFE on intrinsically disordered protein

In recent years IDPs have drawn the interest for their ability of playing a key role in essential cellular processes such as regulation of transcription and translation and assembly of protein. $^{51-54}$ When an IDP MeCP2 (Methyl CpG binding protein 2) is treated with TFE the result may be similar to that of globular proteins. 55 MeCP2 is a 53-kDa nuclear protein that gets its name from its capacity to recognise methylated DNA with specificity. 56 The unstructured residue of C-terminal and N-terminal domain of MeCP2 is converted to α -helix at 70% TFE. Prosystemin, a tomato prohormone is another example of IDP which consists of 200 amino acids. Experiments reveal that this protein, despite having significant residual secondary structure, lacks a compact fold and a hydrophobic packed core. CD spectra Also indicates a little increase in α -helical structure in the range between 5 and 15% TFE whereas

20-30% TFE region reflects the highest disorder-to-order transition.⁵⁷ The above study clarifies that TFE also works as helix inducer like in globular protein and makes the system more ordered as compared to the native state of the disordered protein.

1.4. References

- 1. Schrier, R. R; Scherega, H. A. The effect of aqueous alcohol solutions on the transition of ribonuclease. *Biochim. Biophys. Acta.* **1962**, *64*, 406-408.
- 2. Brandts, J. F. The thermodynamics of protein denaturation. I. The denaturation of chymotrypsinogen. *J. Am. Chem. Soc.* **1964**, *86*, 4291-4301.
- 3. Brandts, J. F.; Hunt, L. The thermodynamics of protein denaturation.III. The denaturation of ribonuclease in water and in aqueous urea and aqueous methanol mixtures. *J. Am. Chem. Soc.* **1967**, 89, 4826-4838
- 4. Mohanta, D.; Jana, M. Can 2,2,2-trifluoroethanol be an efficient protein denaturant than methanol and ethanol under thermal stress. *Phys. Chem. Chem. Phys.* **2018**, *20*, 9886-9896.
- 5. Peller, L. On a model for the helix coil transition in polypeptides. II. The influence of solvent composition and charge interactions on the transition. *J. Phys. Chem.* **1959**, *63*, 1199-1206.
- 6. Tanford, C. Protein denaturation. Adv. Protein Chem. 1968, 23, 121-282.
- 7. Timasheff, S. N. Protein-solvent interactions and protein conformation. *Acc. Chem. Res.* **1970**, *3*, 62-68.
- 8. Timasheff, S. N.; Inoue, H. Preferential binding of solvent components to proteins in mixed water-organic solvent systems. *Biochemistry* **1968**, 7, 2501-2513.
- 9. Franks, F.; Eagland, D. The role of solvent interactions in protein conformation. *CRC Crit. Rev. Biochem.* **1975**, *3*, 165-219.
- 10. Wilkinson, K. D.; Mayer, A. N. Alcohol induced conformational changes of ubiquitin. *Biochem. Biophys.* **1986**, *250*, 390-399.
- 11. Fink, A. L.; Painter, B. Characterization of the unfolding of ribonuclease A in aqueous methanol solvent. *Biochemistry* **1987**, *26*, 1665-1671.

- 12. Kim, P. S.; Baldwin, R. L. Intermediates in the folding reactions of small proteins. *Annu. Rev. Biochem.* **1982**, *59*, 631-60.
- 13. Sashi, P.; Yasin, U. M.; Bhuyan, A.K. Unfolding action of alcohols on a highly negatively charged state of cytochrome *c. Biochemistry* **2013**, *51*, 3273-83.
- 14. Roux, A. H.; Desnoyers, J. E. Association model for alcohol-water mixtures. *Proc. Indian Acad. Sci.* **1987**, *98*, 435-451.
- 15. Pal, J.; Patla, A.; Subramanian, R.; Thermodynamic properties of forming methanol-water and ethanol-water clusters at various temperatures and pressures and implications for atmospheric chemistry: A DFT study. *Chemosphere* **2021**, *272*, 129846.
- 16. Lee, Y-F.; Kelterer, A-M.; Matisz, G.; Kunsagi-Mate, S.; Chung, C-U.; Lee, Y-P. Infrared absorption of methanol-water clusters (CH₃OH)_n(H₂O), n=1-4, recorded with the VUV-ionization/IR-depletion technique. *J. Chem. Phys.* **2017**, *146* (*14*), 144308.
- 17. Kuchuk, V. I.; Shirokova, I. Yu.; Galikova, E. V. Physicochemical properties of water-alcohol Mixtures of a homological Series of lower aliphatic alcohols. *Glass Phys. Chem.* **2012**, *38*(*5*), 460-465.
- 18. Pratt, L. R. Molecular theory of hydrophobic effects: "She is too mean to have her name repeated." *Annu. Rev. Phys. Chem.* **2002**, *53*, 409-436.
- 19. Zhang, X.; Zhu, Y.; Granick, S. Hydrophobicity at a Janus interface. *Science* **2002**, 295, 663-666.
- 20. Chandler, D. Interfaces and the driving force of hydrophobic assembly. *Nature* **2005**, *437*, 640-647.
- 21. Muraka, R. K.; Bagchi, B. Local composition fluctuations in strongly nonideal binary mixtures. *J. Chem. Phys.* **2002**, *117*, 1155-1165.
- 22. Franks, F.; Eves, D. J. G. The Structural properties of alcohol-water mixture. *QUARTERLY REVIEWS* **1966**, *20*(*1*), 1-44.
- 23. Price, W. S.; Ide, H.; Arata, Y. Solution dynamics in aqueous monohydric alcohol systems. *J. Phys. Chem. A.* **2003**, *107*, 4784-4789.
- 24. Banerjee, S.; Bagchi, B. Stability of fluctuating and transient aggregates of amphiphilic solutes in aqueous binary mixtures: studies of dimethylsulfoxide, ethanol, and tert-butyl alcohol. *J. Phys. Chem.* **2013**, *139*(*16*), 164301.

- 25. Iwasaki, K.; Fujiyama, T. Light-Scattering study of clathrate hydrate formation in binary mixtures of tert-butyl alcohol and water. *J. Phys. Chem.* **1977**, *81*(20), 198-1912.
- 26. Harris, K. R.; Newitt, P. J.; Derlacki, Z. J. Alcohol tracer diffusion, density, NMR and FTIR studies of aqueous ethanol and 2,2,2-trifluoroethanol solutions at 25°C. *J. Chem. Soc. Fraday. Trans.***1998**, *94*(*14*), 1963-1970.
- 27. Murthy, S. S. Detailed study of ice clathrate relaxation: evidence for the existence of clathrate structures in some water-alcohol mixtures. *J. Phys. Chem. A.* **1999**, *103*(40), 7927-7937.
- 28. Harris, K. R.; Lam, H. N. Mutual-diffusion coefficients and viscosities for the water-2-methylpropane-2-ol system at 15 and 25°C. *J. Chem. Soc. Faraday. Trans.* **1995,** *91*, 4071-4077.
- 29. Yoshida, K.; Kitajo, A.; Yamaguchi, T. 170 NMR relaxation study of dynamics of water molecules in aqueous of methanol, ethanol, and 1-propanol over a temperature range of 283-403 K. *J. Mol. Liq.* **2006**, *125*, 158-163.
- 30. Mizuno, K.; Miyashita, Y.; Shindo, Y.; Ogawa, H. NMR and FT-IR Studies of hydrogen Bonds in ethanol-water mixtures. *J. Phys. Chem.* **1995**, *99*, 3225-3228.
- 31. Buck, M.; Trifluoroethanol and colleagues: cosovents come of age. Recent studies with peptides and proteins, *Q. Rev. Biophys.* **1998**, *31*, 297-355.
- 32. Myers, J. K.; Pace, C. N.; Scholtz. J. M.; Trifluoroethanol effects on helix propensity and electrostatic interactions in the helical peptide from ribonuclease T₁. *Protein Science* **1998**, 7, 383-388.
- 33. Jasanoff, A.; Fersht, A. R.; Quantitative determination of helical propensities from trifluoroethanol curves. *Biochemistry* **1994**, *33*(8), 2129-2135.
- 34. Bodkin, M. J.; Goodfellow, J. M.; Hydrophobic solvation in aqueous trifluoroethanol solution. *Biopolymers* **1996**. *39*(1), 43-50.
- 35. Rajan, R.; Awasthi, S.K.; Bhattacharjya, P.; Balaram, P. Teflon-coated peptides: hexafluoroacetonetrihydrate as a structure stabilized for peptides. *Biopolymers* **1997**, 42(2), 125-8.
- 36. Hirota, N.; Mizuno, K.; Goto, Y. Group additive contribution to the alcohol induced alpha-helix formation of melittin: implication for the mechanism of the alcohol effects on protein. *J. Mol. Bio.* **1998**, 275(2), 365-78.

- 37. Cammers-Goodwin, A.; Allen, T. J.; Osclick, S. L.; McClure, K. F.; Lee, J. H.; Kemp, D. S. Mechanism of stabilization of helical conformers polypeptides by water containing trifluoroethanol. *J. Am. Chem. Soc.* **1996**, *118*(*13*), 3082-3090.
- 38. Rajan, R.; Balaram, P.; A model for the interaction of trifluoroethanol with peptides and proteins. *Int. J. Peptide Protein Res.* **1998,** *48*, 328-336.
- 39. Khan, M. V.; Rabbani, G.; Kham, R. H. Fluoroalcohols-induced modulation and amyloid formation in conalbumin. *Int. J. Biol. Macromol.* **2014**, *70*, 606-14.
- 40. Kuwajima, K.; Hiroka, Y.; Ikeghuchi, M.; Sugai, S. Comparison of the transient folding intermediates in lysozymes and α-lactabumin. *Biochemsitry* **1985**, *24*, 874-881.
- 41. Buck, M.; Boyd, J.; Redfield, C.; Mackenzie, D.A.; Archer, D. B.; Dobson, C.M. Structural determination of protein dynamics: an analysis of 15N relaxation measurements for main-chain and side-chain nuclei of hen egg white lysozyme, *Biochemistry* **1995**, *34*, 4041-4055.
- 42. Radford, S. E.; Dobson, C.M.; Evans, P. A. The folding of hen lysozyme involves partially structured intermediates and multiple pathways. *Nature* **1992**, *358*, 302-307.
- 43. Blake, C. C. F.; Koenig, D. F.; Mair, G. A.; North, A. C. T.; Philips, D. C.; Sarma, V. R. Structure of hen egg white lysozyme. *Nature* **1965**, *206*, 757-761.
- 44. Buck, M.; Schwalbe, H.; Dobson, C.M. Characterization of conformational preferences in a partly folded protein by heteronuclear NMR spectroscopy assignment and secondary structure analysis of hen egg-white lysozyme in trifluoroethanol. *Biochemistry* **1995**, *34*(*40*), 13219-13232.
- 45. Kraules, P. J. Molscript: s program to produce both detailed and schematic plots of protein structure. *J. Appl. Cryst.* **1991**, *24*, 946-950.
- 46. Hong, D-P.; Hoshino, M.; Kuboi, R.; Goto, Y.; Clustering of fluorine-substituted alcohols as a factor responsible for their marked effects on proteins and peptides. *J. Am. Chem. Soc.* **1999**, *121*(*37*), 8427-8433.
- 47. Shiraki, K.; Nishikawa, K.; Goto, Y. Trifluoroethanol induced stabilization of the alphahelical structure of beta-lactoglobulin: implication for non-hierarchical protein. *J. Mol. Biol.* **1995**, *245*(2), 180-94.
- 48. Mendieta, J.; Folque, H.; Tauler, R. Two phase induction of the non-native alpha helical for of β-lactoglobulin in the presence of trifluoroethanol. *Biophysical Journal.* **1999**, *76*, 451-457.

- 49. Kumar, S.; Modig, K.; Halle, B. Trifluoroethanol induce β→α Transition in β-Lactoglobulin: hydration and co-solvent binding studied by 2 H, 17 O and 19 F Magnetic Relaxation Dispersion. *Biochemistry.* **2003**, *42*, 13708-13716.
- 50. Sashi, P.; Singarapu, K. K.; Bhuyan, A. K. (2018). Solution NMR structure and Backbone dynamics of partially disordered Arabidopsis thaliana phloem protein 16-1, a putative RNA transporter. *Biochemistry* **2018**, *57*, 912–924.
- 51. Uversky, V. N.; Gillespie, J. R.; Fink, A. L.; Why are Natively Unfolded Proteins Unstructured Under Physiologic Conditions? *Proteins: Struct. Funct. Genet.* **2000,** *41*(*3*), 415-427.
- 52. Fink, A. L. Natively Unfolded Proteins, Curr. Opin. Struct. Biol. 2005, 15(1), 35-41.
- 53. Uversky, V. N.; Oldfield, C. J.; Dunker, A.K. Showinng your ID: intrinsic disorder as an ID for recognition, regulation and signalling. *J. Mol. Recognit.* **2005**, 18(5), 343-384.
- 54. Dyson H. J.; Wright, P. E. Coupling of folding and binding for unstructured proteins. *Curr. Opin. Struct. Biol.* **2002**, *12*(*1*), 54-60.
- 55. Hite, K.C.; Kalashnikikova, A.A.; Hansen, J. C. Coil-to-helix transitions in intrinsically disordered methyl CpG binding protein 2 and its isolated domains. *Protein Sci.* **2012**, *21*, 531-538.
- 56. Lewis, J.D.; Meehan, R.R.; Henzel, W.J.; Maurer-Fogy, I.; Jeppesen, P.; Klem, F.; Bird, A. Purification, sequence, and cellular localization of a novel chromosomal protein that binds to a methylated DNA. *Cell.***1992**, *69*, 905-914.
- 57. Buonanno, M.; Coppola, M.; Di Lelio, I.; Molisso, D.; Leone, M.; Pennacchio, F.; Langella, E.; Rao, R.; Monti, S.M. Prosystemin, a prohormone that modulates plant defence barriers, is an intrinsically disordered protein. *Protein Sci.* **2018**, *27*(*3*), 620-632

Chapter 2

Aggregation and diffusive dynamics of some monohydric aliphatic alcohols

Abstract

Self-diffusion dynamics and component associations have been studied for the aqueous solutinos of five monohydric aliphatic alcohols namely, methanol, ethanol, isopropanol, tertiary butanol, and 2,2,2-trifluoroethanol (TFE) by NMR, infrared, and light scattering measurements. Water localization around alcohol cores under water-abundant conditions, and large-scale hydrophobic self-association of alcohols under water-depleting situations describe the two main classes of alcohol associates. Although the results cannot reveal the number density of the components in the associate structures, hydrophobicity dependence of their appearance across the mole fraction scale is clearly noticeable. The mole fraction at which water-hydrated alcohol cores appear is smallest for TFE, indicating significantly large hydrophobicity of the trifluorocarbon group. Activation energy of self-diffusion of aggregates of an alcohol decreases with its mole fraction, suggesting increasing volume fluctuation with the largeness of the aggregates.

2.1. Introduction

Physical properties of both aqueous and organic solvents are almost exclusively determined by their molecular structure. Alcohol solvents, methanol for example, are thought to exist in rolled polymeric chains¹ or cyclic aggregates, which that are less polar compared to the

polarity of the monomers because of hydrogen-bonding between the formative monomers that polarizes the hydroxyl group, resulting in increased affinity for other monomers.² The hydrogen-bonded chain structures, typical of solid states,³ should be more stable with longer lifetime. Although this is a useful picture of neat alcohol used often in synthetic organic chemistry, a large majority of utilities of alcohol requires their aqueous solutions in the form of the binary mixture water:alcohol. This is the genesis of the difficult problem of structural and physical properties of alcohols where water, another liquid of intricately H-bonded molecules, variedly interfers with the properties of the former. The complexity of the water:alcohol system⁴⁻⁶ partly arises from mutual interference with the properties of the component solvents so as to produce structural properties quite different from their neat forms. In the mixed system, alcohol may enhance the water structure at the expense of losing its hydrogen bonding with the latter. In a more physical sense, the molecules of the two components move in each other's force field to not only localize dense forms of water around the solute, but also influence each other's associations coefficients by perturbing the respective chemical potentials. The degree of divergence of structural, physical, and thermodynamic properties of the component solvents will obviously depend on their mole fractions. The problem has been known from the initial report of Frank and Evans⁷ and numerous studies of aqueous solutions of methanol, ethanol, iso-propanol and tert-butanol using neutron scattering,⁸ Rayleigh scattering,⁹ dielectric relaxation,^{10,11} diffusion measurements, 12,13 neutron and X-ray diffraction, 14-16 thermodynamic measurements, 17,18 and molecular dynamics simulation, 16,19-26 have also been reported since then, but uncertainties and controversies about the solution structure of alcohols continue to shroud.

The disinfecting and water-miscibility properties of alcohols have also inspired a large number of nucleic acid and protein denaturation studies since 1956.^{27–45} The reports, however, state the alcohol action on proteins differently. We must also realize that workers

using the water:protein (nucleic acid):alcohol system to study denaturation have been aware of the thermodynamic and structural problems with the components in the alcohol:water binary system. To be able to relay the properties of the solvent components to the protein system held at a constant molarity, it is necessary to understand the changing properties of the former as their mole fractions are modulated. A better understanding of the properties of aqueous solutions of alcohols will not only enhance the basic understanding of solution chemistry but also provide approaches to explain the mechanism by which they denature protein and nucleic acids. The latter was indicated to some detail by Timasheff and coworkers in several of their studies with water:protein:glycerol system. 46-50 Although glycerol is not similar to monohydric alcohols, and hence may act by a different mechanism to denature or stabilize proteins, the importance of preferential solvent exclusion from the protein surface has been amply discussed. To this end, we thought a prerequisite to the study of alcohol denaturation is an analysis of self-association and dynamics of the commonly used alkyl alcohols in their aqueous mixtures.

2.2. Experimental Section

Alcohols used were purchased from different chemical companies; HPLC-grade MeOH from Sigma-Aldrich, laboratory grade absolute ethanol from ChangshuHongsheng Fine Chemicals, iso-propyl alcohol (99.7% GC-assayed) from Fisher Scientific, t-butyl alcohol (99.9% GC-assayed) from Qualigens, and TFE (99.5% assay) from Spectrochem lab. They were used as supplied without further processing. Binary water:alcohol solutions (v/v) were prepared by adding volumes of alcohol to deionized water. Experiments in general were performed at 298 K if not indicated otherwise.

All NMR spectra were taken with samples containing 5% D₂O in a 5 mm room temperature probe of a 500 MHz Ascend spectrometer. Diffusion experiments (PFG NMR) needed z-gradient in the 2–50 Gauss cm⁻¹ range. Spectra were processed and analyzed using Topspin, offline graphing softwares, and codes written for the purpose. Infrared measurements were carried out using an attenuated total reflection infrared (ATR-IR) spectrometer (Nicolet iS5). About 70 μL of the water:alcohol mixture was deposited on the ATR plate for spectral measurement. The scan of the dry ATR plate served for the background spectrum. Steady-state light scattering measurements were done using a fluorometer (FP-8300, Jasco) by setting both excitation and emission wavelengths to 350 nm. Each data point is an average of 24 steady-state scattered intensities accumulated in a 2 min time bin.

2.3. Results and Discussion

2.3.1. Diffusion of alcohol associates in water: alcohol mixture.

Although miscibility (solubility) of shorter alkyl-chain alcohols in water is more than that of longer ones due to reduced apolar surface area of the former, all amphiphilic alcohols associate to varying degrees to produce respective aggregates. These aggregates should be microheterogeneous because not only the extent of self-association at a given alcohol concentration is not restricted to a fixed number, but also the aggregates can interact disparately with water molecules. To a first approximation, the results of simple light scattering experiments (Figure 1) report on the existence of aggregates in water:alcohol mixtures. Since bulk water does not aggregate and therefore does not scatter light, one can surmise that the scattering species are alcohol aggregates whose monomers may plausibly

establish hydrogen bonds with water contingent upon the availability of the latter. Inspection of the data immediately reveals that the alcohol mole fraction (χ_A) corresponding to the appearance of the largest ensemble average size decreases in the order MeOH, EtOH, TBA, TFE (~0.11, 0.08, 0.07, 0.05, respectively), suggesting that the tendency to aggregate increases with hydrophobicity of the aliphatic chain. Note that the $-CF_3$ group is largely hydrophobic than the terminal $-CH_3$ group of alcohols. Since the average size of the aggregates decreases at higher χ_A but continues to remain somewhat larger, it is likely that the water association with the alcohol aggregates or the number density of alcohol molecules in them or both are changed.

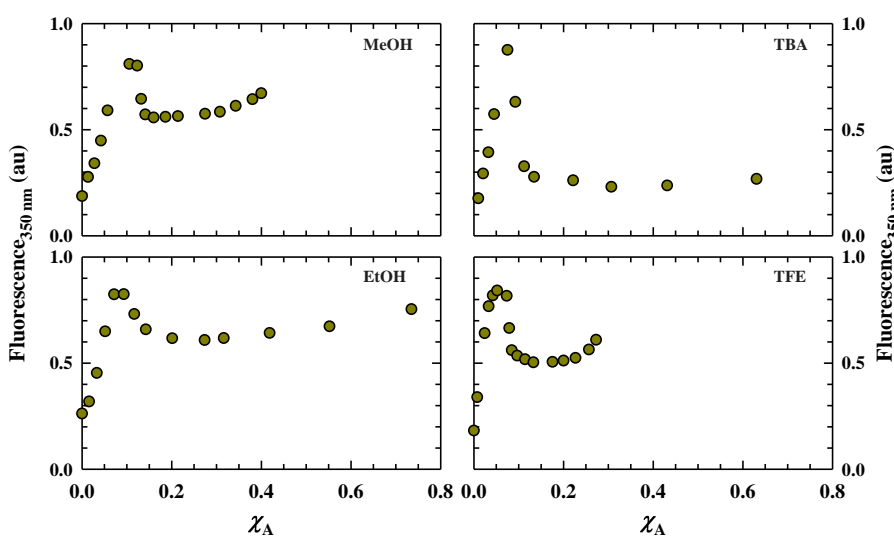


Figure 1. Scattering of 350-nm light by aqueous solutions of the indicated alcohols plotted as a function of mole fraction of alcohol (χ_A) at 298 K. The alcohol solutions were equilibrated at

the same temperature overnight.

The degree of association is determined to a fairly large accuracy by NMR-monitored diffusion coefficient (D_s) that directly measures the average aggregate size and its interaction with the bulk water. Figure 2 shows the variation of $\langle D_s \rangle$ with mole fraction χ_A of the respective alcohols. For all five alcohols, the diffusion rates of water and alcohol, denoted by

 $\langle D_{\rm s} \rangle_{\rm w}$ and $\langle D_{\rm s} \rangle_{\rm A}$, respectively, decrease nonlinearly with $\chi_{\rm A}$ to reach broad minima in the 0.17–0.4 range of $\chi_{\rm A}$. The shallow minimum at $\chi_{\rm A} \sim 0.2$ has also been observed in the $\langle D_{\rm s} \rangle_{\rm A} {\rm vs} \chi_{\rm A}$ graphs for EtOH, IPA, and TBA reported earlier. ^{51–53}Passing the respective minima both $\langle D_{\rm s} \rangle_{\rm w}$ and $\langle D_{\rm s} \rangle_{\rm A}$ increase to register diffusions approaching that of neat alcohols. While this feature can be clearly made out by inspection of the data for MeOH, the response of both $\langle D_{\rm s} \rangle_{\rm w}$ and $\langle D_{\rm s} \rangle_{\rm A}$ to $\chi_{\rm A}$ increasingly flattens out for EtOH, IPA, and TBA.

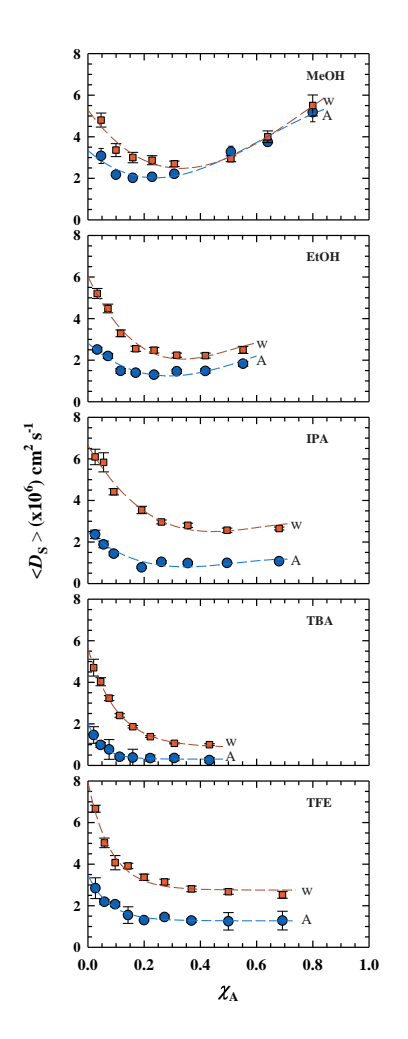


Figure 2.Diffusion coefficients of the indicated alcohols and water at 298 K as a function of respective χ_A at 298 K. The resonances assigned to the $-CH_3$ group of MeOH, EtOH, IPA, and TBA, and the $-CH_2$ – group of TFE were used to calculate the respective diffusion coefficients. The dashed lines through data are drawn to guide to guide the eye, although the data for MeOH, EtOH, and IPA can be approximated by a skewed hyperbola. The labels w and A refer to water and alcohol, respectively.

This result, consistent with earlier experimental observations with MeOH, EtOH, and TBA,⁵⁴ seems to indicate that the flatness of diffusion of alcohol and alcohol-water associates

in binary solutions of higher χ_A is related to the hydrocarbon content of the aliphatic chain. But the invariance of both $\langle D_s \rangle_w$ and $\langle D_s \rangle_A$ with χ_A is also observed for TFE (Figure 2), which is already known to aggregate, ^{13,55–58}has only a two-carbon alkyl chain similar to ethanol. Trifluoroethanol is however more hydrophobic than ethanol through the former's -CF₃ content,^{57,59} indicating that hydrophobicity can account for the χ_A dependence of the coefficients of alcohol association in the binary mixture (see below).

2.3.2. Hydrophobic Hydration Retards Water and Alcohol Diffusion under low χ_A conditions.

We notice that the gradient of self-diffusion of water $\langle D_{\rm s} \rangle_{\rm w}$ with $\chi_{\rm A}$ resembles that of the diffusion of $\langle D_{\rm s} \rangle_{\rm A}$ for all five alcohols considered here (Figure 2). The high similarity index in the response of the two diffusion coefficients to the alcohol content mustarise from specific interaction of water and alcohol in the clustering of the latter. It is well known that the presence of alcohol in water affects the structure of the latter,60-70 but how the uniform pattern of variation of $\langle D_{\rm s} \rangle_{\rm w}$ and $\langle D_{\rm s} \rangle_{\rm A}$ under low $\chi_{\rm A}$ conditions becomes increasingly flat in the order of EtOH, IPA, TBA, and TFE under high χ_A needs careful consideration. To begin with the 'alcohol in water' (low χ_A) condition, a water molecule can be localized reversibly at the -OH end of the alcohol by hydrogen bonding. ²¹Concurrently, the alkyl hydrogens of the alcohol can also interact with the oxygens of water. Since alcohols have higher tendency to self-associate at low χ_A , 71 a hydrophobic core of two or more self-associated alcohol molecules can be also be caged by surrounding water molecules in the form of short-lived alcohol micelles. The water localization by alcohols should strengthen the water structure by which several water molecules can interact to form a cage of water clathrate around the alcohol molecules. Such clathrate hydrates containing ~20 water molecules surrounding a MeOH,8~21 waters associated with TBA,72 and ~5 or 6 waters in the propanol and TBA hydration clathrates¹⁰ have been reported. Existence of cages hydrating EtOH are derived from calculations and experimental data.^{73,74} We assume that TFE being a water structure maker⁷⁵ also acquires a dense surrounding of water. The hydration clathrates under low $\chi_{\rm A}$

conditions occupy interstitial voids of the otherwise open water network, thus reducing not only the self-diffusion coefficient of water molecules $\langle D_{\rm s} \rangle_{\rm w}$, 21,22 but also the binary diffusion coefficient $\langle D_{\rm s} \rangle_{\rm A}$. One should note that increasing $\chi_{\rm A}$ will lead to utilization of larger number of water molecules to form hydration clathrates around the alcohol molecules, depleting the waters in the open hydrogen-bonded network.

2.3.3. Hydrophobic Self-Association of alcohols at high χ_A .

The water-structuring effect of alcohol will be increasingly redundant as water is depleted due to increasing χ_A . The alcohol molecules now exist in hydrophobic self-associated forms with reduced hydrating water structure around, but with a fewer water molecules trapped. Self-diffusion of alcohol is now related to the size of the alcohol clusters determined by the coefficient of self-association of respective alcohols in the water:alcohol mixture. It may be useful here to briefly recall the definition of self-association constant of the components in the water:alcohol system. Denoting water and alcohol by 1 and 2, respectively, we represent the liquid solute behaviour of the components by their respective excess chemical potential that can be expressed by

$$\mu_i = \mu_i^{\circ}(T, P) + \log \gamma_i c_i \qquad i=1, 2$$

$$\log \gamma_1 = A_{11}c_1 + A_{12}c_2$$

$$\log \gamma_2 = A_{21}c_1 + A_{22}c_2,\tag{1}$$

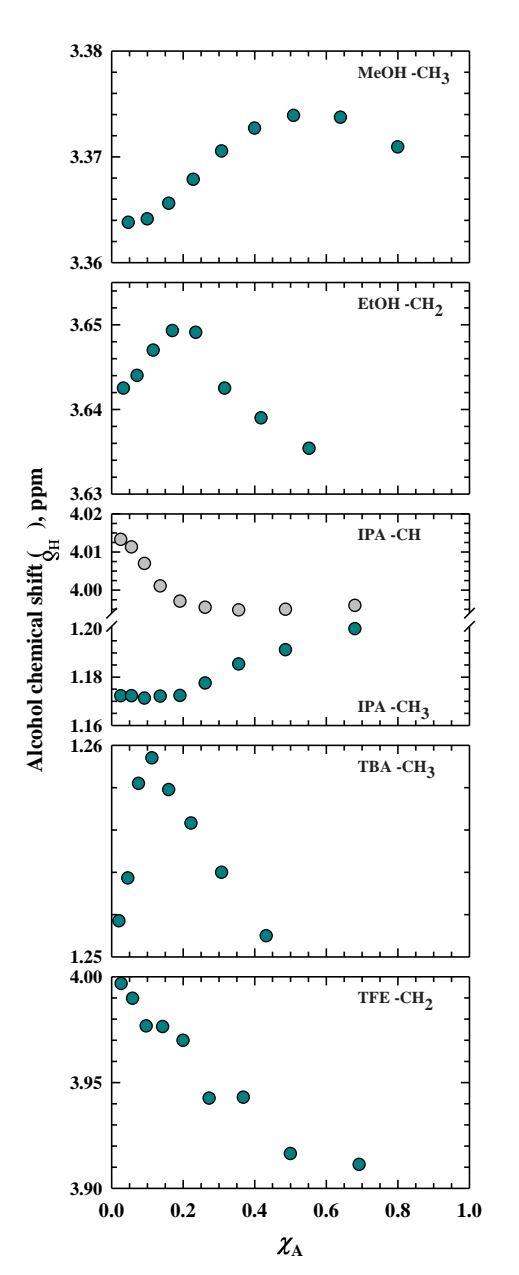
where $\mu_i^{\circ}(T, P)$ is the standard chemical potential. The component interaction coefficients A_{11} , A_{12} , A_{21} , and A_{22} measure the perturbation of γ of a component by intracomponent interaction (A_{11}, A_{22}) and intercomponent intreaction (A_{12}, A_{21}) , yielding the matrix for the thermodynamic interaction coefficients is

Larger numerical value of a coefficient (m⁵ s⁻²) across the mole fraction scale results from increasing association of the appropriate components. The coefficient of hydrophobic self-association (A_{22}) for EtOH and TBA across the respective alcohol mole fraction scales has been measured. 53,71 As discussed in the preceding section, the tendency to self-associate increases rapidly as χ_A becomes smaller (< 0.1). But A_{22} remains nearly constant as the alcohol concentration is increased to obtain the neat form. It is this constant hydrophobic selfassociation accompanied by increasingly depleted water that is reflected in the flat selfdiffusion of alcohol $\langle D_s \rangle_A$ at high χ_A (Figure 2). The data for MeOH and EtOH, however, show an increase in self-diffusion at high χ_A , meaning that neat forms of these alcohols are likely to have lesser tendency to self-associate. Presumably, the tendency to undergo hydrophobic self-association increases with the alkyl chain length; for example, the value of A_{22} for TBA in its water mixture is higher than that for EtOH when $\chi_A > 0.1$. Similarly, higher hydrophobicity of TFE than smaller aliphatic alcohols, EtOH for example, 59 that arises from the highly apolar-CF₃ group and lower electron density on the -OH group lead to weaker hydrogen bonding ability and higher hydrophobic self-association. The self-diffusion coefficient of TFE is therefore small and flat at high χ_A .

2.3.4. NMR Chemical shift of alcohol methyl protons and hydrophobic self-association.

The implications above that both hydroxyl and alkyl hydrogens of alcohol can interact with oxygens of the caging water structure at low χ_A , and that hydrophobic self-association of alcohols dominates under water-depleting conditions (high χ_A) should be reflected in the NMR chemical shift variation with alcohol concentration. Although there will be bulk diamagnetic susceptibility changes to an extent because the water peak in the NMR spectrum also shifts with χ_A , we assume that the susceptibility changes are not large. The

 χ_A dependence of chemical shift of the methyl protons (δ_H) of alcohols (Figure 3) is consistent with the inferences stated above. Following a brief lag (χ_A <0.05), δ_H of the –CH₃ protons of MeOH continues to shift downfield (high-frequency shift) up to χ_A <0.5 and then turns to shift upfield. The initial lag in δ_H means localization of water at the –OH of methanol but the downfield shift that follows translates to deshielding of the –CH₃ protons of one or more core MeOH due to their hydrogen bonding interactions with the surrounding water oxygens, and the upfield shift at χ_A >0.5 implies shielding of the –CH₃ protons due to



hydrophobic self-association of the methyl groups. The same explanation holds for EtOH, IPA, and TBA with the rider that the initial lag phase tends to disappear and the concentration of alcohol (χ_A) at which the deshielding rolls over to shielding decreases with the length of the alkyl chain. A slight deviation from this generalization in the case of IPA is obviously due to the attachment of the –OH group to the middle carbon. The description is also extendible to TFE whose larger hydrophobicity by virtue of the –CF₃ group yields to hydrophobic shielding even at low χ_A .

Figure 3. Absolute chemical shift changes (δ_H)of the indicated resonances and the alcohols with χ_A at 298 K.

2.3.5. IR absorption of alcohol associates.

Infrared absorption of the 3n-6 normal modes of vibration provides information about volume fluctuation and atom displacements giving rise to changes in the dipole strength, and both can be related to the dynamics of alcohol association. Regions of steady-state IR spectra recorded with normal water solution of MeOH, EtOH, IPA, and TBA are given in Figure 4. We subtract the water absorption from each spectrum to focus on the symmetric and antisymmetric C-H stretching, $\nu_{\rm S}$ (C-H)and $\nu_{\rm A}$ (C-H), respectively, of the alcohol with the rationale that they are involved in hydrophobic self-association. Visual inspection of the spectra already shows that the vibrational absorption increases as the alcohol concentration is raised from 5 to 90% which is trivially due to the validity of Beer's law in IR spectroscopy⁷⁶

$$A = \int \alpha_{\nu} d\nu = \frac{1}{n!} \int \ln \frac{l_0}{l} d\nu \tag{3}$$

in which α_{ν} is molar absorption coefficient at frequency ν , n is the alcohol concentration in moles L⁻¹, l is pathlength, and l_0 and l are intensities of incident and transmitted light. To note, however, is that while the absolute absorption due to $\nu_{\rm A}({\rm CH_3})$ increases in the order MeOH, EtOH, IPA, TBA, the order is reversed for the other absorption bands. We explain this result by expressing the IR absorption in terms of the dipole derivative with respect to the normal coordinate of the C-H⁷⁶

$$A = \frac{\pi N_{\rm A}}{3c^2} \left(\frac{\partial \mu}{\partial Q}\right)_{R=R_{\rho}}^2 \tag{4}$$

where N_A is Avogadro number, c is the velocity of light, μ is the dipole moment, and Q is the normal mode displacement with respect to the equilibrium internuclear separation R_e . Clearly, the γ -methyl group (terminal CH₃) is more mobile on account of the large dipole derivative with respect to ν_A (CH₃), and the C-H fluctuations increase with the alkyl chain

length of the alcohol. Conversely, $\nu_s(\text{CH}_2)$ and $\nu_A(\text{CH}_2)$ vibrations produce smaller dipole derivatives, hence lower absorption with increasing number of carbons in the alcohol chain. This interpretation of results suggests that hydrophobic self-association of alcohols motionally restrict the α - and β -methylene groups more than the terminal γ -methyl group.

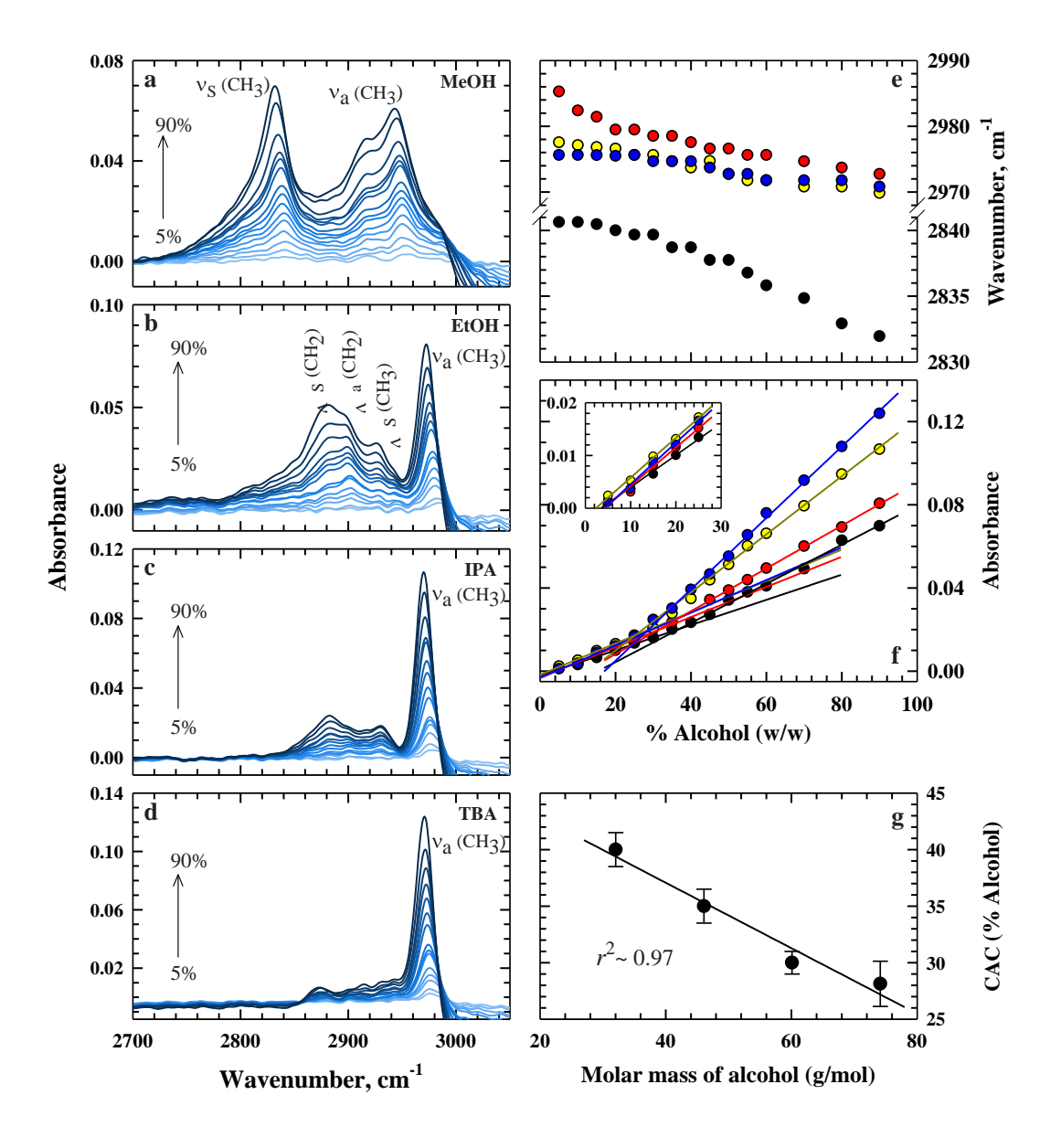


Figure 4.(a–d) IR absorption due to –CH₂– and –CH₃ stretching modes of the alkyl alcohols plotted after subtracting after subtracting the absorption due to water. The increase in absorption from 5 to 90% alcohol of each alcohol is due to the validity of Beers law. (e) Shift in the absorption of antisymmetric stretching mode of –CH₃ toward lower frequency with %

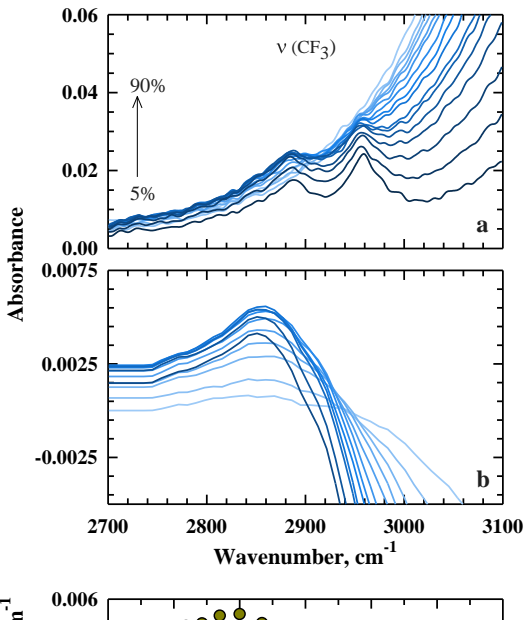
alcohol of MeOH (black), EtOH (red), IPA (yellow), and TBA (blue). (f) The % alcohol dependence of IR absorption due to the antisymmetric stretching of –CH₃ of MeOH (black), EtOH (red), IPA (yellow), and TBA (blue)., showing a break in the Beer law absorption for each alcohol. The *inset* enlarges the initial linear phase. (g) The linearity of critical association concentration (CAC) of alcohols with their molar mass.

Figure 4e shows the shift of the $v_A({\rm CH_3})$ band maximum to lower frequency. Generally, low-frequency shift of IR absorption reflect excitation of lesser density of normal modes at the expense of larger root-mean-square volume ($\delta V_{\rm RMS}$) fluctuation. This holds for protein-like large molecules, ⁷⁷ and should also be true for alcohol associates. The χ_A distribution of vibrational frequency is nonlinear (Figure 4e), apparently due to extensive water hydrates around the alcohol core when the water level is high and larger self-association of the alcohols under water-depleted conditions. While the number density of the normal modes excited may decrease with increasing alcohol concentration, the predicted large $\delta V_{\rm RMS}$ is experimentally verifiable (see below).

The alcohol concentration dependence of the $\nu_{\rm A}({\rm CH_3})$ absorption is plotted in Figure 4f. The Beer law is valid for all four alcohols at low concentrations (~5–40%, Figure 4f, *inset*) as well as at high (>30%). The absorbance in these two regions is, however, distinguished by a sharp break in the region of 25–40% alcohol, similar to the instructive specific conductivity of micelle-forming surfactants. It is likely that packing of the alkyl groups in the alcohol core supported by peripheral water localization on the –OH groups of alcohols produce short-lived micelle-like species, reasoned also by an earlier study. We call the % alcohol corresponding to the absorbance break point critical association concentration (CAC), which is plotted against the molar mass of the four alcohols in Figure 4g. This clarifies that the entry into the micelle-like packing of alcohols is related to their chain

hydrophobicity. We cannot tell at this stage as to how many alcohol molecules associate to qualify for micelle assembly, but note that micellization is not an abrupt all-or-none process; small premicellar hydrophobic aggregates have been observed in surfactant solutions,^{79–81} and are implied in the theory of concentration fluctuations in binary liquids.⁸² Any form of alcohol micelles will not exist at high χ_A where their –OH ends are not supported due to increasing unavailability of water.

To end this section, we provide the IR data for TFE in Figure 5. Since the absorption bands due to $\nu(\text{CF}_3)$ modes (2800–3000 cm⁻¹) are buried in the wings of the water absorption band the spectrum of water alone was consistently subtracted from the TFE:water spectra, which resulted in some shift of the TFE band to lower frequency (Figure 5a,b). We ignore the shift and read the absorbance values from the water-subtracted spectra with χ_A



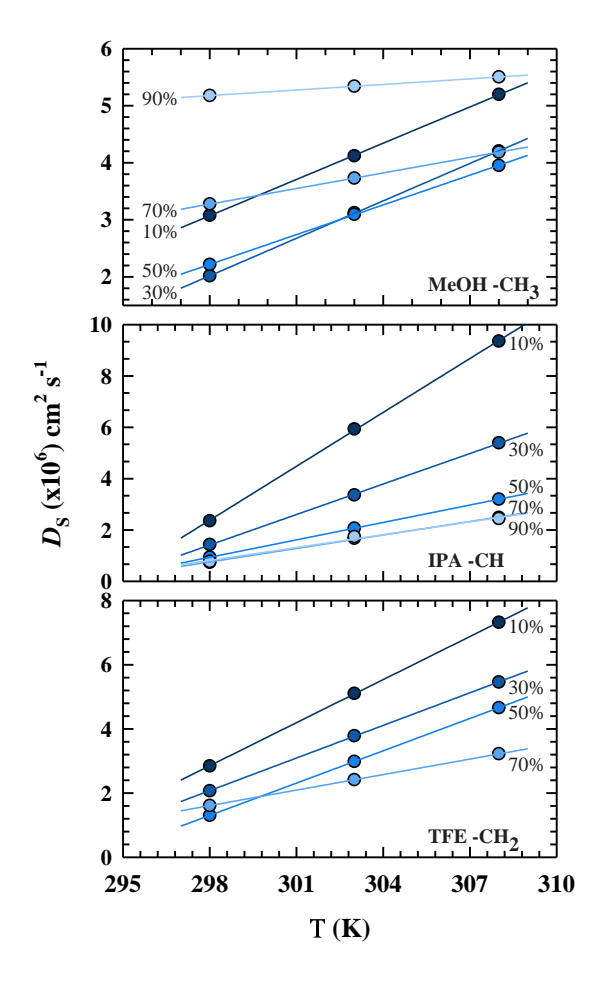
(Figure 5c). Deviation of absorbance from the Beer law starts at χ_A <0.1, levels off in the region about 0.2, and inverts thereafter, reflecting our working theme of initial hydration, growth of hydrated cores of alcohol aggregates, and the collapse of hydrophobic hydration to water bereft hydrophobic self-association.

0.000 0.0002 0.0002 0.0000 0.0 0.1 0.2 0.3 0.4 0.5 0.6 χ_A

Figure 5. (a) IR absorption of the stretching modes of $-CF_3$ in 5 to 90% alcohol. (b) The same set of spectra plotted after subtracting the water spectrum from each. The subtraction leads to an apparent shift in the spectrum toward lower wavelength by ~ 25 cm⁻¹. (c) The skewed

hyperbola of absorbance $vs\chi_A$, the maximum of which corresponds to the changeover from hydrophobic hydration to hydrophobic self-association.

2.3.6. Activation energy of diffusion of alcohol aggregates. The assertion above that the low-frequency shift of vibrational excitation of $v_A(CH_3)$ implies large δV_{RMS} of the alcohol associates led us to determine the activation energy of their diffusion. The rationale is that the molecular volume of alcohols and their diffusion are linearly correlated. We measured the diffusion coefficient of MeOH, IPA, and TFE, each at different concentrations, at 298, 303, and 308 K (Figure 6), and calculated the activation energy for each by the Arrhenius equation $D_s = D_s^o \exp(-E_a/RT)$, where D_s^o is the front factor and E_a is activation energy. The E_a



values listed in Table 1 clarifies that volume fluctuation increases as alcohol associates become larger at higher χ_A , suggesting that hydrophobic self-association may give rise to a compact core but increased volume, plausibly due to reduced water localization at the –OH terminus of alcohol molecules.

Figure 6.Temperature dependence of diffusion coefficient at various concentrations of MeOH, IPA, and TFE. The activation energies extracted are listed in Table 1.

Table 1. Activation energy of diffusion of alcohol aggregates

E _a (kcal mol ⁻¹)				
Methanol	iso-Propanol	TFE		
9.6	25.2	17.3		
13.4	24.3	17.7		
10.5	22.5	23.3 [*]		
4.5	22.3	12.6		
1.2	21.2	_		
	Methanol 9.6 13.4 10.5 4.5	Methanol iso-Propanol 9.6 25.2 13.4 24.3 10.5 22.5 4.5 22.3		

^{*} Likely to have large error

2.4. References

- 1. Reichardt, C. Solvents and Solvent Effects in Organic Chemistry; Wiley-VCH: Weinheim, Germany, 1988.
- 2. Henkel, S.; Misuraca, M. C.; Troselj, P.; Davidson, J.; Hunter, C. A. Polarisation Effects on the Solvation Properties of Alcohols. *Chem. Sci.* **2018**, *9*, 88–99.
- 3. Hamilton, W. C.; Ibers, J. A. Hydrogen Bonding in Solids; J. Wiley: New York, 1968.
- 4. Franks, F. *Water–A Comprehensive Treatise*; Franks, F., Ed.; Plenum Press: New York, **1972**; Vol. 2, Chapter 5.
- 5. Ben-Naim, A. Water and Aqueous Solutions—Introduction to a Molecular Theory; Plenum Press: London, 1982.
- 6. Rowlinson, J. S.; Swinton, F. L. *Liquid sand Liquid Mixtures*; Butterworths: London, 1982.
- 7. Frank, H. S.; Evans, M. W. Free Volume and Entropy in Condensed Systems III. Entropy in Binary Liquid Mixtures: Partial Molal Entropy in Dilute Solutions; Structure and Thermodynamics in Aqueous Electrolytes. *J. Chem. Phys.* **1945**, *13*, 507–532.

- 8. Soper, A. K.; Finney, J. L. Hydration of Methanol in Aqueous Solution. *Phys. Rev. Lett.* **1993**, *71*, 4346–4350.
- 9. Micali, N.; Trusso, S.; Vasi, C.; Blaudez, D.; Mallamace, F. Dynamical Properties of Water-Methanol Solutions Studied by Depolarized Rayleigh Scattering. *Phys. Rev. E* **1996**, *54*, 1720–1724.
- 10. Murthy, S. S. N. Detailed Study of Ice Clathrate Relaxation: Evidence for The Existence of Clathrate Structures in Some Water-Alcohol Mixtures. *J. Phys. Chem.* A **1999**, *103*, 7927–7937.
- 11. Petong, P.; Pottel, R.; Kaatze, U. Water-Ethanol Mixtures at Different Compositions and Temperatures. A Dielectric Relaxation Study. *J. Phys. Chem.* A **2000**, *104*, 7420–7428.
- 12. Harris, K. R.; Goscinska, T.; Lam, H. N. Mutual Diffusion Coefficients for The Systems Water-Ethanol and Water-Propan-1-ol at 25°C. *J. Chem. Soc.*, *Faraday Trans.* **1993**, 89, 1969–1974.
- 13. Harris, K. R.; Newitt, P. J.; Derlacki, Z. J. Alcohol Tracer Diffusion, Density, NMR, and FTIR Studies of Aqueous Ethanol and 2,2,2-trifluoroethanol Solutions at 25°C. *J. Chem. Soc.*, *Faraday Trans.* **1998**, *94*, 1963–1970.
- 14. Nishi, N.; Takahashi, S.; Matsumoto, M.; Tanaka, A.; Muraya, K.; Takamuku, T.; Yamaguchi, T. Hydrogen-Bonded Cluster Formation and Hydrophobic Solute Association in Aqueous Solutions of Ethanol. *J. Phys. Chem.* **1995**, *99*, 462–468.
- 15. Nishi, N.; Matsumoto, M.; Takahashi, T.; Takamuku, T.; Yamagami, M.; Yamaguchi, T. *Structure and Dynamics of Clusters*; Universal Academy Press: Tokyo **1996**; 00 113–120.
- 16. Benmore, C. J.; Loh, Y. L. The Structure of Liquid Ethanol: A Neutron Diffraction and Molecular Dynamics Study. *J. Chem. Phys.* **2000**, *112*, 5877–5883.
- 17. Larkin, J. A. Thermodynamic Properties of Aqueous Non-Electrolyte Mixtures I. Excess Enthalpy for Water+Ethanol at 298.15 to 383.1 K. *J. Chem. Thermodynamics* **1975**, *7*, 137–148.
- 18. Tanaka, S. H.; Yoshihara, H. I.; Ho, A. W. C.; Lau, F. W.; Westh, P.; Koga, Y. Excess Partial Molar Enthalpies of Alkane-Mono-ols in Aqueous Solutions. *Can. J. Chem.* **1996**, *74*, 713–721.
- 19. Okazaki, S.; Touhara, H.; Nakanishi, K. Computer Experiments of Aqueous Solutions.

- V. Monte Carlo Calculation on The Hydrophobic Interaction in 5 mol % Methanol Solution. *J. Chem. Phys.* **1984**, *81*, 890–894.
- Tanaka, H.; Nakanishi, K.; Touhara, H. Computer Experiments of Aqueous Solutions.
 VI. Potential Energy Function for *tert*-Butyl Alcohol Dimer and Molecualr Dynamics Calculation of 3 mol % Aqueous Solution of *tert*-Butyl Alcohol. *J. Chem. Phys.* 1984, 81, 4065–4073.
- 21. Laaksonen, A.; Kusalik, P. G.; Svishchev, I. M. Three –Dimensional Structure of Water-Methanol Mixtures. *J. Phys. Chem. A* **1997**, *101*, 5910–5918.
- 22. Dlugoborski, T.; Hawlicka, E.; Swiatla-Wojcik, D. Effect of a Solute on Water Properties MD Simulation Studies. *J. Mol. Liq.* **2000**, *85*, 97–104.
- 23. Kusalik, P. G., Lyubartsev, A. P.; Bergman, D. L.; Laaksonen, A. Computer Simulation Study of *tert*-Butyl Alcohol. 1. Structure in The Pure Liquid. *J. Phys. Chem. B* **2000**, 104, 9526–9532.
- 24. Banerjee, S.; Bagchi, B. Stability of Fluctuating and Transient Aggregates of Amphiphilic Solutes in Aqueous Binary Mixtures: Studies of Dimethyl Sulfoxide, Ethanol, and *tert*-Butyl Alcohol. *J. Chem. Phys.* **2013**, *139*, 1643001.
- 25. Cassone, G.; Sofia, A.; Sponer, J.; Saitta, A. M.; Sajja, F. *AbInitio* Molecular Dynamics Study of Methanol-Water Mixtures Under External electric Fields. *Molecules* **2020**, *25*, 3371.
- 26. Pršlja, P.; Žibert, T.; Urbic, T. Monte Carlo Simulations of Simple Two-Dimensional Water-Alcohol Mixtures. *J. Mol. Liq.* **2022**, *368*, 120692.
- 27. Rees, E. D.; Singer, S. J. A Preliminary Study of The Properties of Proteins in Some Nonaqueous Solvents. *Arch. Biochem. Biophys.* **1956**, *63*, 144–159.
- 28. Coates, J. H.; Jordan, D. O. Deoxypentose Nucleic Acids XV. The Sedimentation of Calf Thymus Deoxyribonucleic Acid in 95% Ethanol. *Biochim. Biophys. Acta.* **1960**, *43*, 214–222.
- 29. Helmkamp, G. K.; T'so, P. O. P. The Secondary Structures of Nucleic Acids in Organic Solvents. *J. Am. Chem. Soc.* **1961**, *83*, 138–142.
- 30. Herskovits, T. T.; Singer, S. J.; Geiduschek, E. P. Nonaqueous Solutions of DNA. Denaturation in Methanol and Ethanol. *Arch. Biochem. Biophys.* **1961**, *94*, 99–114.
- 31. Herskovits, T. T. Nonaqueous Solutions of DNA. Factors Determining the Stability of

- the Helical Configuration in Solution. Arch. Biochem. Biophys. 1962, 97, 474–484.
- 32. Schrier, E. E.; Ingwall, R. T.; Scheraga, H. A. The Effect of Aqueous Alcohol Solutions on The Thermal Transition of Ribonuclease. *J. Phys. Chem.* **1965**, *69*, 298–303.
- 33. Brandts, J. F.; Hunt, L. The Thermodynamics of Protein Denaturation. 3. The Denaturation of Ribonuclease in Water and in Aqueous Urea and Aqueous Ethanol Mixtures. *J. Am. Chem. Soc.* **1967**, *89*, 4826–4838.
- 34. Herskovits, T. T., Jaillet, H. Structural Stability and Solvent Denaturation of Myoglobin. *Science***1969**, *163*, 282–285.
- 35. Herskovits, T. T.; Gadegbeku, B.; Jaillet, H. On The Structural Stability and Solvent Denaturation of Proteins I. Denaturation by the Alcohols and Glycols. *J. Biol. Chem.* **1970**, 245, 1588–2598.
- 36. Bull, H. B.; Beese, K. Interaction of Alcohols with Proteins. *Biopolymers*. **1978**, *17*, 2121–2131.
- 37. Shiraki, K.; Nishikawa, K.; Goto, Y. Trifluoroethanol-Induced Stabilization of the α-Helical Structure of β-Lactoglobulin: Implication for Non-Hierarchical Protein Folding. *J. Mol. Biol.* **1995**, 245, 180–194.
- 38. Buck, M. Trifluoroethanol and Colleagues: Cosolvents Come of Age. Recent Studies With Peptides and Proteins. *Q. Rev. Biophys.* **1998**, *31*, 297–355.
- 39. Shimizu, S.; Shimizu, K. Alcohol Denaturation: Thermodynamic Theory of Peptide Unit Solvation. *J. Am. Chem. Soc.* **1999**, *121*, 2387–2394.
- 40. Dwyer, D. S.; Bradley, R. J. Chemical Properties of Alcohols and Their Protein Binding Sites. *Cell. Mol. Life Sci.* **2000**, 57, 265–275.
- 41. Sashi, P.; Yasin, U. M.; Bhuyan, A. K. Unfolding Action of Alcohols on a Highly Negatively Charged State of Cytochrome *c. Biochemistry* **2012**, *51*, 3273–3283.
- 42. Nikolaidis, A.; Moschakis, T. On the Reversibility of Ethanol-Induced Whey Protein Denaturation. *Food Hydrocolloids*. **2018**, *84*, 389–395.
- 43. Hossain, M.; Huda, N.; and Bhuyan, A. K. A Surprisingly Simple Three-State Generic Process for Reversible Protein Denaturation by Trifluoroethanol. *Biophys. Chem.* **2022**, 291, 106895.
- 44. Goryanin, I.; Ovchinnikov, L.; Vesnin, S.; Ivanov, Y. Monitoring Protein Denaturation

- of Egg White Using Passive Microwave Radiometry (MWR). *Diagnostics*. **2022**, *12*, 1498.
- 45. Hossain, M.; Huda, N.; and Bhuyan, A. K. A Three-State Mechanism for Trifluoroethanol Denaturation of an Intrinsically Disordered Protein. *J. Biochem.* **2023** (in press).
- 46. Timasheff, S. N.; Inoue, H. Preferential Binding of Solvent Components to Proteins in Mixed Water-Organic Solvent Systems. *Biochemistry* **1968**, 7, 2501–2513.
- 47. Timasheff, S. N. Protein-Solvent Interactions and Protein Conformation. *Acc. Chem. Res.* **1970**, *3*, 62–68.
- 48. Gekko, K.; Timasheff, S. N. Mechanism of Protein Stabilization by Glycerol: Preferential Hydration in Glycerol-Water Mixtures. *Biochemistry* **1981**, *20*, 4667–4676.
- 49. Gekko, K.; Timasheff, S. N. Thermodynamics and Kinetic Examination of Protein Stabilization by Glycerol. *Biochemistry* **1981**, *20*, 4677–4686.
- 50. Timasheff, S. N. Protein-Solvent Preferential Interactions, Protein Hydration, and Modulation of Biochemical Reactions by Solvent Components. *Proc. Natl. Acad. Sci. U.S.A.* **2002**, *99*, 9721–9726.
- 51. Holz, M.; Grunder, R.; Sacco, A.; Meleleo, A. Nuclear Magnetic Resonance Study of Self-Association of Small Hydrocarbon Solutes in Water: Salt Effects and The Lyotropic Series. *J. Chem. Soc. Faraday Trans.* **1993**, *89*, 1215–1222.
- 52. Sacco, A.; Asciolla, A.; Matteoli, E.; Holz, M. NMR Study of the Influence of Urea on the Self-Association of Propan-1-ol in Water and Comparison with Kirkwood-Buff Integral Results. *J. Chem. Soc. Faraday Trans.* **1996**, *91*, 35–40.
- 53. Sacco, A.; Holz, M. NMR Studies on Hydrophobic Interactions in Solution Part 2. Temperature and Urea Effect on the Self-Association of Ethanol in Water. *J. Chem. Soc.*, *Faraday Trans.* **1997**, *93*, 1101–1104.
- 54. Price, W. S.; Ide, H.; Arata, Y. Solution Dynamics in Aqueous Monohydric Alcohol Systems. *J. Phys. Chem. A* **2003**, *107*, 4784–4789.
- 55. Kuprin, S.; Gräslund, A.; Ehrenberg, A.; Koch, M. H. J. Nonideality of Water-Hexafluoropropanol Mixtures as Studies by X-ray Small Angle Scattering. *Biochem. Biophys. Res. Commun.* **1995**, *217*, 1151–1156.
- 56. Gast, K.; Zirwer, D.; Müller-Frohne, M.; Damaschun, G. Trifluoroethanol-Induced

- Conformational Transitions of Proteins: Insights Gained From the Differences Betweenα-Lactalbumin and Ribonuclease A. *Protein Sci.* **1999**, 8, 625–634.
- 57. Hong, D. P.; Hishino, M.; Kuboi, R.; Goto, Y. Clustering of Fluorine-Substituted Alcohols as a Factor Responsible for Their Marked Effects on Proteins and Peptides. *J. Am. Chem. Soc.* **1999**, *121*, 8427–8433.
- 58. Culik, R. M.; Abaskharon, R. M.; Pazos, I. M.; Gai, F. Experimental Validation of the Role of Trifluoroethanol as a Nanocrowder. *J. Phys. Chem. B* **2014**, *118*, 11455–11461.
- 59. Matsugami, M.; Yamamoto, R.; Kumai, T.; Tanaka, M.; Umecky, T.; Takamuku, T. Hydrogen Bonding in Ethanol-Water and Trifluoroethanol-Water Mixtures Studied by NMR and Molecular Dynamics Simulation. *J. Mol. Liq.* **2016**, *217*, 3–11.
- 60. Roney, A. B.; Space, B.; Castner, E. W.; Napoleon, R. L.; Moore, P. B. A Molecular Dynamics Study of Aggregation Phenomena in Aqueous *n*-Propanol. *J. Phys. Chem. B* **2004**, *108*, 7389–7401.
- 61. Egashira, K.; Nishi, N. Low-frequency Raman Spectroscopy of Ethanol-Water Binary Solution: Evidence for Self-Association of Solute and Solvent Molecules. *J. Phys. Chem. B* **1998**, *102*, 4054–4057.
- 62. Dixit, S.; Crain, J.; Poon, W.; Finney, J. L.; Soper, A. K. Molecular Segregation Observed in a Concentrated Alcohol-Water Solution. *Nature* **2002**, *416*, 829–832.
- 63. Vrhovšek, A.; Gereben, O.; Jamnik, A.; Pusztai, L. Hydrogen Bonding and Molecular Aggregates in Liquid Methanol, Ethanol, and 1-Propanol. *J. Phys. Chem. B* **2011**, *115*, 13473–13488.
- 64. Gupta, R.; Patey, G. N. Aggregation in Dilute Aqueous *tert*-Butyl Alcohol Solutions: Insights from Large-Scale Simulations. *J. Chem. Phys.* **2012**, *137*, 034509.
- 65. Gupta, R.; Patey, G. N. How Aggregation in Aqueous 2-Butoxyethanol Solutions is Influenced by Temperature. *J. Mol. Liq.* **2013**, *177*, 102–109.
- 66. Indra, S.; Biswas, R. Heterogeneity in (2-Butoxyethanol + Water) Mixtures: Hydrophobicity-Induced Aggregation or Critically-Driven Concentration Fluctuations? *J. Chem. Phys.* **2015**, *142*, 204501.
- 67. Ghoufti, A.; Artzner, F.; Malfreyt, P. Physical Properties and Hydrogen-Bonding Network Water-Ethanol Mixtures from Molecular Dynamics Simulations. *J. Phys. Chem. B* **2016**, *120*, 793–802.

- 68. Mochizuki, K.; Pattenaude, S. R.; Ben-Amtoz, D. Influence of Cononsolvency on the Aggregation of Tertiary Butyl Alcohol in Methanol-Water Mixtures. *J. Am. Chem. Soc.* **2016**, *138*, 9045–9048.
- 69. Kaur, S.; Kashyap, H. K. Three-Dimensional Morphology and X-ray Scattering Structure of Aqueous tert-Butanol Mixtures: A Molecular Dynamics Study. *J. Chem. Sci.* **2017**, *129*, 103–116.
- 70. Choi, S.; Parameswaran, S.; Choi, J-H. Understanding Alcohol Aggregates and The Water Hydrogen Bond Network Towards Miscibility in Alcohol Solutions: Graph Theoretical analysis. *Phys. Chem. Chem. Phys.* **2020**, 22, 17181.
- 71. Mayele, M.; Holz, M.; Sacco, A. NMR Studies on Hydrophobic Interactions in Solution. *Phys. Chem. Chem. Phys.* **1999**, *1*, 4615–4618.
- 72. Iwasaki, K.; Fujiyama, T. Light Scattering Study of Clathrate Hydrate Formation in Binary Mixtures of *tert*-Butyl Alcohol and Water. *J. Phys. Chem.* **1977**, *81*, 1908–1912.
- 73. Dolenko, T. A.; Burikov, S. A.; Dolenko, S. A.; Efitorov, A. O.; Plastinin, I. V.; Yuzhakov, V. I.; Patsaeva, S. V. *J. Phys. Chem. A* **2015**, *119*, 10806.
- 74. Ghoraishi, M. S.; Hawk, J. E.; Phani, A.; Khan, M. F.; Thundat, T.; *Sci. Rep.* **2016**, *6*, 23966.
- 75. Macdonald, D. D.; Dolan, B.; Hyne, J. B. The Influence of Substituted Alcohols on the Temperature and Maximum Density of Water. *J. Solution Chem.* **1976**, *5*, 405–416.
- 76. Bhuyan, A. K. *Fundamental Concepts of Molecular Spectroscopy*; CRC Press, Taylor & Francis Group: Boca Raton, Fl, 2023.
- 77. Swarupini, D. S.: Joshi, K.; Bhuyan, A. K. Negative Thermal Expansion of a Disordered Native Protein. *Chem. Phys.* **2022**, *560*, 111569.
- 78. Hawlicka, E.; Garbowski, R. Influence of Urea on Hydrophobic Phenomena in Aqueous Aolutions of Alcohols. *Chem. Phys. Lett.* **1995**, *236*, 64–70.
- 79. Aniansson, E. A. G.; Wall, S. N.; Almgen, M.; Hoffman, H.; Kielmann, J.; Ulbricht, W.; Zana, R.; Lang, J.; Tondre, C. Theory of The Kinetics of Micellar Equilibria and Quantitative Interpretation of Chemical Relaxation Studies of Micellar Solutions of Ionic Surfactants. *J. Phys. Chem.* **1976**, *80*, 905–922.
- 80. Cui, X.; Mao, S.; Liu, M.; Yuan, H.; Du, Y. Mechanism of Surfactant Micelle Formation. *Langmuir* **2008**, *24*, 10771–10775.

- 81. Hadgiivanova, R.; Daimant, H. Premicellar Aggregation of Amphiphilic Molecules. *J. Phys. Chem. B* **2007**, *111*, 8854–8859.
- 82. Rupprecht, A.; Kaatze, U. Model of Concentration Fluctuation in Binary Liquids. Verification by Ultrasonic Spectrometry of Aqueous Systems and Evidence of Hydrophobic Effect. *J. Phys. Chem. A* **1999**, *103*, 6485–6491.
- 83. Welle, F. Diffusion Coefficients and Activation Energies of Diffusion of Organic Molecules in Polystyrene Below and Above Glass Transition Temperature. *Polymers* **2021**, *13*, 1317

CHAPTER 3

A Surprisingly Simple Three-State Generic Process for Reversible Protein Denaturation by Trifluoroethanol

Abstract

Despite the rich knowledge of the influence of 2,2,2-trifluoroethanol (TFE)on the structure and conformation of peptides and proteins, the mode(s) of TFE-protein interactions and the mechanism by which TFE reversibly denatures a globular protein remain elusive. This study systematically examines TFE-induced equilibrium transition curves for six paradigmatic globular proteins by using basic fluorescence and circular dichroism measurements under neutral pH conditions. The results are remarkably simple. Low TFE invariably unfolds the tertiary structure of all proteins to produce the obligate intermediate (I) which retains nearly all of native-state secondary structure, but enables the formation of extra α -helices as the level of TFE is raised higher. Inspection of the transitions at once reveals that the tertiary structure unfolding is always a distinct process, necessitating the inclusion of at least one obligate intermediate in the TFE-induced protein denaturation. It appears that the intermediate in the minimal unfolding mechanism $N \rightleftharpoons I \rightleftharpoons D$ somehow acquires higher α helical propensity to generate α -helices in excess of that in the native state to produce the denatured state (D), also called the TFE state. The low TFE-populated intermediate I may be called a universal intermediate by virtue of its α -helical propensity. Contrary to many earlier suggestions, this study dismisses molten globule (MG)-like attribute of I or D.

3.1. Introduction

It has been about 60 years since 2,2,2-trifluoroethanol was introduced in protein chemistry to look at the conformational aspects of polypeptide oligomers and co-oligomers. Helix induction by TFE in peptides isolated from globular proteins was reported soon. ^{2,3} followed by the seminal demonstration of TFE-induced discrete conformational transitions involving helix formation in protein.⁴ Such studies in the course of time opened upa plethora of important questions concerning the response of peptide and protein structures to aqueous TFE. Interests were aroused on the role of amino acid sequence in α -helical propensity, ⁵⁻⁸the development of a sequence-based helix propensity metric 9-13, the mode of protein-TFE interactions the which the affects and mechanism by latter chain conformation, ^{13,14–24}hydrophobic clustering and declustering in TFE solution, ^{21,25–28} the TFEinduced stabilization of β -turns^{29–32}and β -hairpin, ^{33,34} β -sheet formation in a designed protein, ³⁵ and transitions from random coil to α -helix, ¹⁷ β -sheet to α -helix, ^{17,36,37} and coil to β -sheet to α -helix transition with increasing TFE. ³⁸The investigations listed above are hardly exhaustive, but the wealth of information they provide on peptide-TFE and globular protein-TFE system is admirable. A basic problem though is that the available results fail to evolve a consensus regarding an essential framework of structures as to how TFE might denature a globular protein across the scale of cosolvent composition. A part of the problem arose from the effort of accommodating a molten globule (MG) species in the mechanism of TFE denaturation. This is not surprising because the influential MG model of protein folding39-47was postulated concurrent with much of the protein-TFE investigations cited above. Lysozyme for example at pH 2 - the condition under which the protein exists in a molten globule state, shows a single transition to the TFE state that was dubbed as the MG state, 48 but the results for the same cooperative transition 49 were taken to provide no evidence

for involvement of MG because the compactness of a typical molten globule is more than that of the TFE state. ⁵⁰ On the other hand, the TFE transition for Ca^{2+} -free α -lactalbumin at pH 7 was interpreted to proceed via the MG state ⁵⁰ when it should not be. It is still unclear as to which one is the MG state – the end TFE state or an intermediate expected to populate at low TFE or both. In fact, a version of this difficulty of associating a MG in the TFE-induced protein transition has already been mentioned by Goto and coworkers as non-hierarchical protein folding. ¹⁷

A fundamental understanding emerging from the vast information made available is that no matter what elements the initial protein chain contains – coil, turns, β -sheets, 3_{10} helix, α -helix, or some combination of these in a single or more domains, relatively higher TFE invariably induces α -helical propensity irrespective of the pH of the medium, producing the final denatured state (D) or the TFE state whose α -helical content exceeds that of the initial native state (N). But the intermediary structure(s) between the initial and final states and its accumulation is unclear. Studying this reversible process is vital to understand if and how proteins fold to the native state, in vitro at least. One may solubilize aggregated proteins or inclusion bodies in high TFE to obtain the D-state and refold or purify the protein to generate the N state. Even though the highly α -helical D-state is produced artificially by TFE, the N-state forms upon removal of the TFE perturbant. We thought if the content and the extent of structures in the N state do not decide upon the α -helical outcome of D or vice versa, there must be a universal intermediate state (I) that is somehow poised to acquire α helical propensity. If the I state exists, it must represent a state with unfolded tertiary structure but having considerable secondary structure because of the helix-inducing attribute of TFE present already.

The purpose of this manuscript is to test the simple idea above by measuring TFE-induced transitions for six proteins diverse by the extent and content of secondary structure types. They all undergo respective reversible transitions to the TFE state via the hypothesized I state under several near-neutral pH conditions, asserting the operation of the minimal $N \rightleftharpoons I \rightleftharpoons D$ pathway, where the intermediate has unfolded tertiary structure. Occasionally, more than one intermediate is detected depending on the protein type and the dimeric status of the native state. Specifically, no MG-like state is obvious in the reversible TFE denaturation of any of the proteins tested.

3.2. Materials and methods

Proteins cytochrome c (Cyt c), myoglobin (Mb), hen egg white lysozyme, α -lactalbumin (α -LA), β -lactoglobulin (β -LG), and trypsin purchased from Sigma were used without further purification. Buffer components were highly pure, and TFE purchased from Spectrochem had 0.1% water and 0.005% non-volatile substances as declared impurities. Protein solutions were buffered with 20 mM sodium phosphate for use in the pH range 4–8 and 20 mM Tris for pH above 8. Samples for titration of proteins with TFE were prepared by mixing two stock solutions that were identical in all respects except that one contained 60% (v/v) TFE and the other not. Samples containing TFE in 0–60% range were obtained by appropriately combining the two stocks solutions. This approach of sample preparation in which two protein solutions initially held at the two extremes of TFE are mixed to produce intermediate solvent compositions provides a basis to assume reversibility of the protein-TFE reaction. The final protein concentration for fluorescence and far-UV CD measurements was uniformly 7μ M for all six proteins. The concentration used for near-UV CD measurements

measurements were carried out at 25°C using a AVIV SF420 CD spectrometer and a Jasco FP-8300 fluorometer. Sample pHs were also measured at the end of experiments to confirm that they did not change.

We assume that mole fraction-based activity coefficients are applicable to the binary mixture of the non-electrolyte TFE and water. Activity coefficient of TFE are calculated from the empirical relation

$$\gamma_{\pm} = a + be^{-cx} + de^{-fx} \tag{1}$$

obtained by further analysis of literature data.⁵¹ The mass-based mole fraction of TFE in the aqueous solution is denoted by x, and the constants are a = 0.0677, b = 0.4680, c = 20.8253, d = 0.4596, and f = 6.3429.

3.3. Results

3.3.1. TFE binding can expose or bury aromatics: no general principle

The changes in tertiary structure brought about by TFE binding were examined by tryptophan fluorescence. A representative set of emission spectra recorded with α -lactalbumin (α -LA) at pH 7, 8, and 9(Figure 1) shows cooperative red shift of the wavelength of maximum emission (λ_{max}) by ~13 nm within 20% TFE at pH 7. The same shift occurs at lower TFE when the pH is raised to 8 and 9. The Stokes shift reflects the TFE-induced exposure of tryptophan side chains. The cooperative nature of the surface exposure implies break down of weak intraprotein interactions leading to unfolding of tertiary structure.

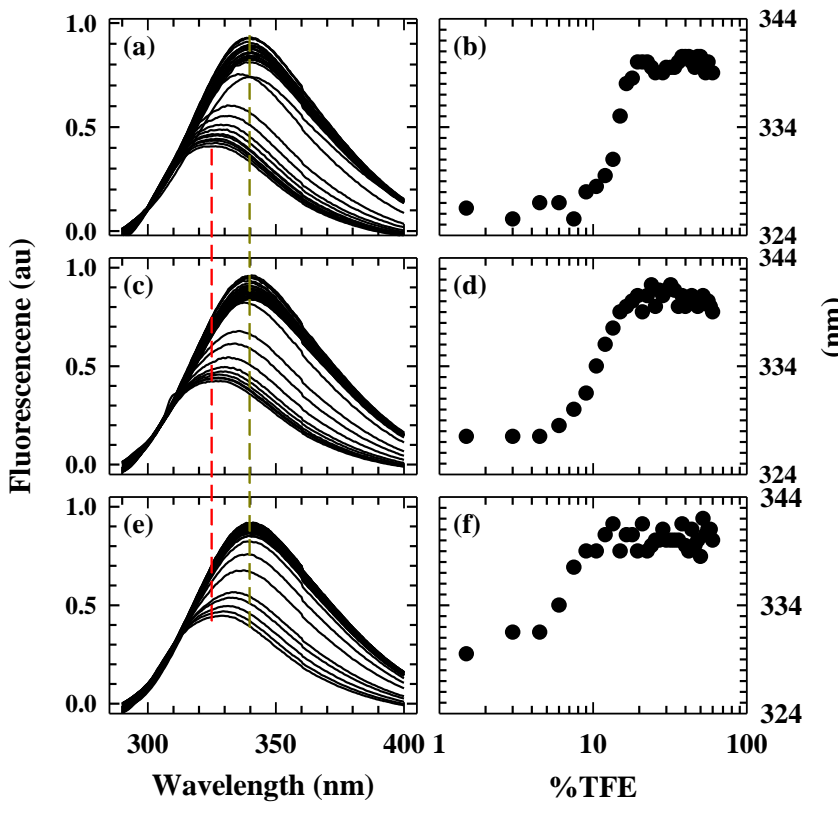


Figure 1. Fluorescence spectra and Stokes shift of emission maxima (λ_{max}) of α -lactalbumin at pH 7 (a,b), pH 8 (c,d), and pH 9 (e,f). The red and yellow dashed lines running from panel (a) to panel (e) compare the appearance of λ_{max} at low and high TFE at pH

7,8, and 9.

The λ_{max} for each of the six proteins studied showed cooperative shifts (Figure 2), suggesting a generic tertiary structure unfolding effect of TFE. The generality is however not maintained with regard to the positioning of the tryptophans with TFE. The λ_{max} for myoglobin, lysozyme, α -LA, and β -lactoglobulin (β -LG) undergoes red shift, indicating that the tertiary structure unfolding results in exposure of the aromatic side chains from the low dielectric interior of the protein to the solvent. On the other hand, the TFE-induced blue shift of the λ_{max} for cyt c and trypsin is indicative of burial of aromatic side chains in the respective unfolded states. This implies that TFE unfolding of tertiary structure affects the aromatic side chains either way –relocating them to the surface or burying in the low dielectric interior.

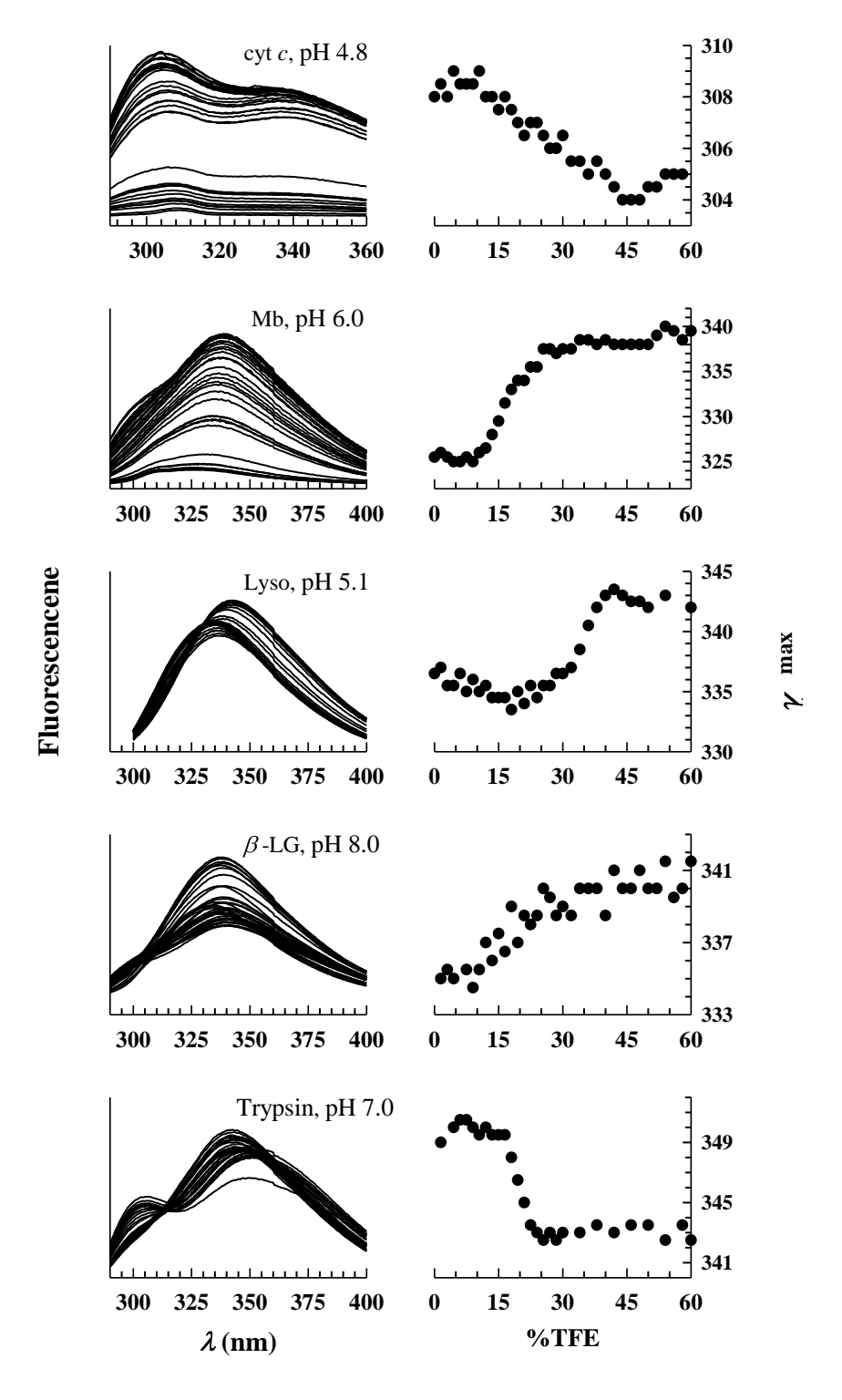


Figure 2. Fluorescence spectra and Stokes and anti-Stokes shift of emission maxima λ_{max} for the proteins under the indicated pH conditions.

One may also ask, can the Stokes shifts of the different proteins be connected to the positioning of the aromatic chains in the native state and/or their local sequence that will likely affect their environment in the unfolded state? Based on the hydropathy and charge content of the 20 amino acid residues near the neutral-pH region we performed a comparison of local sequences containing tryptophans. It appears that proteins showing blue shift (cytochrome c and trypsin) have tryptophans buried in comparatively more positively charged environment, and the numbers of hydrophobic and hydrophilic amino acids within 5 Å of the tryptophan side chain are nearly equal. On the other hand, proteins showing red shift (lysozyme, α -lactalbumin, β -lactoglobulin and myoglobin) have tryptophans surrounded by neutral or comparatively negatively charged amino acids. Also, the numbers of hydrophobic and hydrophilic amino acids surrounding the tryptophan side chains are considerably different.

3.3.2. *Unfolding of tertiary structure*

Parametric analysis of protein denaturation by TFE is not as straightforward as the unfolding transitions obtained with ionic and non-ionic denaturants is. To see if a general qualitative trend of tertiary structure unfolding can be observed, we examine the fluorescence emission and near-UV CD absorption of all six proteins at the λ_{max} of the respective denatured states. Near-UV CD measurements in protein-TFE experiments in particular are necessary to supplement the fluorescence results because quenching of indole fluorescence by high dielectric of TFE ($\gtrsim 20\%$) affects the tryptophan fluorescence intensity to ~25%.On the other hand, near-UV CD only reflects the change in structure around the aromatic residues.

Each protein was titrated with TFE at three different pH values so as to find out the effect of the net protein charge on the respective structural transition monitored by fluorescence, although only one of the pH conditions was used for near-UV CD

measurement. Fluorescence data for four proteins are shown in Figure 3 and the other two are in Figure 4. The fluorescence transitions for cytochrome c (Figure 3a-c), myoglobin (Figure 3e-g), and α -LA (Figure 3i-k) shift to lower or higher TFE% according to the pH-dependent stability of the respective protein. The shifts are not due to pH-dependent protein-TFE interactions because TFE is a very weak proton donor (pKa \sim 12.5) and its interaction with protein groups is not expected to change with pH employed here. Varying the net charge content by a pH perturbation essentially translates to poising the protein at different energetic stability, and this difference is reflected in the shift of the transition along the %TFE coordinate. In this respect the action of TFE is comparable to any chaotrope, since urea or GdnHCl-induced structural transitions shift across the denaturant scale commensurate with the extent of pH-perturbation of a protein.

In the near-UV CD measurements, we initially recorded a few spectra (Figure 5) to identify the bands for time-base averaging of ellipticity at the band wavelength. The single-wavelength data averaged sufficiently are plotted alongside the fluorescence transitions in Figure 3. The near-UV CD transitions for cytochrome c, myoglobin, and α -LA (Figure 3d, h,l) qualitatively complement the corresponding fluorescence transitions. Curiously, both fluorescence (Figure 3e-g) and near-UV CD (Figure 3h)-monitored transitions for myoglobin show a two-step transition, suggesting that TFE populates an equilibrium unfolding intermediate not reported in numerous studies of myoglobin unfolding by urea and GdnHCl published earlier. We introduce the intermediate by inspection of the transitions alone. This intermediate populated by the early transition preceding the major transition may not have a connection with the acid-stabilized intermediate I'of myoglobin in the pH range 3.5–4.5 observed previously, 52 but the implication is the role of TFE in the stabilization of structural intermediates.

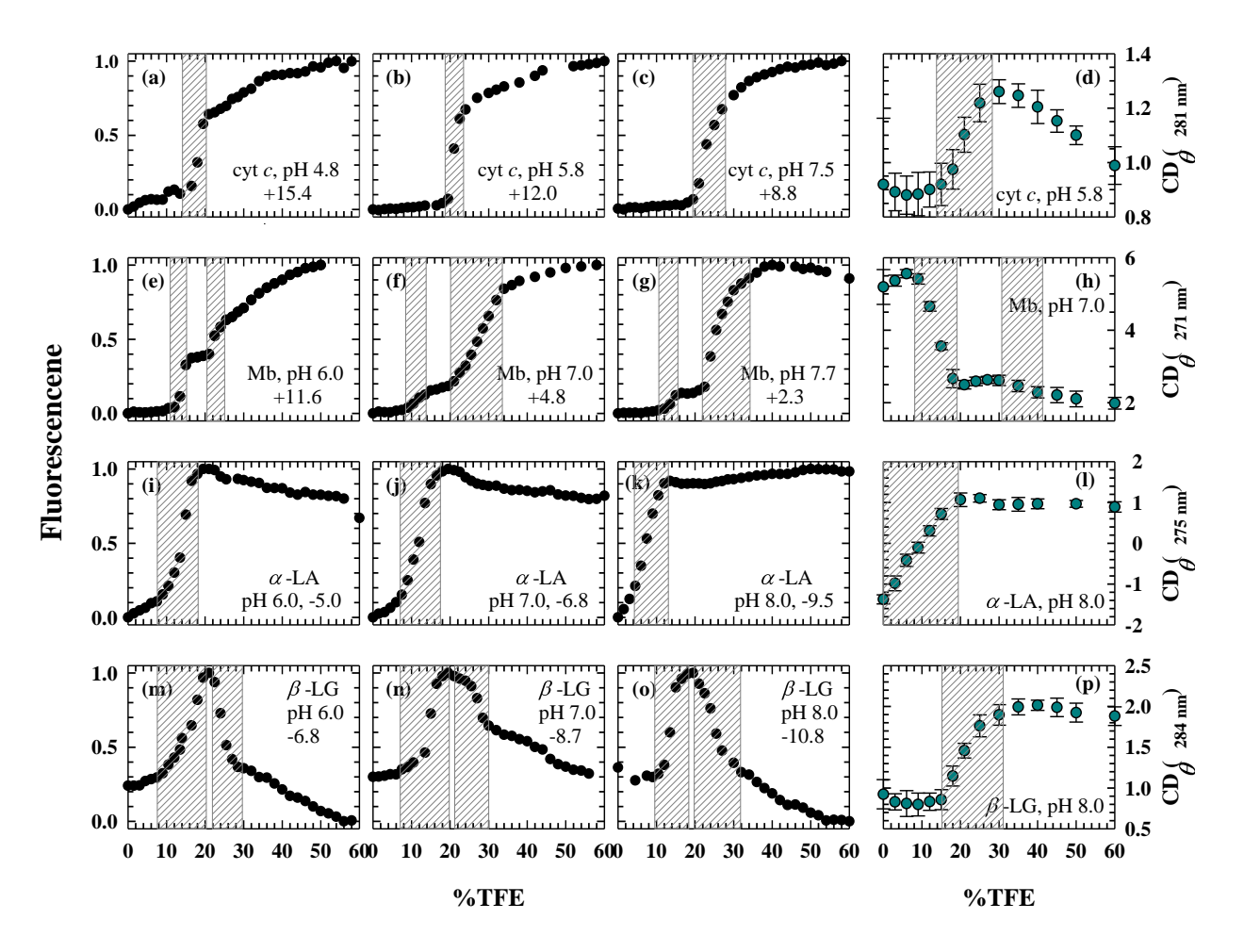


Figure 3. Unfolding of tertiary structure of proteins by TFE under indicated conditions. Each stippled box straddles a transition.

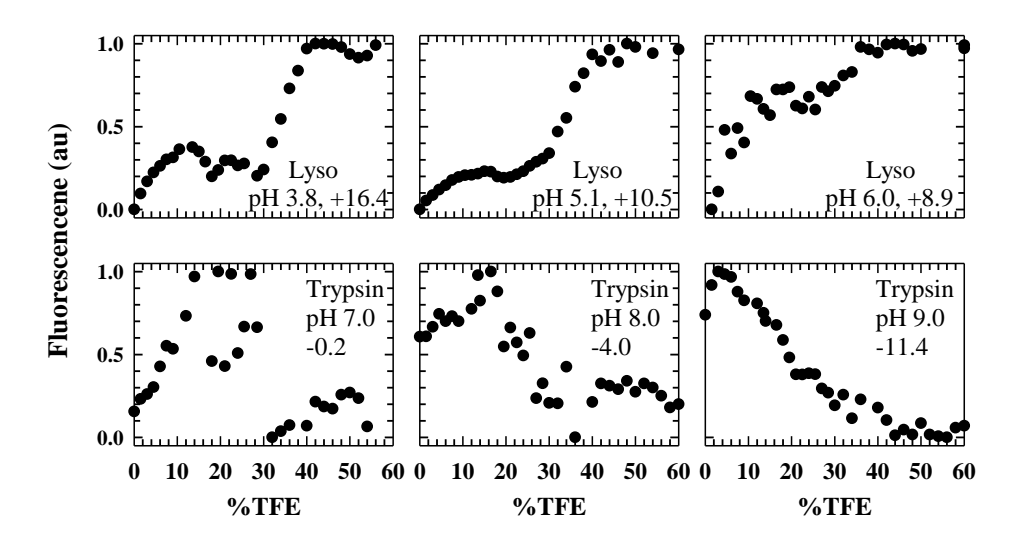


Figure 4.Unfolding of tertiary structures of lysozyme and trypsin. The pH and the charge content in each case are indicated.

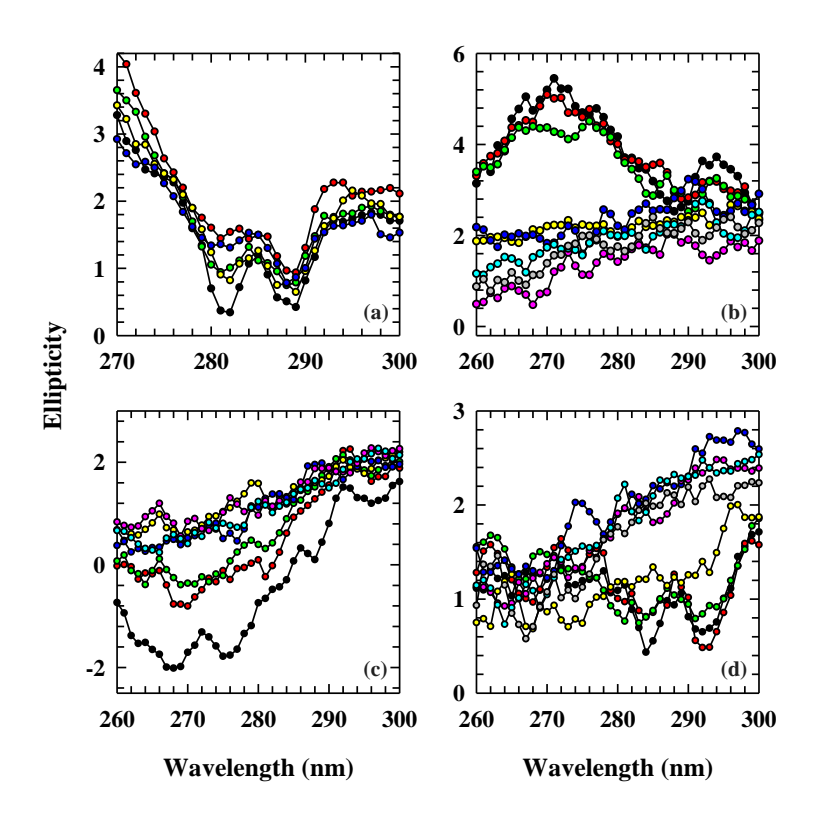


Figure 5.Near-UV CD spectra. (a) cytochrome c in 0, 17, 20, 23, and 26% TFE; (b)myoglobin in 0, 9, 12, 15, 18, 40, 50, and 60% TFE; (c) α -lactalbumin in 0, 6, 12, 20, 30, 40, and 50% TFE; (d) β -lactoglobulin in 0, 3, 9, 18, 25, 30, 45, and 60% TFE. The increment in symbol colour corresponds to the specified increase in TFE%.

The fluorescence-monitored transition of β -LG with TFE simulate a bell shape with distorted flanks (Figure 3m–o), giving the impression of folding and unfolding in tandem. Since β -LG is a dimer at pH>5,⁵³ we attribute the transition at lower TFE to dimer \rightleftharpoons monomer equilibrium in which the quenched fluorescence in the native dimeric state is revoked as the dimer dissociates to monomers. This dimer \rightarrow monomer suggestion can be tested by measuring the transition at an elevated protein concentration (Figure 6). The second transition associated with decreasing fluorescence then reflects the unfolding of tertiary structure of the monomers. The near-UV CD transition (Figure 3p) does not distinguish the dissociation and unfolding processes, which is likely due to insensitivity of the rotational

strength of the aromatic side chains to subunit dissociation. The dissociation-coupled unfolding of β -LG with TFE is consistent with the denaturation study of the protein in urea.⁵⁴ We see again that the action of TFE on the tertiary structure of this protein is comparable with that of urea. On the other hand, intermediates on the urea-induced equilibrium pathway of β -LG implied by simulation studies⁵⁵, are not populated by urea or TFE.

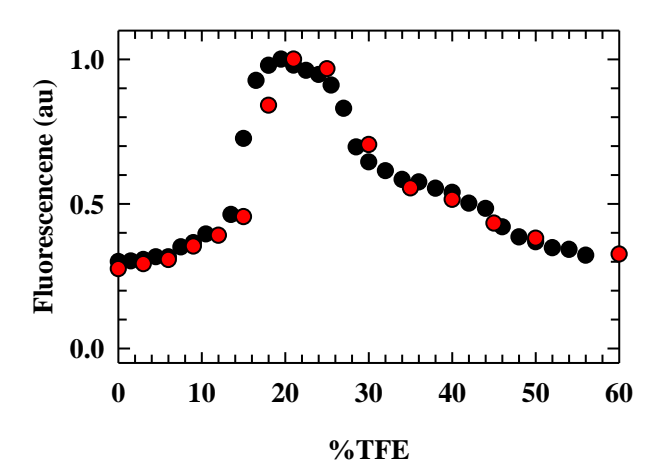


Figure 6.TFE-induced tertiary structure unfolding of β -LG when the protein concentration is held at 7 μ M (black circles) and 70 μ M (red circles). The early transition associated with increasing fluorescence is due to dimer \rightarrow monomer transition.

3.3.3. Denaturation of Secondary Structure by TFE

The samples employed above for fluorescence were further subjected to determine secondary structure content of the six proteins. Typical changes in the far-UV CD spectrum due to TFE addition are shown in Figure 7, and the ellipticity values at 222 and 207 nm read by averaging time-base runs are plotted in Figure 8.It is plain that all proteins under all pH conditions show cooperative change of secondary structure. The myoglobin case is a bit different in that an unfolding transition precedes the denaturation as the pH is raised from 6 to 7.7(Figure 8*d-f*). It is possible that these two transitions are related to the accumulation of a

structural intermediate as observed by fluorescence already (Figure 3e-g). The transition for β -LG at lower TFE (Figure 8m) is most likely due to dissociation of the dimer to monomers, which is consistent with the occurrence of a three-turn α -helix and a β -strand in the dimerization interface. The absence of this biphasic transition at pH 7 and 8 (Figure 8n-o) is likely due to tight coupling of the dimerization transition with secondary structure denaturation such that the monomer is not populated.

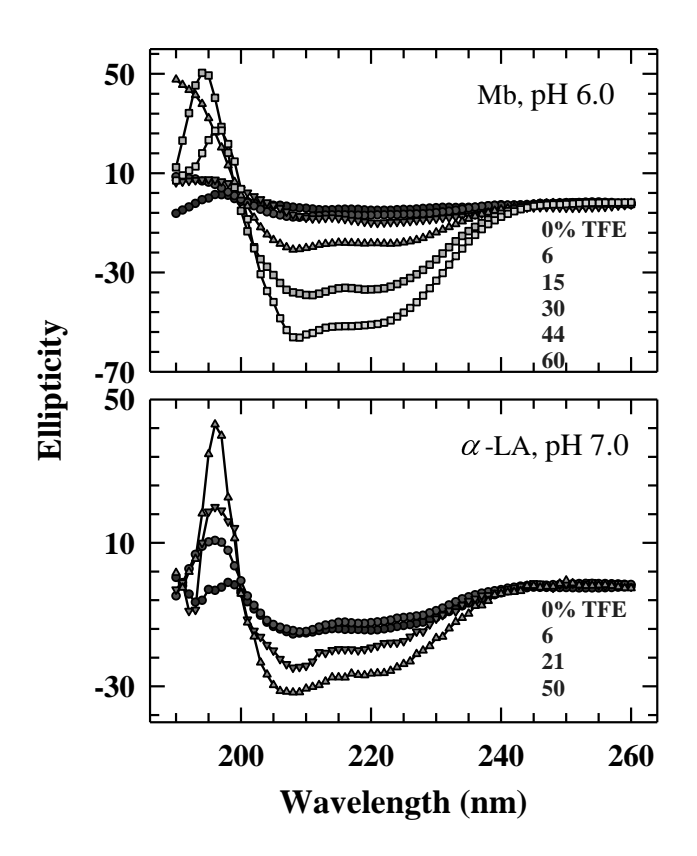


Figure 7.Typical changes in the far-UV CD spectra of myoglobin and α -lactalbumin with TFE.

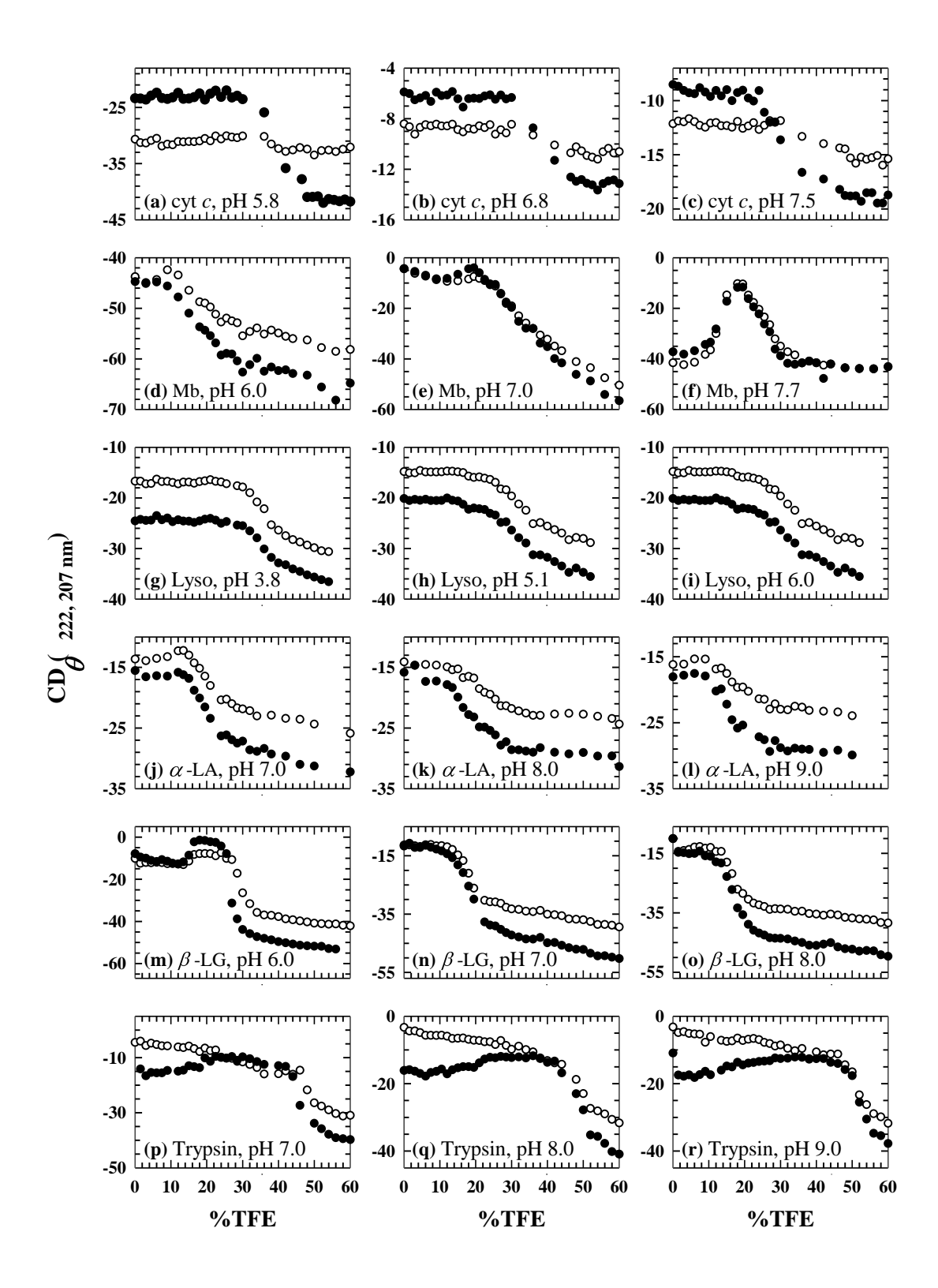


Figure 8. The TFE dependence of 222-nm (open circles) and 207-nm (closed circles) ellipticity.

The key result is the formation of additional secondary structure with TFE. This process can be called neither unfolding because of the accumulation of extra secondary structure nor refolding because there is little scope of structure acquisition in excess of what the native state already has. We therefore name the process denaturation of secondary structure.

3.3.4. Denaturation is associated with accumulation of α -helical structure

Studies earlier have established that TFE stabilizes α -helices and enhances helical propensity of β -sheetproteins. ^{7,9,12,15,17,37,50,56,57} The CD data can also be analyzed to check for the accumulation of additional α -helical structure (Figure 9) in the denatured protein by using the method of Greenfield and Fasman, ⁵⁸ call GF, that we have used earlier to quantify the SDS-induced α -helix formation in proteins . ⁵⁹ The % α -helix is estimated by

%
$$\alpha$$
-helix $\sim \frac{[\theta]_{207}-4000}{-33000-4000}$,

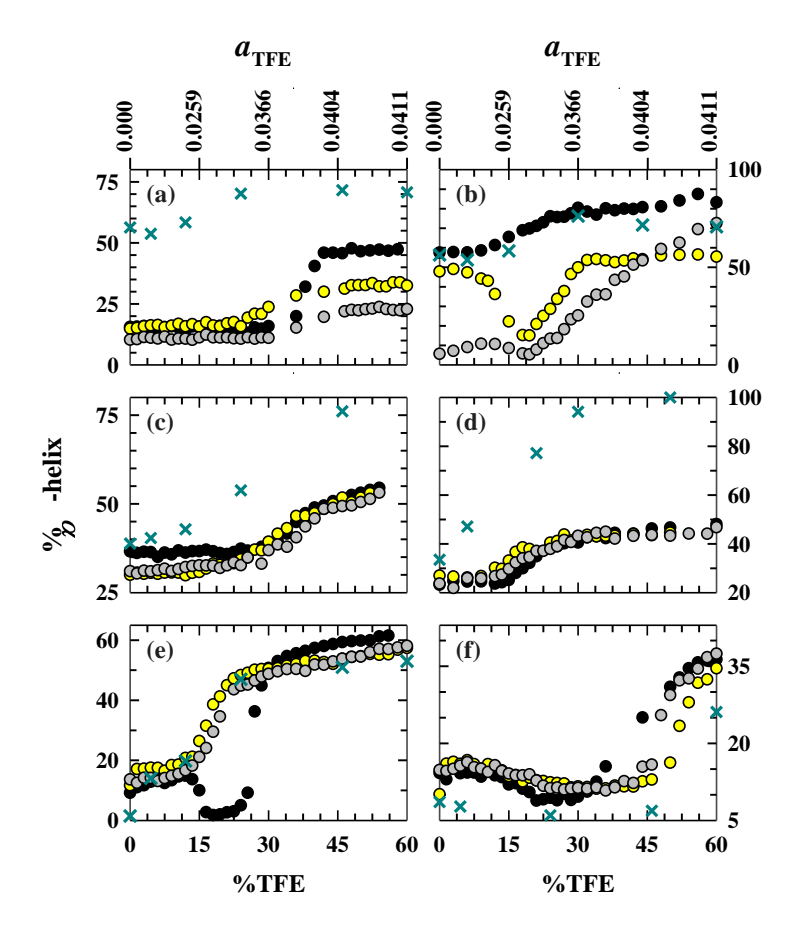


Figure 9. The TFE dependence of % α-helix content estimated from the 207-nm ellipticity. The black, gray, and yellow symbols in each panel correspond to pH values in ascending order: (a) cytochrome c, pH 5.8, 6.8, 7.5, (b) myoglobin, pH 6, 7, 7.7, (c) lysozyme, pH 3.8, 5.1, 6, (d) α-LA, pH 7, 8, 9, (e) β-LG, pH 6, 7, 8, (f) trypsin, pH 7, 8, 9. The symbol × in cyan represent estimations obtained from BeStSelTM. The % α-helix is also listed in Table 1.

in which θ_{207} is the mean residue ellipticity (MRE in deg cm²dmol⁻¹), -4000 is the MRE of β -structure plus random coil at 208 nm, and -33000 is the MRE of α -helical structure of poly-L-lysine. ⁵⁸

Table 1. Structure content in the native and TFE-denatured proteins					
	Heli	x %	β-sheet %	Turn %	Others %
	GF	BeStSel TM			
Native	15	56	34	0	10
Denatured	48	71	29	0	0
Native*	57	70			
Denatured	83	99	1		
Native	37	39	24	11	26
Denatured	55	76			
Native	23	33	44	23	
Denatured	50	82	18		
Native	9	2	28	13	57
Denatured	61	53	43	4	0
Native	14	9	20	13	58
Denatured	37	26	34	7	33
	Native Denatured Native* Denatured Native Denatured Native Denatured Native Denatured Native Denatured Native	Heli GF Native 15 Denatured 48 Native* 57 Denatured 83 Native 37 Denatured 55 Native 23 Denatured 50 Native 9 Denatured 61 Native 14	Helix % GF BeStSel TM	Helix % β-sheet % GF BeStSel TM Native 15 56 34 Denatured 48 71 29 Native* 57 70 70 Denatured 83 99 1 Native 37 39 24 Denatured 55 76 Native 23 33 44 Denatured 50 82 18 Native 9 2 28 Denatured 61 53 43 Native 14 9 20	Helix % β-sheet % Turn % GF BeStSel TM Native 15 56 34 0 Denatured 48 71 29 0 Native* 57 70 70 70 70 Denatured 83 99 1 11 Native 37 39 24 11 Denatured 55 76 76 Native 23 33 44 23 Denatured 50 82 18 Native 9 2 28 13 Denatured 61 53 43 4 Native 14 9 20 13

^{*} The myoglobin sequence shows the occurrence of 121 of 153 residues in α -helical stretches; this should account for ~80% helix content.

3.3.5. Accumulation of structural intermediate in TFE

The large extent of data allows for a qualitative comparison of the tertiary and secondary structure transition curves of the protein under given conditions of solvent and pH. Figure 10 samples some of the transition curves showing that tertiary structure unfolding and secondary structure denaturation are clearly distinct and separated along the TFE scale for all proteins studied. The observation of two non-superimposable transitions determined by two different probes is a classic criterion for the accumulation of an unfolding intermediate. ⁶⁰The separation of fluorescence and CD curves for β -LG appears a bit less clear (Figure 10e) due to the rider of dimer to monomer dissociation already mentioned above. Since the separation of the tertiary and secondary structure probes is distinct, we suggest that TFE unfolding universally populates a structural intermediate I whose tertiary structure is largely disrupted but the secondary structure persists. The intermediate denatures with higher TFE to produce a denatured state D that contains excess α -helical structure. We suggest that the equilibrium mechanism of TFE unfolding of globular proteins can be generically given by the minimal three-state scheme

$$N \stackrel{K_1}{===} I \stackrel{K_2}{===} D$$

Additional intermediates can be accommodated depending on observations and interpretations in a protein specific manner.

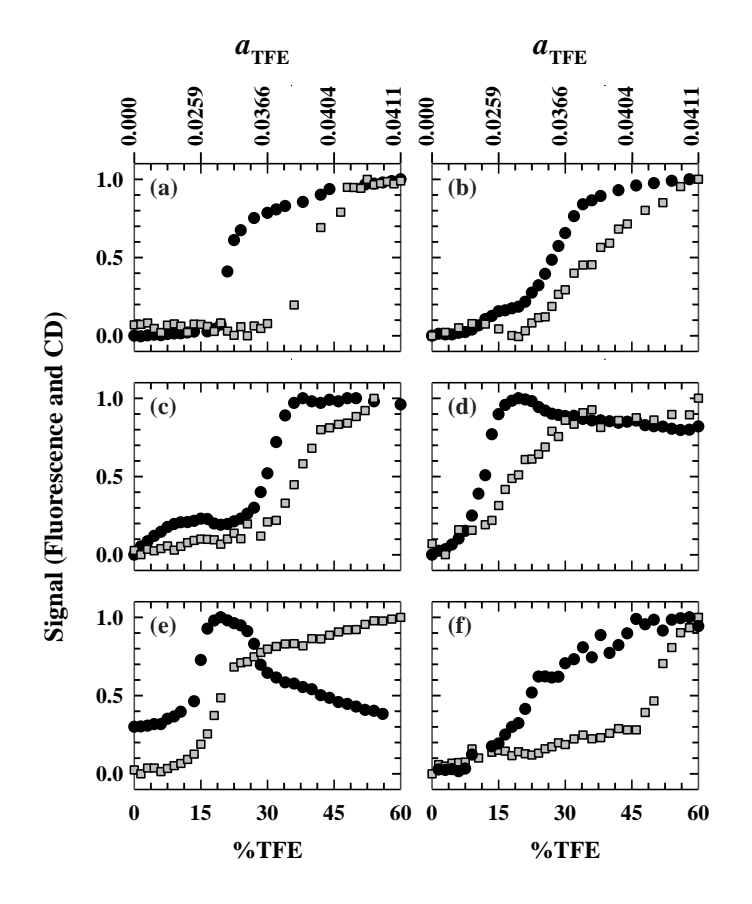


Figure 10. The separation of tertiary structure unfolding transition (circle in black) from secondary structure denaturation transition (square in gray) along the TFE scale: (a) cytochrome c, pH 5.8, (b) myoglobin, pH 7, (c) lysozyme, pH 5.1, (d) α -LA, pH 8, (e) β -LG, pH 7, (f) trypsin, pH 9. The activity of TFE (a_{TFE}) is scaled on top of each row.

3.3.6. Free energy of unfolding and denaturation

The estimation of thermodynamic parameters characterizing TFE unfolding of proteins is fraught with large errors in observables possibly due to aggregation tendency of TFE, frequent lack of well-defined baselines, and the dearth of practical knowledge of the applicability of the empirical 'Pace procedure' to two-component water-alcohol solvent denaturation. We therefore invoke the Wyman's binding polynomial function in conjunction with multicomponent solution theory model championed by Schellman. 61–63 It has also been suggested earlier that the protein-alcohol interaction is best modelled by the preferential exclusion of alcohol from the protein surface. 64,65 Briefly, denoting water, protein, and TFE by components 1, 2, and 3, respectively, the free energy of protein conformational transitions brought about by the water—TFE cosolvent system can be calculated by

$$\Delta G_{\rm U} = \mu_2^{\rm I} - \mu_2^{\rm N}$$

$$\Delta G_{\rm D} = \mu_2^{\rm D} - \mu_2^{\rm I}, \eqno(2)$$

where μ_2^N , μ_2^I , and μ_2^D are chemical potentials of the protein with respect to the native (N), the unfolded intermediate (I), and the denatured TFE state (D). As detailed in several earlier work on protein-cosolvent interaction, ^{59,65,66} the change in the free energy is calculated by

$$\Delta G = -RT \left(\frac{\partial \ln K}{\partial \ln a_3}\right)_{m_2},\tag{3}$$

where $a_3 = a_{TFE}$ is the activity of TFE, K is the equilibrium constant for the $N \rightleftharpoons I$ or $I \rightleftharpoons U$ transition, and m_2 is the molal concentration of the protein.

To extract the values of K, both pre- and post-transition baselines of the transitions (Figure 10) were assumed to be linear in $a_{\rm TFE}$

$$S(a_{\rm TFE}) = S^{\rm o} + ma_{\rm TFE}, \tag{4}$$

in which S denotes the observed baseline signal, S^o is the value of S in water, and m is the slope of the baseline. Figure 11 a, b shows the baselines for the $N \rightleftharpoons I_1$ and $I_1 \rightleftharpoons I_2$ transitions of myoglobin observed by fluorescence alone (Figure 10b). The baseline generation is somewhat burdensome, especially when the quality of data is poor. Since invocation of a second order polynomial results in large errors, the pre-transition baseline for the fluorescence transition of lysozyme (Figure 10c), was calculated by using data in the 18 to 24% TFE range. The S^o and m-values are used to calculate K by

$$K = \frac{S_{\text{obs}} - (S_{\text{pre}}^{\text{o}} + m_{\text{pre}} a_{\text{TFE}})}{(S_{\text{post}}^{\text{o}} + m_{\text{post}} a_{\text{TFE}}) - S_{\text{obs}}},$$
[5]

where $S_{\rm obs}$ is the observed signal at a given value of $a_{\rm TFE}$, $S_{\rm pre}^{\rm o}$ and $S_{\rm post}^{\rm o}$ refer to intercept signal values corresponding to pre- and post-transition baselines, and $m_{\rm pre}$ and $m_{\rm post}$ are the respective slopes. The $\ln K$ vs $\ln a_{\rm TFE}$ plots for the proteins under conditions indicated are produced in Figure 11 and the ΔG values are listed in Table 2.

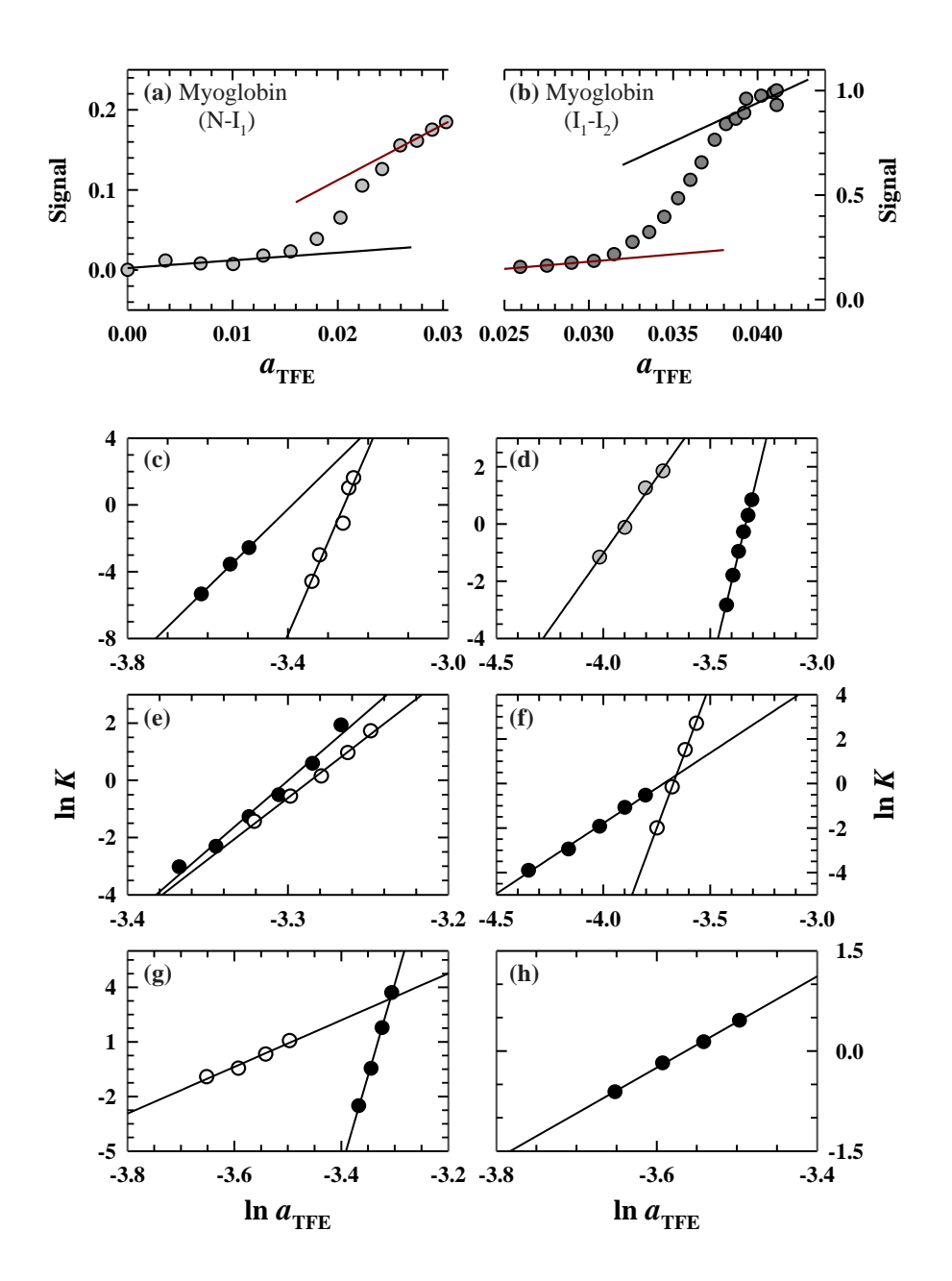


Figure 11. (a,b) Calculation of baselines for N, I_1 , and I_2 states of myoglobin (N \rightleftharpoons $I_1 \rightleftharpoons I_2$) detected by fluorescence. The baseline corresponding to the I-state (in red) acts as the post transition baseline for N \rightleftharpoons I_1 and pretransition baseline for $I_1 \rightleftharpoons I_2$. Double natural logarithm plots are shown for cytochrome c, pH 5.8 (c), myoglobin, pH 7 (d), lysozyme, pH 5.1 (e), α -LA, pH 8 (f), β -lactoglobulin, pH 7 (g), and trypsin, pH 9 (h). The data points in solid black correspond to the N \rightleftharpoons I transition, and those shown by empty circles correspond to the I \rightleftharpoons D transition. The free energy values calculated are listed in Table 2.

Table 2. Free energy ΔG (kcal mol⁻¹) of TFE-induced unfolding and denaturation

pН	Charge	unfolding (fluorescence)	Denaturation (CD ₂₀₇)
5.8	+12	13.8(±1.0)	32.7(±3.5) 14.4(±1.1)
7.0	+4.8	6.3(±0.5)*	14.4(±1.1) -
	10.5		27.7(.10)
		,	25.5(±1.0)
	-9.5	$3.9(\pm 0.5)$	15.3(±1.0)
		` '	5.0(±0.5)
7.0	-8.7	59.4(±2.0)	$7.7(\pm 0.3)$
9.0	-11.4	$4.1(\pm 0.5)$	_
	7.5 7.0 5.1 8.0 9.0 7.0	5.8 +12 7.5 +8.8 7.0 +4.8 5.1 +10.5 8.0 -9.5 9.0 -15.4 7.0 -8.7	$5.8 + 12$ $13.8(\pm 1.0)$ $7.5 + 8.8$ $17.4(\pm 0.6)$ $7.0 + 4.8$ $6.3(\pm 0.5)^*$ $18.2(\pm 1.0)^{**}$ $5.1 + 10.5$ $28.6(\pm 2.0)$ $8.0 - 9.5$ $3.9(\pm 0.5)$ $9.0 - 15.4$ $3.0(\pm 0.2)$ $7.0 - 8.7$ $59.4(\pm 2.0)$

 $^{^*}N \rightleftharpoons I_1, **I_1 \rightleftharpoons I_2$

Because the modes of action of alcohol and chaotropes like urea and guanidine hydrochloride on protein are different, the ΔG values found from our TFE experiments are not expected to match those that are obtained from denaturation experiments using the latter two.^{67,68} A partial list of folding free energy of proteins determined from chaotrope denaturation of the proteins is given in Table 3. In the present study, however, the increase in ΔG for TFE unfolding (N \rightleftharpoons I) of cytochrome c with pH (Table 2) is due to increasing stability of the protein.⁶⁹Likewise, the decrease in ΔG for the unfolding (N \rightleftharpoons I) of α -LA arises from decreasing stability of the protein as the pH increases from 8 to 9.⁷⁰The results reveal that TFE acts on proteins as other denaturants such as GdnHCl and urea do; the measured value of ΔG changes commensurate with the stability of the protein. Yet, the ΔG values for the TFE-induced denaturation process (I \rightleftharpoons D) are not straightforward to interpret because this process largely reflects α -helical propensity rather than secondary structure

Table 3. Unfolding free energy from urea and GdnHCl unfolding of proteins

Protein	рН	Temp (°C)	ΔG (kcal mol ⁻¹)	Ref
Cytochrome c	6.0	25	7.55 ± 0.32	F. Ahmed et al. (1994) J. Biochem. 115,322-327.
	7.0	25	9.30 ± 0.30	D. Ramakrishna (2016) Unpublished
Myoglobin	6.0	25	9.50	C.N. Pace, K.E. Vanderburg (1979)Biochemistry 18, 288-292.
	7.0	25	7.6	F. Ahmad, C.C Bigelow (1982) J. Biol.Chem. 257, 12935–12938.
Lysozyme	3.0	25	5.92±0.08	F. Ahmad et al (1994) J. Biochem. 115, 322-327.
	5.0	25	9.0	F. Ahmad et al (1983) J Biol. Chem. 258, 7960-7963.
α-Lactalbumin	7.0	25	7.29 ± 0.11	M. Mizuguchi et al (2002) Proteins 49,95-103.
β-Lactoglobulin	6.0	25	11.5 ± 0.5	L. D'alfonso et al (2005) Proteins 58,70-79.
	7.0	20	6.62	D. Trofimova et al (2004) Langmuir 20,5544-5552.
Trypsin	7.0	25	7.2 ± 0.4	L.C. Ma, S. Anderson (1997) Biochemistry 36, 3728-3736.
	7.5	22	14.17	H. Outzen et al (1996) Comp. Biochem.Physiol. 115, 33-45.

3.4. Discussion

3.4.1. Obligate unfolding intermediate in TFE denaturation of proteins under neutral pH

The salient finding of this work is the general minimal $N \rightleftharpoons I \rightleftharpoons D$ model, where I is a structural intermediate whose tertiary structure is largely unfolded by TFE. The intermediate acquires additional α -helices at higher TFE to transform to a denatured state, often called the TFE state. Even though the experimental database used to project the general intermediate is small, the depth of the data clearly establishes the provision for the intermediate. To what extent the intermediate I populates depends on the protein species and the solvent conditions that regulate its stability. While the widely separated $N \rightleftharpoons I$ and $I \rightleftharpoons D$ transitions of cytochrome c at pH 5.8 and trypsin at pH 9.0 (Figure $10a_s f$) depict the emergence of the fully populated intermediates, relatively reduced resolution of the transitions for myoglobin, lysozyme, and α -LA (Figure 10b-d) suggests that the intermediate may populate to a lesser extent.

Simple qualitative footings can be provided to project the $N \rightleftharpoons I \rightleftharpoons D$ model. It is thought that TFE deploys the fluoromethyl–CF₃ group to weaken the hydrophobic patches of the protein. ^{16,19,25}It is also likely that TFE penetrates into the interior of globular proteins as hydrophobic alcohols do, ^{71,72}in which case both the energetic cost of burying the slightly negatively charged –CF₃ group in the low dielectric interior and the interactions between –CF₃ and hydrophobic patches of the protein will effectively unfold the tertiary structure. This is the expected occurrence irrespective of the details of the content and the type of secondary structure in the protein, and the outcome is the population of the intermediate I lacking tertiary structure. We suggest that the formation of I is conducive to additional helix induction in the I \rightleftharpoons D step.

The above argument warrants further discussion. The first point pertains to the protein-TFE interactions even though the details of the interactions are still open to investigation. It is believed that there are a few easily accessible high-affinity binding sites on the protein surface [22,23] to which alcohols may bind directly by H-bonding and van der Waals interactions [73]. Such interactions are visualized in Figure 12 produced by docking TFE to two crystal structures of lysozyme. This high-affinity surface binding of alcohol can perturb the intraprotein interactions facilitating access of alcohol molecules to the protein interior. When the alcohol bears a charge, as does TFE by virtue of half a unit of negative charge on the fluorines- $CF_3^{\delta-}$, its access to the low dielectric apolar interior of the protein is energetically expensive, which is the reason for low-affinity binding of charged alcohols to the inner hydrophobic patches. The TFE binding results in a gain of protein entropy and hence an increase in the number of degrees of freedom, leading to unfolding of tertiary conformation.

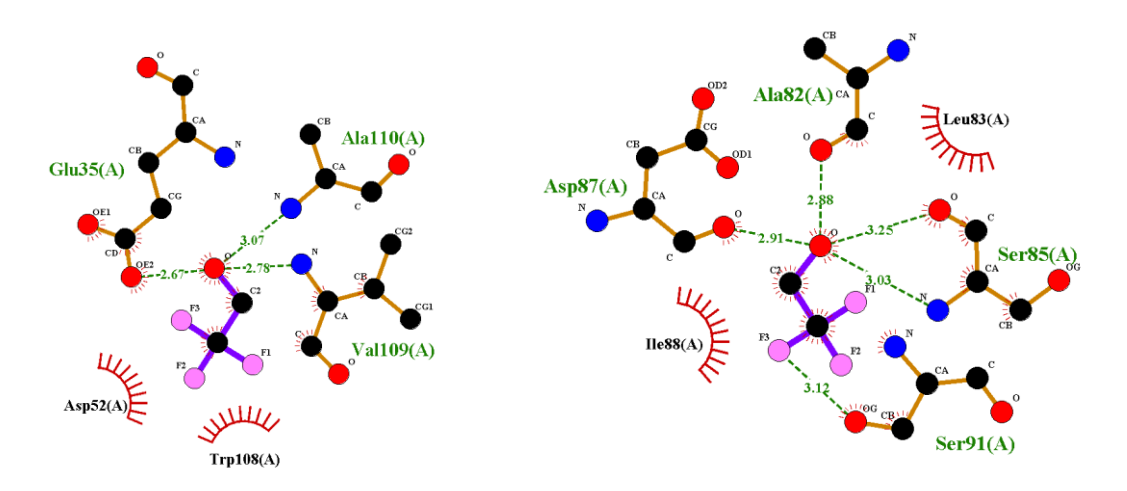


Figure 12.A cartoon of hypothetical TFE binding sites in two structures of lysozyme. *Left*, structure 1DPX: the side chain of Glu35 and the main chain nitrogens of Val109 and Ala110 form H-bonds with TFE. Additionally, Asp52 and Trp108 establish hydrophobic interactions with TFE. *Right*, structure 2WUN: main chain carbonyls of Asp87, Ala82, and Ser85, and the side chain carbonyl of Ser 91 form H-bonds with TFE. A putative H-bond also exists between

the side chain carbonyl of Ser91 and one of the partially negatively charged fluorines of TFE. Hydrophobic interactions between TFE and Leu8 and Ile88 are also shown.

The second point concerns the aftermath of the tertiary structure unfolding, guiding to the formation of the TFE state that has α -helices in excess of that of the native state. Again, there are inconsistencies among suggested factors that favour α -helical structuration of the TFE state. For example, the idea that intrinsically high α -helical propensity arises from pre-existing α -helical regions of the native state^{7,12,56} is inconsistent with observations that native states containing predominantly β -sheet structures are also transformed to the TFE state under equilibrium conditions¹⁷ as well as in kinetic refolding. ^{17,74–78} Evidences appear to suggest that helical propensity arises predominantly from local helical interactions. ^{16,17,79} Limited experimental results also imply that the TFE state is formed irrespective of whether the primary structure of a protein has sequence propensity to form α -helices or not. However, intricate the process of helix induction could be, the unfolding of the protein tertiary structure is a prerequisite⁸⁰ and perhaps a sufficient condition for TFE-induced acquisition of extra α -helices.

3.4.2. *Is the TFE intermediate similar to the MG state?*

The discovery of the molten globule state^{40,81,82} also called the third thermodynamic state distinct from the native and unfolded states, was so imposing that many studies took it as an inspiration to look for the MG state in the presence of solvent additives. Since the MG states are easily formed at pH extremes, some TFE-protein studies have been selectively carried out at acid pH and the results interpreted as TFE stabilization of MG states.^{48,83,84} The invocation of the MG state in this context has however been hardly helpful. Closer examination of results, as found in references^{48,50} for example, would reveal that TFE interacted proteins

often lack the rigor of properties used to define the molten globule state. It has indeed been pointed out earlier that TFE-induced protein states are different from the equilibrium molten globule state.¹⁷ Further, there are instances where acid molten globule is not found to populate in the presence of TFE.⁴⁹

A direct dismissal of MG in TFE-induced protein denaturation is suggested by the experimental data and the simpleN \rightleftharpoons I \rightleftharpoons D model of this study. We list the basic characteristics of the MG state and specify how it differs from the intermediate (I) or the TFE state (D). One, the MG state is compact by definition and hence is largely fluorescence-quenched. The states I and D however contain unfolded tertiary structure and are largely fluorescent (Figures 3,10), suggesting their non-MG character. Two, the canonical near-UV CD signal of MG is weak, but one detects no near-UV CD strength in any of the TFE-transformed proteins (Figure 3). Three, the MG state is described to have native-like secondary structure, which is not the case for the TFE state (D) that contains excess of α -helical structure (Figure 9).

Finally, even if a remotely related molten globule state stabilized by TFE is considered, its placement in the TFE-induced unfolding pathway would appear less realistic in the light of results with various globular proteins that imply that molten globules could actually be unproductive off-pathway species.^{85–90}

Reports have also appeared that organic solvents, dimethyl sulfoxide and hexafluoroacetone hydrate for example, promote MG states. 91,92 Although credited for the rigor of a large body of such work, it will be worth scrutinizing the properties of the proposed intermediates to ascertain whether they are MGs, MG-like, closer to MG, or not MG.

3.4.3. Beyond the three-state model of TFE unfolding

It is suggested that the $N \rightleftharpoons I \rightleftharpoons D$ scheme is the minimal model for protein denaturation with TFE. The results obtained for holomyoglobin (Figures 3e-g, 8d-f)also indicates the scope for stabilization of additional intermediates at low TFE, and we extend the three-state model to $N \rightleftharpoons I_1 \rightleftharpoons I_2 \rightleftharpoons D$, where I_1 is a stable intermediate whose tertiary structure is unfolded to a lesser extent. Incidentally, this is an important result by itself because unfolding intermediates of holomyoglobin at neutral pH has not been hitherto reported. Similarly, the incorporation of the native dimer \rightleftharpoons monomer dissociation equilibrium of β -lactogobulin (Figures 3m-o, 8m-o) yields the denaturation scheme $N_{Dimer} \rightleftharpoons N_{Monomer} \rightleftharpoons I \rightleftharpoons D$. The TFE-induced dimer to monomer dissociation has also been described recently for the protein superoxide dismutase. 93 These examples suggest that TFE acts as a general denaturant, even though it disrupts hydrophobic surfaces by the solvent exclusion mechanism 23,65 unlike urea and GdnHCl that establish poly functional interactions with no regard to the type of amino acids $^{94-98}$

3.5. Conclusions and prospect

TFE denatures proteins by interacting with a few high-affinity binding sites on the surface of the native state N followed by low-affinity binding to hydrophobic regions in the protein interior. The internalization of TFE is energetically expensive because of partial charges on the fluorines of the $-CF_3$ group. This energy cost also contributes to entropy increase and unfolding of the tertiary structure. We have called this unfolded state a universal intermediate I populated in relatively low TFE-containing aqueous medium. The unfolded tertiary structure intricately guides the intermediate to acquire additional α -helices in the presence of higher TFE to yield the TFE state. Since the TFE state is not native and still contains α -helical structures in excess, we have called this a general TFE-denatured state D. The TFE

denaturation of all globular proteins under neutral pH conditions can be described by the minimal three-state model $N \rightleftharpoons I \rightleftharpoons D$. Occasionally, additional intermediates with respect to the extent of unfolding of the tertiary structure may also accumulate. The study opens up avenues for structural characterization of the putative intermediates.

3.6. References

- 1. Goodman, M; Rosen, I. G. Conformational aspects of polypeptide structure XVI. Rotatory constants, cotton effects, and ultraviolet absorption data for glutamate oligomers and co-oligomers. *Biopolymers* **1964**, *2*, 537-559.
- 2. Tamburro, A. M.; Scatturin, A.; Rocchi, R.; Marchiori, F.; Borin, G.; Scaffone, E. Conformational transitions of bovine pancreatic ribonuclease S-petide. *FEBS Lett.* 1 **1968**, 298-300.
- 3. Brown, J.E.; Klee, W.A. Helix-coil transition of the isolated amino terminus of ribonuclease. *Biochemistry* **1971**, *10*, 470-476.
- 4. Liebes, L. F.; Zand, R.; Phillips, W. D. Solution behaviour, circular dichroism and 220 MHz NMR studies of the bovine myelin basic protein. *Biochim. Biophys. Acta* **1975**, *405*, 27-39.
- 5. Marquesee, S.; Baldwin, R. L. Helix stabilization by Glu⁻···Lys⁺ salt bridges in short peptides of de novo design. *Proc. Natl. Acad. Sci.* **1987**, *84*, 8898-8902.
- 6. Lehrman, S. R.; Tuls, J. L.; Lung, M. Peptide α -helicity in aqueous trifluoroethanol. Correlations with predicted α -helicity and the secondary structure of the corresponding regions of bovine growth hormone. *Biochemistry* **1990**, *29*, 5590-5596.
- 7. Segawa, S-I.; Fukuno, T.; Fujiwara, K.; Noda, Y. Local structures in unfolded lysozyme and correlation with secondary structure in the native conformation. *Biopolymers* **1991**, *31*, 497-509.
- 8. Yang, J. J.; Buck, M.; Pitkeathly, M.; Kotik, M.; Haynie, D. T.; Dobson, C. M.; Radford, S. E. Conformational preferences of four peptides spanning the sequence pf hen lysozyme. *J. Mol. Biol.* **1995**, 252, 485-491.

- 9. Storrs, R. W.; Truckses, D.; Wemmer, D. E. Helix propagation in trifluoroehanol solutions. *Biopolymers* **1992**, *32*, 1695-1702.
- 10. Jasanoff, A.; Fersht, A.R. Quantitative determination of helical propensities from trifluoroethanol titration curves. *Biochemistry* **1994**, *33*, 2129-2135.
- 11. Rohl, C. A.; Chakrabartty, A.; Baldwin, R. L. Helix propagation and N-cap propensity of the amino acids measured in alanine-base peptides in 40 volume percent trifluoroethanol. *Protein Sci.* **1996**, *5*, 2623-2637.
- 12. Luo, P.; Baldwin, R. L. Mechanism of helix induction by trifluoroethanol: a framework for extrapolating the helix-forming properties of peptides from trifluoroethanol-water mixtures back to water. *Biochemistry* **1997**, *36*, 8413-8421.
- 13. Myers, J. K.; Pace, C. N.; Scholtz, J. M. Trifluoroethanol effects on helix propensity and electrostatic interactions in the helical peptide from ribonuclease T1. *Protein Sci.* **1998**, *7*, 383-388.
- 14. Mizuno, K.; Kaido, H.; Kimura, K.; Miyamoto, K.; Yoneda, N.; Kawabata, T.; Tsurusaki, T.; Hashizume, N.; Shindo, Y. Studies of the interaction between alcohols and amides to identify factors in the denaturation of globular proteins in halogenalcohol + water mixtures. *J. Chem. Soc. Soc. Faraday Trans. I.* **1984**, *80*, 879-984.
- 15. Nelson, J. W.; Kallenbach, N. R. Stabilization of the ribonuclease S-peptide α -helix by trifluoroethanol. *Proteins: Struct. Funct. Genet. I.* **1986**, 211-217.
- 16. Thomas, P. D.; Dill, K. A. Local and non-local interactions in globular proteins and mechanism of alcohol denaturation. *Protein Sci.* **1993**, *2*, 2050-2065.
- 17. Shiraki, K.; Nishikawa, K.; Goto, Y. Trifluoroethanol-induced stabilization of the α -helical structure of β -lactoglobulin: implication for non-hierarchical protein folding. *J. Mol. Biol.* **1995**, 245, 180-194.
- 18. Cammers-Goodwin, A.; Allen, T. J.; Oslick, S. L.; McClure, K. F.; Lee, J. H.; Kemp, D. S. Mechanism of stabilization of helical conformations of polypeptides by water containing trifluoroethanol. *J. Am. Chem. Soc.* **1996**, *118*, 3082-3090.
- 19. Rajan, R.; Balaram, P. A model for the interaction of trifluoroethanol with peptides and proteins. *Int. J. Peptide Protein Res.* **1996**, *48*, 328-336.
- 20. Kentsis, A.; Sosnick, T. R. Trifluoroethanol promotes helix formation by destabilizing backbone exposure: desolvation rather than native hydrogen bonding defines the kinetic pathway of dimeric coiled coil folding. *Biochemistry* **1998**, *37*, 14613-14622.

- 21. Roccatano, D.; Colombo, G.; Fioroni, M.; Mark, A. E. Mechanism by which 2,2,2-trifluoroethanol/water mixtures stabilize secondary-structure formation in peptides: a molecular dynamics study. *Proc. Natl. Acad. Sci U. S. A.* **2002**, *99*, 12179-12184.
- 22. Ghuman, J.; Zunszain, P. A.; Petipas, I.; Bhattacharya, A. A.; Otagiri, M.; Curry, S. Structural basis of the drug-binding specificity of human serum albumin. *J. Mol. Biol.* **2005**, *353*, 38-52.
- 23. Chong, Y.; Kleinhammes, A.; Tang, P.; Yan, X.; Yue, W. Dominant alcohol-protein interaction via hydration enabled enthalpy-driven binding mechanism. *J. Phys. Chem. B* **2015**, *119*, 5367-5375.
- 24. Mahanta, D.; Jana, M. Can 2,2,2-trifluoroethanol be an efficient protein denaturant than methanol and ethanol under thermal stress. *Phys. Chem. Chem. Phys.* **2018**, *20*, 9886-9896.
- 25. Albert, J. S.; Hamilton, A. D. Stabilization of helical domains in short peptides using hydrophobic interactions. *Biochemistry* **1995**, *34*, 984-990.
- 26. Blanco, F. J.; Ortiz, A. R.; Serrano, L. Role of a non-native interaction in the folding of the protein G B₁ domain as inferred from the conformational analysis of the α -helix fragment. Folding & Design 1997,2, 123-133.
- 27. Demarest, S. J.; Fairman, R.; Raliegh, D. P. Peptide models of local and long-range interactions in the molten globule state of human α -lactalbumin. *J. Mol. Biol.* **1998**, 283, 279-291.
- 28. Chatterjee, C.; Gerig, J. T. Interactions of trifluoroethanol with the Trp-Cage peptide. *Biopolymers* **2007**, 87, 115-123.
- 29. Greff, D.; Fermandijan, S.; Fromageot, P.; Khosla, M. C.; Smeby, R. R.; Bumpus, F. M. Circular-dichroism spectra of truncated and other analogs of angiotensin II. *Eur. J. Biochem.* **1976**, *61*, 297-305.
- 30. Siligardi, G.; Drake, A. F.; Mascagni, P.; Neri, P.; Lozzi, L.; Niccolai, N.; Gibbons, W.A. Resolution of conformational equilibria in linear peptides by circular dichroism in cryogenic solvents. *Biochem. Biophys. Res. Commun.* **1987**, *143*, 1005-1011.
- 31. Mabrouk, K.; Rietschoten, Van J.; Rochat, H.; Loret, E.P. Correlation of antiviral activity with beta-turn types for V3 synthetic multibranched peptides from HIV-1 gp120. *Biochemsitry* **1995**, *34*, 8294-8298.

- 32. Riersen, H.; Rees, A. R. Trifluoroethanol may form a solvent matrix for assisted hydrophobic interactions between peptide side chains. *Protein Eng.* **2000**, 13, 739-743.
- 33. Blanco, F. J.; Jiménez, M. A.; Pineda, A.; Rico, E.; Santoro, J.; Nieto, J. L. NMR solution structure of the isolated N-terminal fragment of protein G B₁ domain. Evidence of trifluoroethanol induced native-like β-hairpin formation. *Biochemistry* **1994**, *33*, 6004-6014.
- 34. Santiveri, C. M.; Pantoja-Uceda, D.; Rico, M.; Jiménez, M. A. Beta-hairpin formation in aqueous solution and in the presence of trifluoroethanol: a ¹H and ¹³C nuclear magnetic resonance conformational study of designed peptides. *Biopolymers* **2005**, *79*, 150-162.
- 35. Kortemme, T.; Ramírez-Alvarado, M.; Serrano, L. Design of a 20-amino acid, three-stranded β -sheet protein. *Science*. **1998**, 281, 253-256.
- 36. Yang, J. J.; Pitkeathly, M.; Radford, S. E. Far-UV CD reveals a conformational switch in a peptide fragment from the β -sheet of hen lysozyme. *Biochemistry* **1994**, *33*, 7345-7353.
- 37. Buck, M.; Schwalbe, H.; Dobson, C. M. Characterization of conformation preferences in a partly folded protein by heteronuclear NMR spectroscopy: assignment and secondary structure analysis of hen egg-white lysozyme in trifluoroethanol. *Biochemistry* **1995**, *34*, 13219-13232.
- 38. Shibata, A.; Yamamoto, M.; Yamashita, T.; Chiou, J-S.; Kamaya, H.; Ueda, I. Biphasic effects of alcohols on the phase transition of poly(L-lysine) between α -helix and β -sheet conformations. *Biochemistry* **1992**, *31*, 5728-5733.
- 39. Dolgikh, D. A.; Gilmanshin, R. I.; Brazhnikov, E. V.; Bychkova, V.E.; Semisotnov, G. V.; Venyaminov, S. Y.; Ptitsyn, O.B.α-lactalbumin: compact state with fluctuating tertiary structure. *FEBS Lett.* **1981**, *136*, 311-315.
- 40. Ohgushi, M.; Wada, A. 'Molten globule state': a compact form of globular proteins with mobile side-chains. *FEBS Lett.* **1983**, *164*, 21-24.
- 41. Ikeguchi, K.; Kuwajima, K.; Mitani, M.; Sugai, S. Evidence for identity between the equilibrium unfolding intermediate and a transient folding intermediate: a comparative study of the folding reactions of α -lactalbumin and lysozyme. *Biochemistry* **1986**, 25, 6965-6972.
- 42. Kuwajima, K. The molten globule state as a clue for understanding the folding and coopertivity of globular-protein structure. *Proteins* **1989**, *6*, 87-103.

- 43. Jennings, P. A.; Wright, P. E. Formation of a molten globule intermediate early in the kinetic folding pathway of apomyoglobin. *Science* **1993**, *262*, 892-896.
- 44. Ptitsyn, O. B.; Molten globule and protein folding. Adv. Protein Chem. 1995, 47, 83-229.
- 45. Wolynes, P. G.; Onuchic, J. N.; Thirumalai, D. Navigating the folding routes. *Science* **1995**, 267, 1619-1620.
- 46. Pandey, V. S.; Rokhsar, D. S. Is the molten globule a third phase of proteins. *Proc. Natl. Acad. Sci. USA.* **1998**, *95*, 1490-1494.
- 47. Arai, M.; Kuwajima, K. Role of the molten globule state in protein folding. *Adv. Protein Chem.***2000**, *53*, 209-271.
- 48. Buck, M.; Radford, S. E.; Dobson, C. M. A partially folded state of hen egg-white lysozyme in trifluoroethanol: structural characterization and implication for protein folding. *Biochemistry* **1993**, *32*, 669-678.
- 49. Hoshino, M.; Hagihara, Y.; Yamada, D.; Kataoka, M.; Goto, Y. Trifluoroethanol induced conformational transition of hen egg-white lysozyme studied by small-angle X-ray scattering. *FEBS Lett.* **1997**, *416*, 72-76.
- 50. Gast, K.; Zirwer, D.; Müller-Frohne, M.; Damaschun, G. Trifluoroethanol-induced conformational transitions of proteins: Insights gained from the differences between α -lactalbumin and ribonuclease A. *Protein Sci.* **1999**, 8, 625-634.
- 51. Chitra, R.; Smith, P. E. Properties of 2,2,2-trifluoroethanol and water mixtures. J. *Chem. Phys.* **2001**, *114*, 426-435.
- 52. Barrick, D.; Baldwin, R.L. The molten globule intermediate of apomyoglobin and the process of protein folding. *Protein Sci.* **1993**, *2*,869-876.
- 53. Mercadante, D.; Melton, L. D.; Norris, G. E.; Loo, T.S.; Williams, M. A. K.; Dobson, R. C. J.; Jmeson, G. B. Bovine β-lactroglobulin is dimeric under imitative physiological conditions: dissociation equilibrium and rate constants over the pH range of 2.5–7.5. *Biophys. J.* 2012, 103, 303-312.
- 54. Galani, D.; Apenten, R. K. O. Beta-lactoglobulin denaturation by dissociation-coupled unfolding. *Food Red. Int.* **1999**, *32*, 93-100.
- 55. Singh, R.; Meena, N. K.; Das, T.; Sharma, R. D.; Prakash, A.; Lynn, A. M. Delineating the conformational dynamics of intermediate structures on the unfolding pathway of β-

- lactoglobulin in aqueous urea and dimethyl sulfoxide. *J. Biomol. Struct. Dyn.* **2020**, *38*, 5027-5036.
- 56. Dyson, H. J.; Wright, P. E. Peptide conformation and protein folding. *Curr. Opin. Struct. Biol.* **1993**, *3*, 60–65.
- 57. Culik, R. M.; Abaskharon, R. M.; Pazos, I. M.; Gai, F. Experimental validation of the role of trifluoroethanol as a nanocrowder. *J. Phys. Chem. B* **2014**, *118*, 11451-11461.
- 58. Greenfield, N.; Fasman, G. D. Computed circular dichroism spectra for the evaluation of protein conformation. *Biochemistry* **1969**, *8*, 4108-4116.
- 59. Huda, N.; Hossain, M.; Bhuyan, A. K. Complete observation of all structural, conformational, and fibrillation transitions of proteins at submicellar SDS. *Biopolymers* **2019**, e23255.
- 60. Ikai, A.; Fish, W. W.; Tanford, C. Kinetics of unfolding and refolding of proteins. II. Results for cytochrome *c. J. Mol. Biol.* **1973**, *73*, 165-184.
- 61. Schellman, J. A. Selective binding and solvent denaturation. *Biopolymers* **1987**, *26*, 549-559.
- 62. Schellman, J. A. A simple model for salvation in mixed solvents. Applications to the stabilization and destabilization of macromolecular structures. *Biophys. Chem.* **1990**, *37*, 121-140.
- 63. Schellman, J. A. The relation between the free energy of interaction and binding. *Biophys. Chem.* **1993**, *45*, 273-279.
- 64. Yang, Y.; Barker, S.; Chen, M. J.; Mayo, K. H. Effect of low molecular weight aliphatic alcohols and related compounds on Platelet Factor 4 subunit association. *J. Biol. Chem.* **1993**, *268*, 9223-9229.
- 65. Timasheff, S. N.; Protein-solvent preferential interactions, protein hydration, and the modulation of biochemical reactions by solvent components. *Proc. Natl. Acad. Sci. USA*. **2002**, *99*, 9721-9726.
- 66. Sashi, P.; Yasin, U. M.; Balasubramanian, H.; Usha Sree, M.; Ramakrishna, D.; Bhuyan, A. K. Preferential water exclusion in protein unfolding. *J. Phys. Chem. B* **2014**, *118*, 717-723.
- 67. Ahmad, F. Free energy changes in ribonuclease A denaturation. *J. Biol. Chem.* **1983**, 258, 11143-11146.

- 68. Biswas, B.; Muttathukattil, A. N.; Reddy, G.; Singh, P. C. Contrasting effects of guanidiniun chloride and urea on the activity and unfolding of lysozyme. *ACS Omega* **2018**, *3*, 14119-14216.
- 69. Elove, G. A.; Bhuyan, A. K.; Roder, H. Kinetic mechanism of cytochrome c folding: involvement of the heme and its ligands. *Biochemistry* **1994**, *33*, 6925-6935.
- 70. Griko, Y. V.; Remeta, D. P. Energetics of solvent and ligand-induced conformational changes in α-lactalbumin. *Protein Sci.* **1999**, *8*, 554-561.
- 71. Segawa, S-I.; Sugihara, M. Characterization of the transition state of lysozyme unfolding. I. Effect of protein-solvent interactions on the transition state. *Biopolymers* **1984**, *23*, 2473-2488.
- 72. Buck, M. Trifluoroethanol and colleagues: cosolvents come of age. Recent studies with peptides and proteins. *Q. Rev. Biophys.* **1998**, *31*, 297-355.
- 73. Boer, de J. H. The dynamical character of adsorption (2nd ed. Oxford, UK: Clarendon Press, **1968**).
- 74. Radford, S. E.; Dobson, C. M.; Evans, P. A. The folding of hen lysozyme involves partially structured intermediates and multiple pathways. *Nature* **1992**, *358*, 302-307.
- 75. Liu, Z.-P.; Rizo, J.; Gierasch, L. M. Equilibrium folding studies of cellular retinoic acid binding protein, a predominantly β-sheet protein. *Biochemistry* **1994**, 33, 134-142.
- 76. Kuwajima, K.; Yamaya, H.; Sugia, S. The burst phase intermediate in the refolding of β -lactoglobulin studied by stopped flow circular dichroism and absorption spectroscopy. *J. Mol. Biol.* **1996**, 264, 806-822.
- 77. Hamada, D.; Goto, Y. The equilibrium intermediate of β -lactoglobulin with non-native α -helical structure. *J. Mol. Biol.* **1997**, 269,479-487.
- 78. Arai, M.; Ikura, T.; Semisotnov, G. V.; Kihara, H.; Amemiya, Y.; Kuwajima, K. Kinetic refolding of β -lactoglobulin. Studies by synchrotron X-ray scattering, circular dichroism, absorption and fluorescence spectroscopy. *J. Mol. Biol.* **1998**, 275, 149-162.
- 79. Sivaraman, T.; Kumar, T. K. S.; Yu, C. Destabilization of native tertiary structural interactions is linked to helix induction by 2,2,2-trifluoroethanol. *Int. J. Bio. Macromol.* **1996**, *19*, 235-239.
- 80. Sivaraman, T.; Kumar, T. K. S.; Hung, K. W.; Yu, C. Influence of disulfide bonds on the induction of helical conformation in proteins. *J. Protein Chem.* **1999**, *18*, 481-488.

- 81. Dolgikh, D. A.; Kolomiets, A. P.; Bolotina, I. A.; Ptitsyn, O. B. 'Molten-globule' state accumulates in carbonic anhydrase folding. *FEBS Lett.* **1984**, *165*, 88-92.
- 82. Kuroda, Y.; Endo, S.; Nakamura, H. How a novel scientific concept was coined the "molten globule state". *Biomolecules* **2020**, *10*, 269.
- 83. Alexandrescu, A. T.; Ng, Y-L.; Dobson, C. M. Characterization of a trifluoroethanol-induced partially folded state of α-lactalbumin. *J. Mol. Biol.* **1994**, *235*, 587-599.
- 84. Uversky, V. N.; Narizhneva, N. V.; Kirschstein, S. O.; Winter, S.; Löber, G. Conformational transitions provoked by organic solvents in β-lactoglobulin: can a molten globule like intermediate be induced by the decrease in dielectric constant. *Folding & Design* **1997**, *2*, 163-172.
- 85. Fink, A. L. Oberg, K. A.; Seshadri, S. Discrete intermediates versus molten globule models for protein folding: characterization of partially folded intermediates of apomyoglobin. *Folding & Design* **1997**, *3*, 19-25.
- 86. Nabuurs, S. M.; Westphal, A. H.; Mierlo, van C. P. M. Noncooperative formation of the off-pathway molten globule during folding of the α-β parallel protein apoflavodoxin. *J. Am. Chem. Soc.* **2009**, *131*, 2739-2746.
- 87. Bhuyan, A. K. Off-Pathway Status for the Alkali Molten Globule of Ferricytochrome *c. Biochemistry* **2010**, *49*, 7764-7773.
- 88. Bhuyan, A. K. The Off-pathway Status of the Alkali Molten Globule is Unrelated to Heme Misligation and trans-pH Effects: Experiments with Ferrocytochromec. *Biochemistry* **2010**, *49*, 7774-7782.
- 89. Lindhoud, S.; Westphal, A. H.; Borst, J. W.; Mierlo, van C. P. M. Illuminating the off-pathway nature of the molten globule folding intermediate of an α - β parallel protein. *PLOS One.* **2012**, *7*, e45746.
- 90. Lindhoud, S.; Pirchi, M.; Westphal; Haran, G.; Mierlo, van C. P. M. Gradual folding of an off-pathway molten globule detected at the single molecule level. *J. Mol. Biol.* **2015**, 427, 3148-3157.
- 91. Bhattacharjya, S.; Balaram, P. Effects of organic solvents on protein structures: observation of a structured helical core in hen egg-while lysozyme in aqueous dimethylsulfoxide. *Proteins* **1997**, 29, 492-507.

- 92. Bhattacharjya, S.; Balaram, P. Hexafluoroacetone hydrate as a structure modifier in proteins: characterization of a molten globule state of hen egg-white lysozyme. *Protein Sci.* **1997**, *6*, 1965-1073.
- 93. Niu, B.; Mackness, B. C.; Zitzewitz, J. A.; Matthews, C. R.; Gross, M. L. Trifluoroethanol partially unfolds G93A SOD1 leading to protein aggregation: a study by native mass spectrometry and FPOP protein foot printing. *Biochemistry* **2020**, *59*, 3650-3659.
- 94. Hibbard, L. S.; Tulinsky, A. Expression of functionality of α-chymotrypsin. Effects of guanidine hydrochloride and urea in the onset of denaturation. *Biochemistry*. **1978**, *17*, 5460-5468.
- 95. Makhatadze, G. I.; Privalov, P. L. Protein interactions with urea and guanidinium chloride: a calorimetric study. *J. Mol. Biol.* **1992**, *226*, 491-505.
- 96. Pike, A. C. W.; Acharya, R. Structural basis for the interaction of urea with lysozyme. *Protein Sci.* **1994**, *3*, 706-710.
- 97. Dunbar, J.; Yennawar, H.P.; Banerjee, S.; Luo, J.; Farber, G.K. The effect of denaturants on protein structure. *Protein Sci.* **1997**, *6*, 1727-1733.
- 98. Bhuyan, A. K. Protein stabilization by urea and guanidine hydrochloride. *Biochemistry* **2002**, *41*, 13386-13394.

CHAPTER 4

A Three-State Mechanism for Trifluoroethanol Denaturation of an Intrinsically Disordered Protein (IDP)

Abstract

Relating the amino acid composition and sequence to chain folding and binding preferences of intrinsically disordered proteins (IDPs) has emerged as a huge challenge. While globular proteins have respective 3D structures that are unique to their individual function, IDPs violate this structure-function paradigm because rather than having a well-defined structure an ensemble of rapidly interconverting disordered structures characterize an IDP. This work measures 2,2,2-trifluoroethanol (TFE)-induced equilibrium transitions of an IDP called AtPP16-1 (Arabidospsis thaliana phloem protein type 16-1) by using fluorescence, circular dichroism, infrared, and NMR methods at pH 4, 298 K. Low TFE reversibly removes the tertiary structure to produce an ensemble of obligate intermediate (I) retaining the native-state (N) secondary structure. The I ensemble has higher helical propensity conducive to the acquisition of an exceedingly large level of α -helices by a reversible denaturation transition of I to the denatured state Das the TFE level is increased. Strikingly, it is the same $N \rightleftharpoons I \rightleftharpoons D$ scheme typifying the TFE transitions of globular proteins. The high-energy state I characterized by increased helical propensity is called a universal intermediate encountered in both genera of globular and disordered proteins. Neither I nor D strictly show molten globule (MG)-like properties, dismissing the belief that TFE promotes MGs.

4.1. Introduction

The applications of the amphiphilic alcohol TFE in peptide and protein science include cosolvent engineering of structure and conformation, solubilization and induced folding of insoluble recombinant proteins, conferring desired dynamics to folded states, adding secondary structure propensity, and engineering catalytic activity of enzymes. Many of such applications were recognized soon after the seminal introduction of TFE to study conformations of polypeptide oligomers and co-oligomers², leading to a large volume of reports on TFE-induced helix formation, $^{3-5}\alpha$ -helical propensity, $^{6-14}$ conformational transitions, $^{14,15-25}$ hydrophobic assembling and disassembling, $^{20, 26-29}$ stabilization of β -type secondary structures, 30-36 helix-coil transition, 18 and transitions from one to another type of secondary structure, ^{18, 37–39} of proteins. One may note that the number of reports on the TFEprotein system rose sharply during 80's and 90's of the concluded century and receded thereafter. Many questions remained unanswered however, the most important one being the mechanism of TFE-induced protein transitions. For example, one was not sure if the transition is a two- or a three-step process, and whether a species like molten globule (MG) is promoted by TFE. Fewer studies of recent years nonetheless have continued to examine TFE interaction with globular proteins, 1,22,24,25,29,33,35 and have included sundry topics such as the properties of TFE-water mixtures⁴⁰ and nanocrowding effect of TFE on protein surroundings.41

All studies referenced above provide results for globular proteins alone, and the key understanding emanating is the induction of high helical propensity by TFE with no regard to the content and extent of secondary structure elements in the initial native state. As a result, the final denatured state D at high TFE, also called the TFE-state by some, contains α -helices specifically in excess of that in the native state. This dogma can also be stated by including a

generic tertiary unfolded intermediate, such that a minimal three-state mechanism $N \rightleftharpoons I \rightleftharpoons$ Dis applicable to TFE denaturation of globular proteins.

On the other hand, little has been learned on the TFE interaction with IDP. This should be an important problem not merely because IDPs account for about a half of cellular proteins in the eukaryotic proteome, but principally due to a host of characteristics surrounding the amino acid composition and sequence^{42–45}, the disordered regions and the conformers, and the overall size of them. 46–49 Unlike a well-defined 3D structure of a globular protein, the IDP chain folds poorly to produce an ensemble of rapidly interconverting conformers containing disordered regions. It is of interest to know how TFE approaches the ensemble of structures, whether TFE binding causes folding of certain segments unlike the initial tertiary structure unfolding of globular proteins, 50 and how the overall denaturation transitions of the two protein genera are different.

This work measures the TFE-induced transitions of the IDP AtPP16-1 in the 0–60% (v/v) range of aqueous TFE at pH 4.1, 298(±1) K, by using basic spectroscopic methods. The IDP whose solution NMR structure was determined by us⁵¹has only ~19% of the residues in secondary structure regions – an α -helix (residues 96–105) and three antiparallel β -strands, β I (residues 3–9), β II (residues 56–62), and β III (residues 133–135). Many surface overhangs arising from side chains and disordered regions are observed, and the conspicuous disordered region appears as a lobe (residues 10–55) straddling strands β I and β II (Fig. 1). The IDP undergoes reversible transitions according to the N \rightleftharpoons I \rightleftharpoons D scheme generalized for globular proteins. The species I of the IDP chain ensemble is a high-energy tertiary unfolded intermediate that denatures to the helix-rich D state. It would appear that TFE is indifferent to the chain residue characteristics and surface irregularities of the protein.

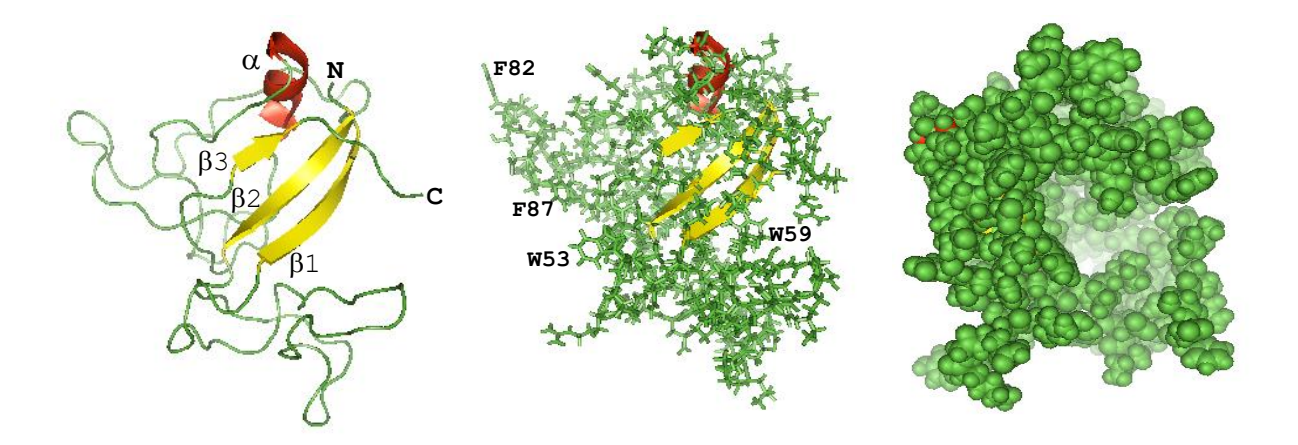


Figure.1. From *left* to *right*: a ribbon diagram of the lowest energy conformer,a ribbon and stick diagram showing the surface ledges, and a space-fill model showing a large grove important for binding nucleic acids.

4.2. Materials and Methods

TFE, TFE-d3 (Cambridge Isotope Laboratories), and acetate buffer components were of highest purity available commercially. Recombinant *At*PP16-1 used for all experiments was produced in the laboratory using the procedure described earlier. Isotope enrichment of the protein for heteronuclear NMR experiments was done by growing the cells in M9 medium containing NH₄Cl and/or Recombination on whether double or single isotope labelling was required. The conditions for cell growth in M9 medium, harvesting and lysis, and purification of the protein have also been described. The purified protein solution was dialyzed exhaustively against 7 mM acetate buffer, pH 4.1.

Samples for TFE titration of the protein were prepared by a procedure that also tests the reversibility of the protein-TFE reaction. Two stock solutions are prepared in a way that they are identical with respect to the buffering condition (7 mM acetate, pH 4.1) and the protein concentration ($12\mu M$ for fluorescence, CD, and IR measurements) except that one contains TFE (60% by volume) and the other does not. These two stock solutions are

combined appropriately to obtain samples containing TFE in 0–60% range. The samples are equilibrated at ~25°C for ~6 h before measurements are carried out at 25 °C. Fluorescence emission spectra were recorded by 280-nm excitation using a Jasco FP-8300 fluorimeter, CD spectra and single-wavelength time-base measurements were taken in a JASCO 715 instrument, and IR spectra were measured in a FTIR-ATR instrument (ThermoFisher Scientific). That the sample pH did not change after the preparation of the solutions was confirmed by pH measurement after completion of the measurements.

Samples for $[^{1}H^{-15}N]$ HSQC NMR spectra were also prepared by the procedure described above, although the dispersion of chemical shifts in the spectra was increasingly poor beyond ~5.7% TFE-d3. Protein concentration was ~100 μ M. Typically 128 experiments each of 32 scans were acquired in the ^{15}N dimension. Spectra were recorded in a 500 MHz Bruker spectrometer using a TXI probe.

The activity coefficient of TFE was determined by the empirical relation⁵⁰

$$\gamma_{\pm} = a + be^{-cx} + de^{-fx} \tag{1}$$

where the mole fraction of TFE in the aqueous solution is denoted by x, and the constants are a=0.0677, b=0.4680, c=20.8253, d=0.4596, and f=6.3429.

4.3. Results

4.3.1. *TFE* stabilization of a tertiary structure intermediate

A study of the response of tertiary structure to the added TFE is fruitful in order to see if the melting of the former is related to helix-promoting activity of TFE. Monitoring tertiary structure of IDP could be even more interesting because aromatic amino acids have the lowest disorder propensity, meaning their side chains hardly promote intrinsic disorder. In the

present pursue, we notice TFE-induced quenching of tryptophan fluorescence (Fig. 2a) concomitant with the appearance of a blue-shifted emission peak centered at ~300 nm (Fig. 2b). The wavelength of maximum fluorescence (λ_{max}) due to the three tryptophans W53, W59, and W150 of AtPP16-1 red-shifts cooperatively by 9 nm as the TFE level is raised to ~30% and stays constant thereafter (Fig. 2c). The cooperativity of the Stokes shift to the red must mean TFE-induced melting of weak tertiary interactions causing larger surface exposure of the tryptophan side chains. The fluorescence however quenches in two distinct steps irrespective of the use of the native-state λ_{max} or the λ_{max} corresponding to different levels of TFE (Fig. 2d), suggesting the accumulation of an equilibrium intermediate characterized by partly unfolded tertiary structure. One might like to label the intermediate as Iwonly to indicate its identification by tryptophan fluorescence, and place it in the $N \rightleftharpoons I_W \rightleftarrows Ipathway$ in which N and I refer to native and tertiary structure-unfolded intermediate states of the IDP. The term unfolding is being used here in the true sense, not meaning denaturation but complete loss of tertiary structure. While unfolding leads to quenching of indole fluorescence at high TFE, the new peak appearing at ~300 nm implies the emergence of tyrosine fluorescence (Fig. 2b,e). The TFE dependence of the latter is monotonous however, showing relocation of one or more of the 5 tyrosines whose fluorescence is not quenched in the unfolded state.

The observation of the tertiary structure unfolded intermediate is significant because the role of TFE in the stabilization of partly melted tertiary structure of certain globular proteins is a very recent finding,⁵⁰ not documented in extensive studies carried out both experimentally and computationally. It emerges that TFE can stabilize such an intermediate in the case of an IDP also, even though the latter does not have a tertiary structure as well-defined as in globular proteins. One may conclude that TFE unfolding structurally resembles unfolding by urea and guanidinium chloride (GdnHCl) such that all three agents unfold

tertiary structures and stabilize partly unfolded structures under thermodynamically favorable conditions irrespective of the order and disorder in the native state structure. Data are also provided in support of this conclusion vide infra.

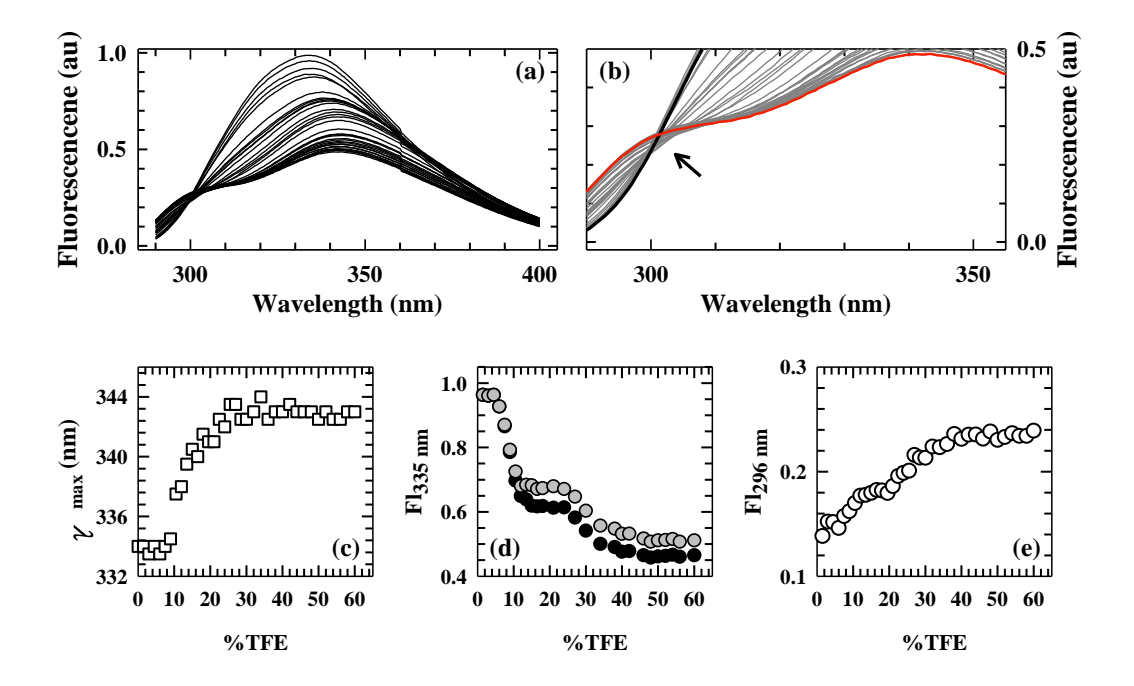


Figure 2. Fluorescence detection of TFE action on AtPP16-1. (a) The tryptophan fluorescence quenches with TFE with a concomitant red shift of the λ_{max} . (b) A second emission peak centered at ~300 nm, likely due to fluorescence of tyrosines, appear as the TFE level is raised. (c) The Stokes shift of the λ_{max} of tryptophan emission is cooperative with TFE and amounts to ~9 nm. (d) The TFE-induced quenching of tryptophan fluorescence occurs in two steps separated by a distinct baseline. The curves correspond to the fluorescence with respect to the λ_{max} at different %TFE (gray), and fluorescence at 332 nm (black). (e) The increase of emission at λ =296.5 nm appears to have a parabolic dependence on TFE, suggesting that tyrosine fluorescence does not indicate the population of a tertiary structural intermediate.

The fluorescence intensity presented above is in error by ~10% due to the sensitivity of indole fluorescence to the apolarity (dielectric constant) of TFE. The error margin was determined by a control experiment in which the fluorescence of indole was measured with

variable aqueous % TFE. This is one of the reasons why fluorescence results should be buttressed by near-UV CD which only reflects the changes in optical rotatory strength of the aromatic side chains irrespective of their surrounding dielectric. Weak optical rotatory strength of aromatic side chains in the $\pi \rightarrow \pi^*$ region of the absorption spectrum requires sufficient averaging of the signal; so we recorded the near-UV spectrum only for a few samples to determine the λ_{max} (Fig. 3a), and then measured time-base average of the CD signal at the determined λ_{max} . The TFE dependence of the 271-nm CD absorption due to tyrosine and phenylalanine is shown in Fig. 3b where the single step change in ellipticity is complete in ~25% TFE, suggesting unfolding of the tertiary structure around these residues in atwo-state manner,N \rightleftharpoons I.

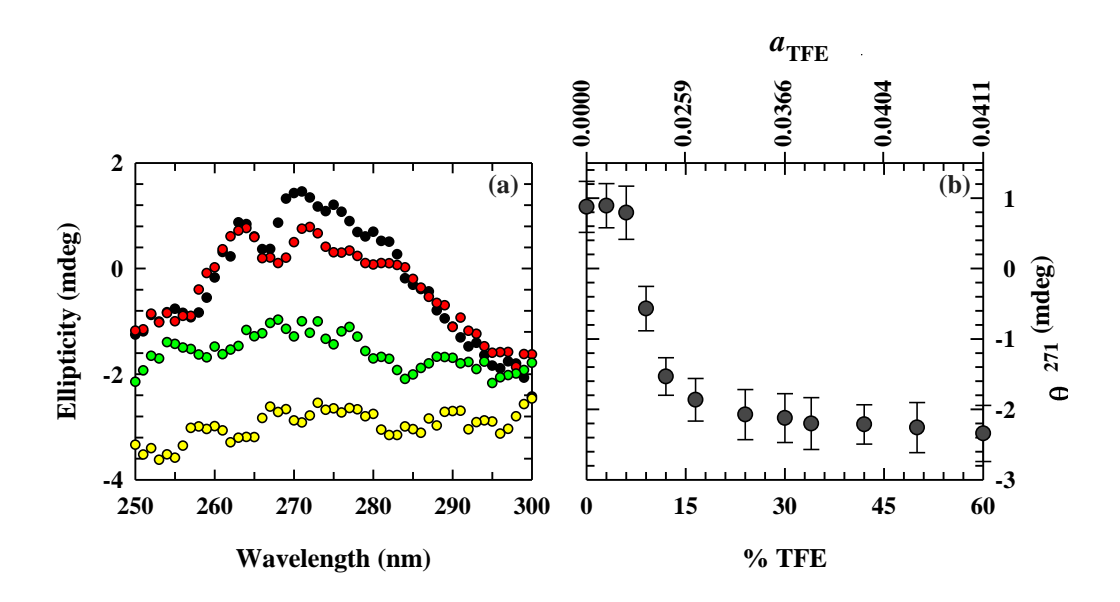


Fig.3. (a) The near-UV CD spectrum in 0 (black), 6 (red), 16.5 (green), and 30 (yellow) %TFE. (b) The change in the θ_{271} values from 0 to 60 %TFE. The error bars represent standard deviations of mean values.

The identification of the intermediateI_Wexplicitly by fluorescence implies the formation of a specific structural cluster which contains one or more tryptophan residues such

that the cluster protects the residues from the solvent. Occurrence of localized, stereochemically sensitive apolar clusters specifically containing tryptophan side chains have been documented in earlier studies of globular protein unfoldingby urea. ^{52–54}The finding of such an intermediate of the IDP *At*PP16-1 suggests that intermediates can accumulate in TFE unfolding as it does in urea and GdnHCl unfolding. Tertiary structural intermediates may populate in IDP folding as they do for globular proteins, even though the tertiary structure in the former ill-defined to variable degree.

4.3.2 Changes in the side-chain C=O bond polarity with TFE

IDP chains are characteristically rich in charged amino acid residues; Asp and Glu account for 25 of the 156 residues of AtPP16-1. To look at how TFE might affect their side chain motions, we monitored the TFE-induced transition by IR in the 1400–1820 cm⁻¹ region. The absorption due to the C=O stretching of the polypeptide backbone (Amide I normal mode, ~1630 cm⁻¹) is completely masked by the C=O stretching absorption of the acetate buffer, the latter however does not interfere with the Asp and Glu C=O stretching absorption at 1737 cm⁻¹ (Fig.4a). The C=O of these side chains are presumably not H-bonded, and the observation of no shift in the $\nu(C=O)$ plausibly reflects no effect of the low dielectric constant of TFE.⁵⁵ The band intensity decreases in two steps, each showing a power-law dependence on % TFE (Fig.4b). The break at ~40% TFE may be a reflection of the response of the C=O side chains to the formation of additional helices. The problem however enters into the realm of infrared spectroscopy, where the intensity of absorption is determined by the derivative of the permanent $C^{\delta+}=O^{\delta-}$ dipole with respect to the oscillating C and O distance evaluated at equilibrium nuclear configuration r_e . The 1740 cm⁻¹ band should arise as a single quantum absorption from the excitation of a vibrational level in ground electronic state (v') to one in an excited electronic surface (v), so that the intensity of absorption is given by

$$I = \left(\frac{\partial \mu(r)}{\partial r}\right)_{r=r_e} \int_{-\infty}^{+\infty} \psi_v^*(r - r_e) \,\psi_{v'} \,dr \tag{2}$$

where r is the internuclear $C^{\delta+}=O^{\delta-}$ distance specific to the stretching mode and r_e is the equilibrium separation. The second-order dipole derivative is excluded because of the assumption of single-quantum absorption.

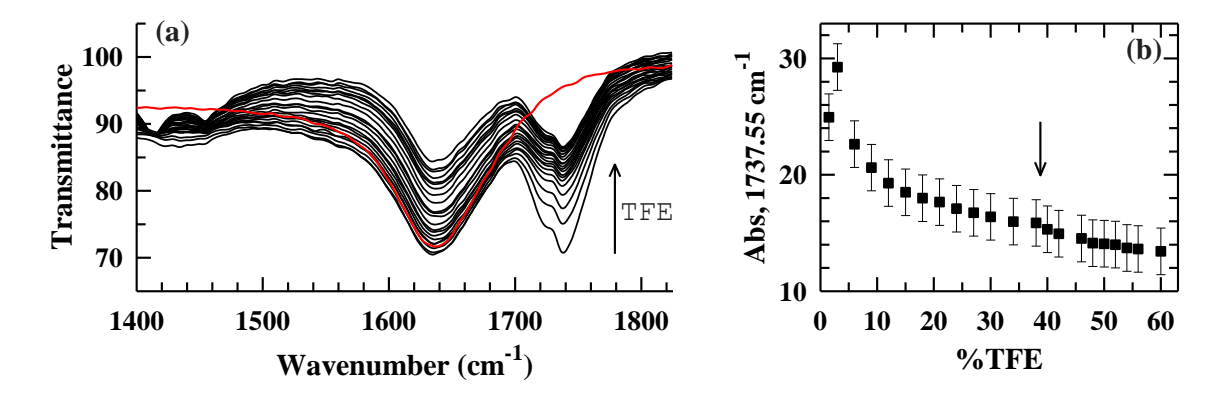


Figure 4. (a) The 1630 and 1737 cm^{$^{-1}$} band intensities with TFE with the acetate buffer spectrum shown in red, (b) TFE dependence of the 1737.55 cm^{$^{-1}$} absorbance. The break at \sim 40% TFE is indicated by the arrow.

The decreasing intensity of the $1740~\rm cm^{-1}$ band – meaning smaller magnitude of the dipole derivative, can be correlated with decreasing polarity of the side chain $\rm C^{\delta+}=\rm O^{\delta-}$ of Asp and Glu as the protein is titrated with TFE. This can happen if an electrophile, most likely $\rm H^+$, reduces the electronegativity of the oxygen. It is also possible that the helical propensity of these amino acids increase in TFE so that the helix macrodipole somehow reduces the polarity of $\rm C^{\delta+}=\rm O^{\delta-}$. These must be taken as conjectures only; more results will be needed to find out how the polarity of the bond decreases. Incidentally, we have used this IR band earlier to study binding of paraben food additives to globular proteins. 56

4.3.3 Denaturation of Secondary Structure by TFE

The rationale for looking at the secondary structure content is found in the long established fact that TFE invariably promotes α -helical structure in globular proteins, often in far excess of what the native state contains. It is of interest to learn as to what extent the helical propensity is increased in IDPs where the native-state secondary structure content is most often marginal; in the present IDP AtPP16-1 only 19% of the residues form the minimal secondary structure framework.

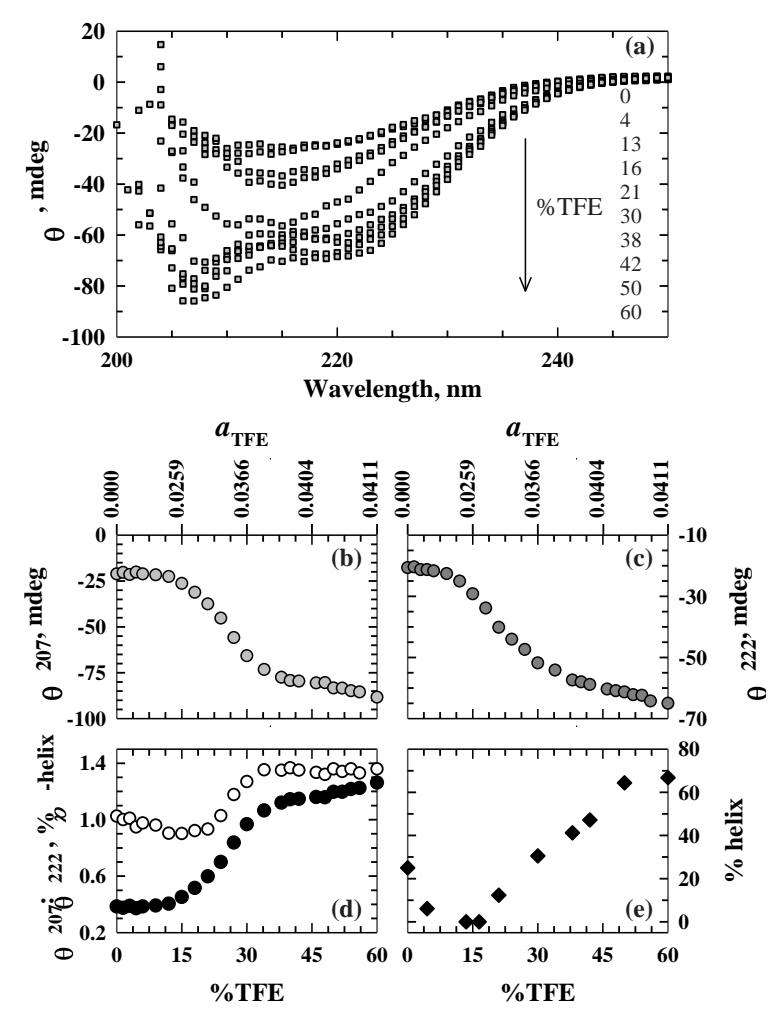


Figure 5. (a) Changes in the far-CD spectrum with the indicated % TFE, (b) cooperative transition monitored by θ_{207} , (c) the same transition observed by θ_{222} , (d) the change in the % helix approximated the θ_{207} : θ_{222} ratio (open circles) and Greenfield-Fasman method (solid circles), (e) helix estimations obtained from BeStSelTM.

An inspection of the representative set of far-UV CD spectra in the 0–60% range of TFE (Fig.5a) shows that the 207- and 222-nm bands can be distinguished only when the level of the solvent rises above ~25%, indicating reorganization of secondary structural elements.

For a clearer result, time-base CD readings at 207 and 222 nm were averaged out to generate the TFE dependence of ellipticities at these wavelengths (Fig.5b,c). The negative ellipticity at both wavelengths increases cooperatively by \sim 50 mdeg across the %TFE scale, suggesting acquisition of secondary structure to a large extent. This is consistent with TFE-induced helical propensity observed for numerous peptides and globular proteins reported over a long time. The result is not unexpected; if TFE induces α -helices in unstructured or nominally structured peptide sequences(I), then structure should be induced in intrinsically disordered proteins as well.

Since both α - and β -structures contribute to the 207-nm CD and the contribution of the former is more, the ratio of ellipticities at 207 and 222 nm could be an approximate indicator of the content of α -helical structure (Fig. 5d). One can also start to estimate the helicity using the Greenfield-Fasman (GF) approach, ⁵⁷ given by

% α-helix
$$\sim \frac{[\theta]_{207}-4000}{-33000-4000}$$

where θ_{207} is the mean residue ellipticity (MRE), -4000 is the MRE of β -structure and random coil at 208 nm, and -33000 is the MRE of α -helical structure given for of poly-L-lysine. The helical structure given for of poly-L-lysine. Although the TFE-promoted α -helicity estimated by the GF method fairly compares with that approximated from the θ_{207} : θ_{222} ratio (Fig.5d), the results do not appear reliable. The NMR structure shows 15 residues (96–110 stretch of the sequence) forming the lone α -helix in the native AtPP16-1(51), accounting for ~10% helicity instead of ~1% seen in Fig.5d. The result that the helicity increases only to ~1.5% across the 0–60% range of TFE also raises doubt. The % helix estimated using BeStSelTM web server (Fig.5e) appears consistent, although no helicity appears in ~15% TFE. Zero helicity might mean an initial destabilization of secondary structure required to achieve helix propensity at higher TFE. The 67% helix content in ~60% TFE is remarkable, reflecting large α -helical propensity of the IDP chain.

We call the TFE state characterized by excess α -helical content the 'denatured state' (D), and denote the reversible transition between the native and the D state by N \rightleftharpoons D only to implicate that no secondary structure intermediate populates. But why is the TFE state dubbed denatured? Since TFE did not unfold the secondary structure but added extra helices, the protein is not unfolded but denatured. It cannot be called a quasinative state even if it has native-like helices, because low TFE has already unfolded the tertiary structure.

4.3.4. Widespread loss of chemical shift dispersion at low TFE

Since we have already had the solution structure of the IDP AtPP16-1 determined⁵¹we also hoped to obtain some insight of TFE-induced structure perturbation by NMR. The chemical shift dispersion however, already poor in the native state, degraded to a large extent upon the addition of a fewer % TFE. As seen in the $^{1}H^{-15}N$ HSQC spectra (Fig.6), the dispersion collapses severely in ~7% TFE. Clearly, the intensity loss is not due to RF damping as occurs in GdnHC1 titration of globular proteins monitored by NMR. Rather, it is a reflection of global perturbation of the protein conformation or aggregation of the protein or both. The protein aggregation problem is not seen in the absence of TFE even when the IDP is ~150 μ Min the solution. It is possibly the widespread perturbation of the conformation that leads to the loss of dispersion, which means the I_W intermediate observed by tryptophan fluorescence (Fig. 2) is a local cluster of structure. We are still interested to look at the helix-rich D-state of the IDP produced at high TFE, but the required rigor of higher level NMR experiments and calculations will take some time.

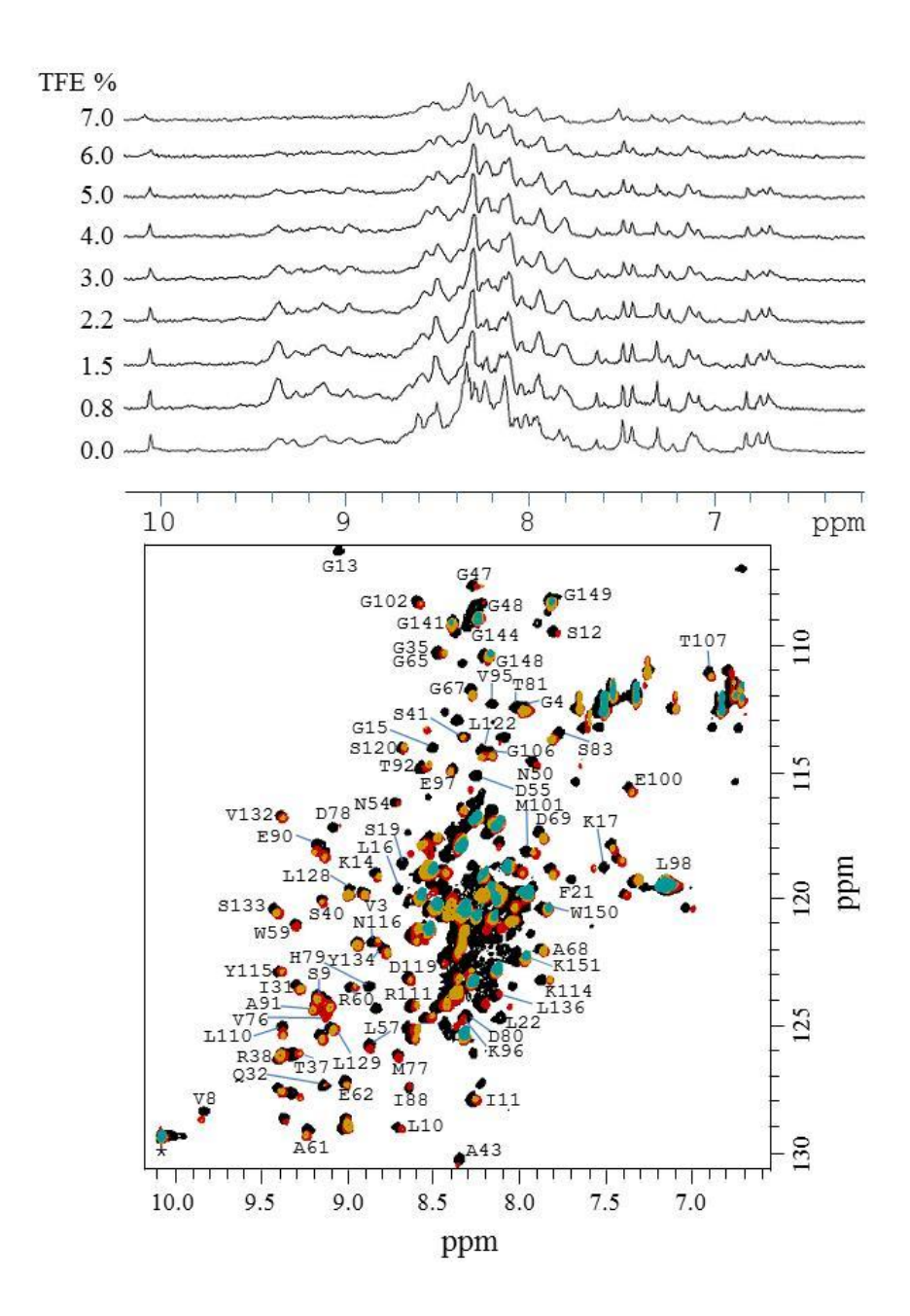


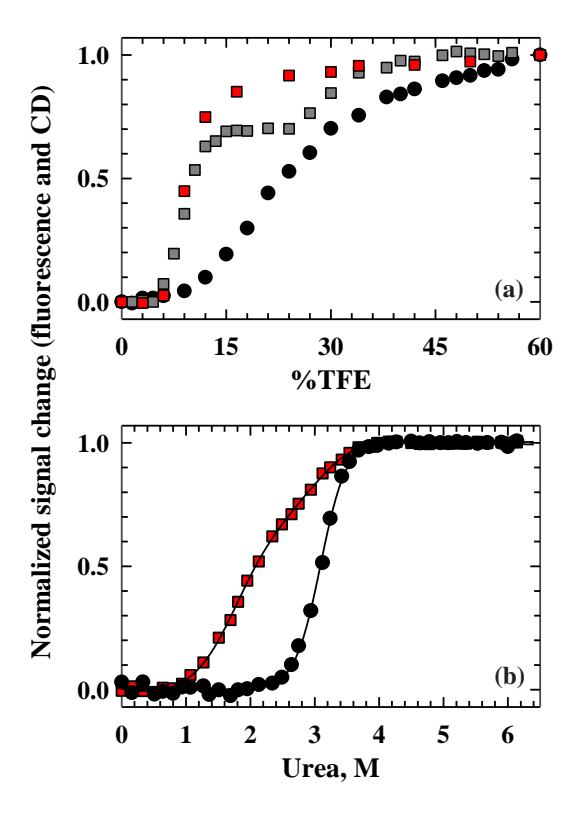
Figure 6. (a) Stack plot of the amide region projected from the first 1D spectrum of each of the $^{1}\text{H}-^{15}\text{N}$ HSQC 2D spectra recorded at the indicated %TFE. (b) Overlay of the HSQC spectra in 0 (black), 1.5 (red), 3 (yellow), and 7 (cyan) %TFE showing increasingly collapsed dispersion. The assignments known for the native protein at pH 4.1, 298 K are indicated.

4.3.5 Accumulation of tertiary structure-unfolded intermediate

Reviewing the fluorescence and CD results discussed earlier, a comparison of tertiary structure unfolding ($N \rightleftharpoons I_W \rightleftharpoons I$) and secondary structure denaturation ($N \rightleftharpoons D$) transitions, normalized individually, shows clear separation of the two across the TFE scale (Fig.7a).

Two non-superimposable transitions observed by two or more different probes is a standard criterion to presume the accumulation of structural intermediate.^{59,60}One can then combine the TFE transitions into

 $N \rightleftharpoons I_W \rightleftharpoons I \rightleftharpoons D$.



Separation **Figure** 7. (a) of nonsuperimposable transitions for tertiary unfolding structure N**≓**I (red square) and N ≠ I_W ≠ I (gray square), and secondary structure denaturation N≠D(solid circles). (b) Separation of urea-induced tertiary (red secondary square) and (solid circle) unfolding transitions of the IDP. The free energy values are listed in Table 1.

If the I_W state did not populate, as it is not observed by the near-UV CD transition in Fig.3, the scheme reduces to the three-state generic model for TFE denaturation of globular proteins described⁵⁰

N≓I≓D,

in which the intermediate I refers to the tertiary structure unfolded state, which presumably determines the α -helical propensity in order to denature to the helix-rich D state. The state I

has been called an universal intermediate because of its accumulation and detection in a diverse set of globular proteins. In essence, the tertiary structure unfolded state is a structural intermediate required for denaturation to a helix-rich TFE-state. It is also suggested that additional intermediate(s) may populate across the N \rightleftharpoons I equilibrium in a protein specific manner— the accumulation of I₁ in TFE unfolding of myoglobin, ⁵⁰ for example. Here we have the first example of an IDP whose response to TFE is consistent with the N \rightleftharpoons I \rightleftharpoons D model for globular proteins. Interestingly, the minimal three-state model also describes the urea-unfolding transitions of the IDP AtPP16-1 (Fig. 7b). The free energy values of the urea transitions calculated by the linear free energy model are comparable to those obtained from the TFE transitions by using the preferential exclusion model as follow (see Table 1).

4.3.6. Free energy of unfolding and denaturation of the IDP

Experimental studies in the past have hardly dealt with the thermodynamic aspects of TFE-induced structural changes in proteins because analysis of TFE unfolding curves is not as straightforward as that of chaotropic denaturants like urea and GdnHCl. An analysis that relies on the principles of solvent denaturation of proteins has however been implemented to extract the free energy changes between the native and TFE-perturbed states. The basic idea due to Schellman, Timasheff, and others⁶¹⁻⁶³is to determine the excess free energy of the protein arising from its binding interaction with the solvent TFE. Earlier studies have in fact indicated that protein-alcohol interaction could be analyzed by the model for preferential exclusion of the cosolvent from the protein surface.^{24,63,64}By convention, the components water, protein, and TFE are denoted by 1, 2, and 3, respectively, and the excess free energy of the protein due to its interaction with TFE takes the form^{61,63}

$$\beta_2 \equiv \Gamma_{23} \cong \left(\frac{\partial m_3}{\partial m_2}\right)_{T,P,\mu_3} \tag{3}$$

in which Γ_{23} represents the coefficient of thermodynamic binding, m stands for molal concentration, and μ is the chemical potential. The change in the chemical potential of the denatured or unfolded protein brought about by TFE binding reflects the free energy of denaturation (unfolding) of the protein,

$$\Delta G = \mu_2^{D(U)} - \mu_2^{N} = -RT(\Gamma_{23}^{D(U)} - \Gamma_{23}^{N}) = -RT\Delta\Gamma_{23}, \tag{4}$$

where $\Gamma_{23}^{D(U)}$ and Γ_{23}^{N} are thermodynamic binding coefficients. When determination of Γ_{23} is difficult, the difference $\Delta\Gamma_{23}$ is estimated from the Wyman linkage equation expressed in terms of TFE activity

$$\Delta\Gamma_{23} = \left(\frac{\partial \ln K}{\partial \ln a_3}\right)_{m_2},\tag{5}$$

in which K is the equilibrium constant of the $N \rightleftharpoons Dreaction$, and a_3 is TFE activity. There will be two equilibrium constants K_1 and K_2 for the $N \rightleftharpoons I_W \rightleftharpoons I$ equilibria.

To determine K we assume linearity of the pre and post-transition baselines with a_{TFE}

$$S(a_{\rm TFE}) = S^{\rm o} + ma_{\rm TFE},\tag{6}$$

where S is normalized observable signal, and S^o is the value of S in the absence of TFE. The baselines for $N \rightleftharpoons I_W \rightleftharpoons I$ transition ($N \rightleftharpoons I_W$ and $I_W \rightleftharpoons I$) are shown in Fig.8a,b. One can then obtain K using the values of S^o and Mby

$$K = \frac{S - \left(S_{\text{pre}}^{\text{o}} + m_{\text{pre}} a_{\text{TFE}}\right)}{\left(S_{\text{post}}^{\text{o}} + m_{\text{post}} a_{\text{TFE}}\right) - S},\tag{7}$$

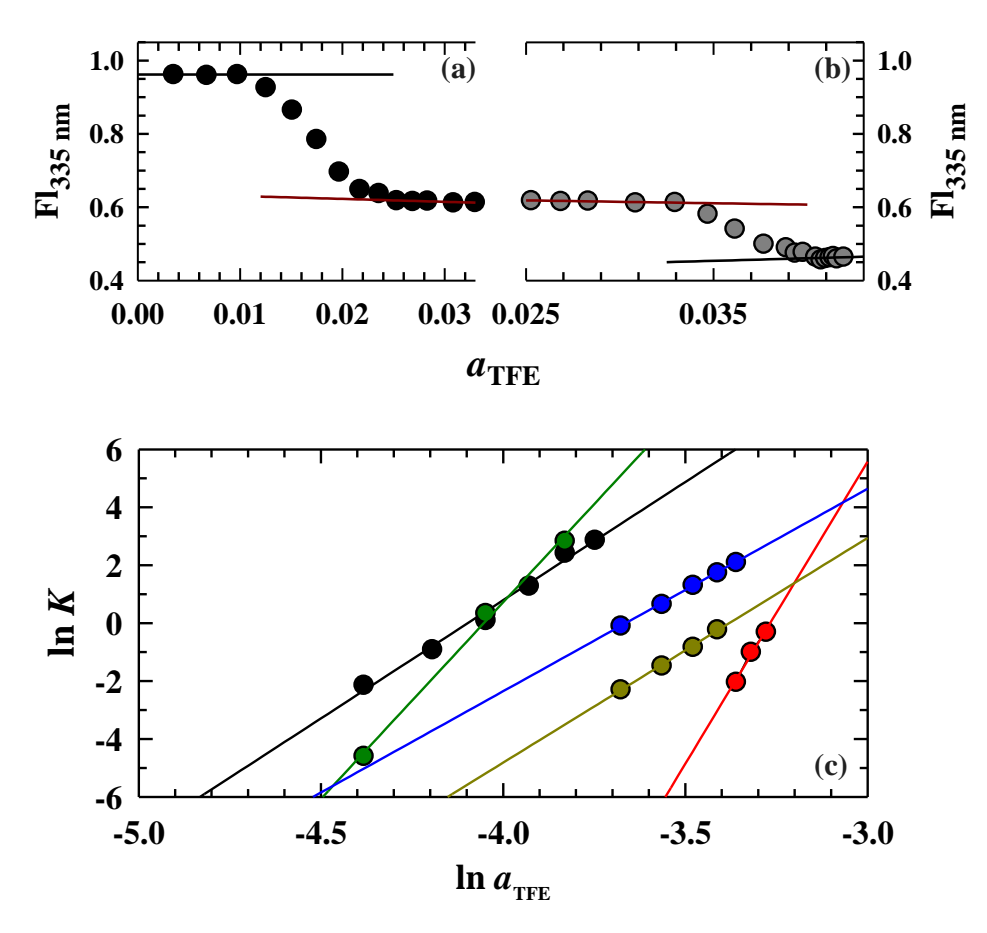


Figure 8. (a,b) Baselines for N, I_W , and I states (N \rightleftharpoons $I_W \rightleftharpoons$ I) detected by fluorescence. The line in red serves for the posttransition baseline of the N \rightleftharpoons I_W transition and pre-transition baseline of the $I_W \rightleftharpoons$ I transition. (c) Double natural logarithmic plots shown for the tryptophan fluorescence transitions N \rightleftharpoons I_W (black) and $I_W \rightleftharpoons$ I (red), near-UV CD transition N \rightleftharpoons I (cyan), and far-UV CD transition N \rightleftharpoons D measured at 222 nm (blue) and 207 nm (gray). Values of free energy extracted are listed in Table 1.

in which $S_{\text{pre}}^{\text{o}}$ and $S_{\text{post}}^{\text{o}}$ refer to intercept signal values with respective slopes m_{pre} and m_{post} . Plots of $\ln K$ vs $\ln a_{\text{TFE}}$ for the $N \rightleftharpoons I_W \rightleftharpoons I$, $N \rightleftharpoons I$ and $N \rightleftharpoons D$ transitions monitored by fluorescence, and near- and far-UV CDs are shown in Fig.8c, in which RT (~0.59 kcal mol⁻¹ at 25 °C) times the slope is the respective value of ΔG (Table 1).

Table 1. Free energy ΔG (kcal mol⁻¹) of TFE-and urea-induced unfolding and denaturation of AtPP16-1, pH 4.1, 298 K

Denaturant	Probe monitor	Transition	$\Delta G (kcal mol^{-1})$
TFE	Trp fluorescence	$N \rightleftharpoons I_W$	4.8(±0.5)
		$I_W \rightleftharpoons I$	12.3(±1.0)
	271-nm CD	$N \rightleftharpoons I$	$8.0(\pm0.8)$
	222-nm CD	$N \rightleftharpoons D$	$4.2(\pm 0.5)$
	207-nm CD	$N \rightleftharpoons D$	$4.6(\pm 0.5)$
Urea	Trp fluorescence	$N \rightleftharpoons I$	$2.4(\pm 0.5)$
	222-nm CD	$N \rightleftharpoons U$	9.0(±1.0)

The interpretation of these ΔG values regarding the schemes $N \rightleftharpoons I_W \rightleftharpoons I$ and $N \rightleftharpoons D$, and the integrated $N \rightleftharpoons I \rightleftharpoons D$ may appear burdensome because the unfolding free energy for the $I_W \rightleftharpoons I$ step monitored by fluorescence is three-fold higher than the $N \rightleftharpoons D$. Considering the accuracy of the data, we interpret the results to accommodate the tertiary structure unfolded intermediate (I) as a high-energy obligate intermediate (Fig.9).

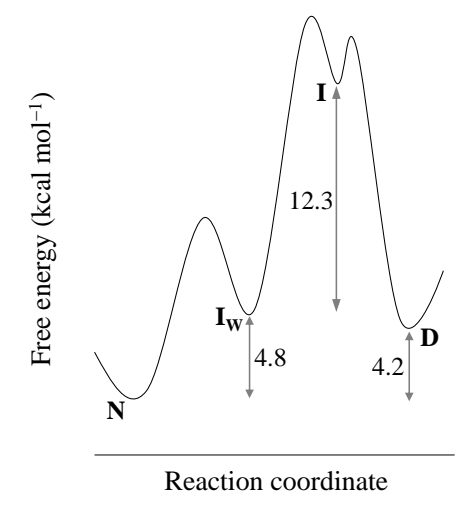


Figure 9.An overly simplified free energy profile indicating the position of the high energy intermediate I.

4.4. Discussion

Even though the TFE-state or the denatured state Dis a helix-rich apparently artificial state, protein denaturation experiments with TFE continue to be important because of various possible applications of the alcohol including, solubilization of proteins and peptides and folding them to the native state by removing the alcohol, modulation of catalytic activity of enzymes, explication of solvent dependent protein dynamics, finding determinants of helix propensity and packing, and enhancement of protein structure. A closer effort to analyze TFE action on proteins is therefore necessary.

In all protein systems irrespective of the extent and typesof ordered structures, and whether globular or not, the TFE-induced structure perturbation is reversible with no known hysteresis between denaturation and refolding transitions.⁵⁰The reversibilitycomes as a windfall because it not only makes the above mentioned TFE applications possible, but also provides a handle to analyze the folding (unfolding) reaction in relation to urea and GdnHCl unfolding. The finding of the stabilization of tertiary unfolded intermediate I by both TFE and urea (Fig. 7) is a good indication of similarity of their structure unfolding effects, although it will be irrational to assume that it is the same intermediate that is stabilized by the two denaturants. That the intermediates must be different is clarified by the free energy change (ΔG) calculated for TFE denaturation vis a vis urea unfolding (Table 1), a result that has also been discussed recently for a sizable set of globular proteins. ⁵⁰Since the modes of action of TFE and urea on protein are different, the ΔG values calculated with the TFE results are not expected be comparable with those determined from ureaunfolding. ^{66,67}A possible argument that ΔG calculated by using the coefficient of thermodynamic binding of the TFE cosolvent (Γ_{23}) in comparison with the ΔG calculated by Pace's linear free energy model may give different results will be untenable, because it can be shown analytically that the folding energy of a given transition calculated by the two procedures is sufficiently consistent. It is

concluded that the folding intermediate populated in TFE unfolding is structurally unrelated to that in urea unfolding.

The TFE intermediate I is not only distinct but also an obligate species recognizable by inspection of the TFE-induced transitions of globular proteins diverse by types and extent of secondary structure content. 50 This work is an attempt to introduce the TFE intermediate in the context of IDPs, although more experiments wait to fully establish its generality. Regarding its universal nature, one can go by naivety and guess – a specific conformation that is somehow poised to acquire α -helices as the TFE level rises irrespective of the primary structure and whether the starting state (N) is an ordered globular structure or disordered less structured chain. This indiscriminate action of TFE toward the common theme of higher α helical structuration has been evasive. The α -helical propensity can arise from not only preexisting α -helical segments of the native state 8,13,68 or local helical interactions 17,18,69 but also predominantly β -sheet favoring regions. ^{18,70}The ability of the TFE intermediate to acquire α helical propensity irrespective of the sequence propensity in the native state is its distinguishing property, which is presumably absent in the classical folding intermediates stabilized by urea and GdnHCl. The universality of the TFE intermediate refers to this fact that tertiary unfolding of the native protein is a prerequisite⁷¹ and a necessary condition to acquire α -helical propensity. Since the amino acid sequences of globular and intrinsically disordered proteins are typically different in that the latter contains abundant disorderpromoting residues, the residue types in the sequence as such do not determine the acquisition of extra α -helices.

A persistent confusion in the protein-TFE literature is whether TFE forces a protein to adopt a molten globule (MG) state. Numerous studies toward the end of the last century endeavoured to show that the TFE intermediate I and/or the denatured state Dresemble the MG state, as reported in references^{72–75} for example, the reason for which was perhaps the

thrust created by the then newly announced 'third thermodynamic state of globular proteins' called the MG state. ^{76–78}A review of those results would however reveal that structural properties of TFE-transformed proteins are not fully consistent with the canonical properties of MG^{18,50}nor does TFE promote acid MG. ⁷⁹It has been argued elsewhere that the MG is an abortive off-pathway species, ^{80,81} implying that the reversibility of TFE-denaturation will not hold even if a MG state is admitted in the equilibria. We notice here that the coarse characteristics of IDP transition by TFE are little different from those observed for globular proteins. The conformational ensemble of an IDP corresponds to an ensemble of a continuous distribution of tertiary structure, ⁸²accounting for an average tertiary structure that is less rigid. Since IDPs may be likened to the native MG, ^{83,84}and we see reversible tertiary unfolding by TFE and the resulting intermediate denatured reversibly to acquire excess α-helices, the possibility of the accumulation of MGs through the action of TFE is abrogated.

That the free energy of the TFE obligate intermediate I is higher than the free energies of both N and D in the N \rightleftharpoons I \rightleftharpoons D pathway (Fig. 9 and Table 1) warrants a comment. High energy intermediates seems to be of common occurrence in the folding of a sizable set of small globular proteins initially unfolded by urea or GdnHCl. For example, Sánchez and Kiefhaber⁸⁵have observed high-energy obligatory intermediates in their analysis of 23 globular proteins. Other instances of such intermediates have also been reported where specific structural features are implicated. But the higher energy of the TFE intermediate in the case of the IDP may stem from the entropy cost associated with reduced fluctuation of the chain ensemble as a result of TFE binding to a few high-affinity surface sites by H-bonding and van der Waals interactions and to a fewer low-affinity inner patches of the protein by hydrophobic interaction. Since TFE has half a unit of negative charge on the fluorines ($-CF_3^{\delta-}$), its access to the low dielectric apolar core of the protein is energetically expensive, hence the affinity is low. The tertiary structure of the IDP is lost nonetheless, the helical

propensity increases, and the entropy loss appears as a penalty. This argument has been provided recently to explain the free energy folding penalty accompanying binding of interacting proteins to disordered α -helical motifs of several IDPs. ⁸⁸

4.5. References

- 1. Buck, M. Trifluoroethanol and colleagues: cosolvents come of age. Recent studies with peptides and proteins, *Q. Rev. Biophys.* **1998**, *31*, 297-355.
- 2. Goodman, M.; and Rosen, I. G. Conformational aspects of polypeptide structure XVI. Rotatory constants, cotton effects, and ultraviolet absorption data for glutamate oligomers and co-oligomers, *Biopolymers* **1964**, *2*, 537-559.
- 3. Tamburro, A. M.; Scatturin, A.; Rocchi, R.; Marchiori, F.; Borin, G.; and Scaffone, E. Conformational transitions of bovine pancreatic ribonuclease S-peptide. *FEBS Lett.* **1968**, *1*, 298-300.
- 4. Brown, J. E.; and Klee W. A. Helix-coil transition of the isolated amino terminus of ribonuclease, *Biochemistry* **1971**, *10*, 470-476.
- 5. Liebes, L. F.; Zand, R.; and Phillips, W. D. Solution behaviour, circular dichroism and 220 MHz NMR studies of the bovine myelin basic protein. *Biochim. Biophys. Acta* **1975**, 405, 27-39.
- 6. Marquesee, S.; and Baldwin, R. L. Helix stabilization by Glu⁻···Lys⁺ salt bridges in short peptides of de novo design. *Proc. Natl. Acad. Sci. U. S. A.* **1987**, *84*, 8898-8902.
- 7. Lehrman, S. R.; Tuls, J. L.; Lung, M. Peptide α -helicity in aqueous trifluoroethanol. Correlations with predicted α -helicity and the secondary structure of the corresponding regions of bovine growth hormone. *Biochemistry* **1990**, *29*, 5590-5596.
- 8. Segawa, S-I.; Fukuno, T.; Fujiwara, K.; and Noda, Y. Local structures in unfolded lysozyme and correlation with secondary structure in the native conformation. *Biopolymers* **1991**, *31*, 497-509.
- 9. Yang, J. J.; Buck, M.; Pitkeathly, M.; Kotik, M.; Haynie, D. T.; Dobson, C. M.; and Radford, S. E. Conformational preferences of four peptides spanning the sequence pf hen lysozyme. *J. Mol. Biol.* **1995**, 252, 485-491.

- 10. Storrs, R. W.; Truckses, D.; and Wemmer, D. E. Helix propagation in trifluoroehanol solutions. *Biopolymers* **1992**, *32*, 1695-1702.
- 11. Jasanoff, A.; and Fersht, A. R. Quantitative determination of helical propensities from trifluoroethanol titration curves. *Biochemistry* **1994**, *33*, 2129-2135.
- 12. Rohl, C. A.; Chakrabartty, A.; and Baldwin, R. L. Helix propagation and N-cap propensity of the amino acids measured in alanine-base peptides in 40 volume percent trifluoroethanol. *Protein Sci.* **1996**, 5, 2623-2637.
- 13. Luo, P.; and Baldwin, R. L. Mechanism of helix induction by trifluoroethanol: a framework for extrapolating the helix-forming properties of peptides from trifluoroethanol-water mixtures back to water. *Biochemistry* **1997**, *36*, 8413-8421.
- 14. Myers, J. K.; Pace, C. N.; Scholtz, J. M. Trifluoroethanol effects on helix propensity and electrostatic interactions in the helical peptide from ribonuclease T1. *Protein Sci.* **1998**, *7*, 383-388.
- 15. Mizuno, K.; Kaido, H.; Kimura, K.; Miyamoto, K.; Yoneda, N.; Kawabata, T.; Tsurusaki, T.; Hashizume, N.; and Shindo, Y. Studies of the interaction between alcohols and amides to identify factors in the denaturation of globular proteins in halogen alcohol + water mixtures, *J. Chem. Soc. Faraday Trans. I.* **1984**, *80*, 879-984.
- 16. Nelson, J. W.; Kallenbach, N. R. Stabilization of the ribonuclease S-peptide α -helix by trifluoroethanol. *Proteins: Struct. Funct. Genet.* **1986**, *1*, 211-217.
- 17. Thomas, P. D.; Dill, K. A. Local and non-local interactions in globular proteins and mechanism of alcohol denaturation. *Protein Sci.* **1993**, *2*, 2050-2065.
- 18. Shiraki, K.; Nishikawa, K.; Goto, Y. Trifluoroethanol-induced stabilization of the α -helical structure of β -lactoglobulin: implication for non-hierarchical protein folding, *J. Mol. Biol.* **1995**, 245, 180-194.
- 19. Cammers-Goodwin, A.; Allen, T. J.; Oslick, S. L.; McClure, K. F.; Lee, J. H.; and Kemp, D. S. Mechanism of stabilization of helical conformations of polypeptides by water containing trifluoroethanol. *J. Am. Chem. Soc.* **1996**, *118*, 3082-3090.
- 20. Rajan, R.; Balaram, P. A. model for the interaction of trifluoroethanol with peptides and proteins. *Int. J. Peptide Protein Res.* **1996**, *48*, 328-336.
- 21. Kentsis, A.; Sosnick, T. R. Trifluoroethanol promotes helix formation by destabilizing backbone exposure: desolvation rather than native hydrogen bonding defines the kinetic pathway of dimeric coiled coil folding. *Biochemistry* **1998**, *37*, 14613-14622.

- 22. Roccatano, D.; Colombo, G.; Fioroni, M.; and Mark, A. E. Mechanism by which 2,2,2-trifluoroethanol/water mixtures stabilize secondary-structure formation in peptides: a molecular dynamics study, *Proc. Natl. Acad. Sci U. S. A.* **2002**, *99*, 12179-12184.
- 23. Ghuman, J.; Zunszain, P. A.; Petipas, I.; Bhattacharya, A. A.; Otagiri, M.; and Curry, S. Structural basis of the drug-binding specificity of human serum albumin, *J. Mol. Biol.* **2005**, *353*, 38-52.
- 24. Chong, Y.; Kleinhammes, A.; Tang, P.; Yan, X.; Yue, W. Dominant alcohol-protein interaction via hydration enabled enthalpy-driven binding mechanism. *J. Phys. Chem. B* **2015**, *119*, 5367-5375.
- 25. Mahanta, D.; Jana, M. Can 2,2,2-trifluoroethanol be an efficient protein denaturant than methanol and ethanol under thermal stress. *Phys. Chem. Chem. Phys.* **2018**, *20*, 9886-9896.
- 26. Albert, J. S.; Hamilton, A. D. Stabilization of helical domains in short peptides using hydrophobic interactions. *Biochemistry* **1995**, *34*, 984-990.
- 27. Blanco, F. J.; Ortiz, A. R.; and Serrano, L. Role of a non-native interaction in the folding of the protein G B_1 domain as inferred from the conformational analysis of the α -helix fragment. *Folding & Design.* **1997**, 2, 123-133.
- 28. Demarest, S. J., Fairman, R., Raliegh, D. P. Peptide models of local and long-range interactions in the molten globule state of human α -lactalbumin, *J. Mol. Biol.* **1998**, 283, 279–291.
- 29. Chatterjee, C.; Gerig, J. T.Interactions of trifluoroethanol with the Trp-Cage peptide. *Biopolymers* **2007**, *87*, 115-123.
- 30. Greff, D.; Fermandijan, S.; Fromageot, P.; Khosla, M. C.; Smeby, R. R.; Bumpus, F. M. Circular-dichroism spectra of truncated and other analogs of angiotensin II, *Eur. J. Biochem.* **1976**, *61*, 297-305.
- 31. Siligardi, G.; Drake, A. F.; Mascagni, P.; Neri, P.; Lozzi, L.; Niccolai, N.; Gibbons, W. A. Resolution of conformational equilibria in linear peptides by circular dichroism in cryogenic solvents. *Biochem. Biophys. Res. Commun.* **1987**, *143*, 1005-1011.
- 32. Mabrouk, M.; Van Rietschoten, J.; Rochat, H.; Loret, E. P. Correlation of antiviral activity with beta-turn types for V3 synthetic multibranched peptides from HIV-1 gp120. *Biochemsitry.* **1995**, *34*, 8294-8298.

- 33. Riersen, H.; Rees, A. R. Trifluoroethanol may form a solvent matrix for assisted hydrophobic interactions between peptide side chains. *Protein Eng.* **2000**, *13*, 739-743.
- 34. Blanco, F. J.; Jiménez, M. A.; Pineda, A.; Rico, E.; Santoro, J.; and Nieto, J. L.NMR solution structure of the isolated N-terminal fragment of protein G B₁ domain. Evidence of trifluoroethanol induced native-like β -hairpin formation. *Biochemistry* **1994**, 33, 6004-6014.
- 35. Santiveri, C. M.; Pantoja-Uceda, D.; Rico, M.; Jiménez, M. A. Beta-hairpin formation in aqueous solution and in the presence of trifluoroethanol: a ¹H and ¹³C nuclear magnetic resonance conformational study of designed peptides. *Biopolymers* **2005**, *79*, 150-162.
- 36. Kortemme, T.; Ramírez-Alvarado, M.; Serrano, L. Design of a 20-amino acid, three-stranded β -sheet protein. *Science*. **1998**, 281,253-256.
- 37. Yang, J. J.; Pitkeathly, M.; and Radford, S. E. Far-UV CD reveals a conformational switch in a peptide fragment from the β -sheet of hen lysozyme. *Biochemistry* **1994**, *33*, 7345-7353.
- 38. Buck, M.; Schwalbe, H.; Dobson, C. M. Characterization of conformation preferences in a partly folded protein by heteronuclear NMR spectroscopy: assignment and secondary structure analysis of hen egg-white lysozyme in trifluoroethanol. *Biochemistry* **1995**, *34*, 13219-13232.
- 39. Shibata, A.; Yamamoto, M, Yamashita, T.; Chiou, J-S., Kamaya, H.; Ueda, I. Biphasic effects of alcohols on the phase transition of poly(L-lysine) between α -helix and β -sheet conformations. *Biochemistry* **1992**, *31*, 5728-5733.
- 40. Chitra, R.; Smith, P. E. Properties of 2,2,2-trifluoroethanol and water mixtures. *J. Chem. Phys.* **2001**, *114*, 426-435.
- 41. Culik, R.M.; Abaskharon, R. M.; Pazos, I. M.; Gai, F. Experimental validation of the role of trifluoroethanol as a nanocrowder. *J. Phys. Chem. B.* **2014**, *118*, 11451-11461.
- 42. Sim, K. L.; and Creamer, T. P. Abundance and distributions of eukaryote protein simple sequences. *Mol. Cell. Proteomics.* **2002**, *1*, 983-995.
- 43. Weathers, E. A.; Paulaitis, M. E.; Woolf, T. B.; and Hoh, J. H. Insights into protein structure and function from disorder-complexity space. *Proteins* **2007**, *66*, 16-28.
- 44. Uversky, V. N.; Gillespie, J. R.; Fink, A. L. Why are "natively unfolded" proteins unstructured under physiologic conditions. *Proteins* **2000**, *41*, 415-427.

- 45. Das, R. K.; Pappu, R. V. Conformations of intrinsically disordered proteins are influenced by linear sequence distributions of oppositely charged residues. *Proc. Natl. Acad. Sci. U. S. A.* **2013**, *110*, 13392-13397.
- 46. Kastano, K.; Erdős, G.; Mier, P.; Alanis-Lobato, G.; Prompons, V. J.; Dosztányi, Z.; Andrade-Navarro, M. A. Evolutinary study of disorder in protein sequences. *Biomolecules* **2020**, *10*, 1413.
- 47. Dunker, A. K.; Olfield, C. J.; Meng, J.; Romero, P.; Yang, J. Y.; Chen, J. W.; Vacic, V.; Obradovic, Z.; Uversky, V. N. The unfoldomics decade: an update on intrinsically disordered protens. *BMC Genomic.* **2018**, *9*, (Suppl 2), S1.
- 48. Babu, M. M. The contribution of intrinsically disordered regions to protein function, cellular complexity, and human disease. *Biochem. Soc. Trans.* **2016**, *44*, 1185-1200.
- 49. Dunker, A. K.; Bondos, S. E.; Huang, F.; Oldfield, C. J. Intrinsically disordered proteins and multicellular organisms. *Semin. Cell. Dev. Biol.* **2015**, *37*, 44-55.
- 50. Hossain, M.; Huda, N.; Bhuyan, A. K. A surprisingly simple three-state generic process for reversible protein denaturation by trifluoroethanol, *Biophys. Chem.* **2022**, *291*, 106895.
- 51. Sashi, P.; Singarapu, K. K.; Bhuyan, A. K. Solution NMR structure and backbone dynamics of partially disordered *Arabidopsis thaliana* phloem protein 16-1, a putative RNA transporter. *Biochemistry* **2018**, *57*, 912-924.
- 52. Garvey, E. P.; Swank, J.; Matthews, C. R. A hydrophobic cluster forms early in the folding of dihydrofolatereductase. *Proteins* **1989**, *6*, 259-266.
- 53. Kuwajima, K.; Garvey, E. P.; Finn, B. E.; Matthews, C. R.; Sugai, S. Transient intermediates in the folding of dihydrofolatereductase as detected by far-ultraviolet circular dichroism spectroscopy. *Biochemistry* **1991**, *30*, 7693-7703.
- 54. O'Neill, J. C.; Matthews, C. R. Localized, stereochemically sensitive hydrophobic packing in ana early folding intermediate of dihydrofolatereductase from *Escherichiacoli*. *J. Mol. Biol.* **2000**, 295, 737-744.
- 55. Barth, A.; Zscherp, C. What vibrations tell us about proteins. *Q. Rev. Biophys.* **2002**, *35*, 369-430.
- 56. Ramesh, H.; Huda, N.; Hossain, M.; Bhuyan, A. K. Food additives benzoic acid and its methyl and propyl parahydroxy derivatives aggregate proteins. *ACS FoodSci. Technol.* **2021**, *1*, 2162-2173.

- 57. Greenfield, N.; Fasman, G. D. Computed circular dichroism spectra for the evaluation of protein conformation. *Biochemistry* **1969**,*8*, 4108-4116.
- 58. Micsonai, A.; Wien, F.; Kernya, L.; Lee,Y-H.; Goto, Y.; Réfrégiers, M.; Kardos, J. Accurate secondary structure prediction and fold recognition for circular dichroism spectroscopy. *Proc. Natl. Acad. Sci. U. S. A.* **2015**,*112*, E3095-3103.
- 59. Ikai, A.; Fish, W. W.; Tanford, C. Kinetics of unfolding and refolding of proteins. II. Results for cytochrome *c. J. Mol. Biol.* **1973**, *73* 165-184.
- 60. Jackson, S. E. How do small single-domain proteins fold. *Folding & Design.* **1998**, *3*, R81-R91.
- 61. Schellman, J. A. Selective binding and solvent denaturation. *Biopolymers* **1987**, *26*, 549-559.
- 62. Schellman, J. A. The relation between the free energy of interaction and binding. *Biophys. Chem.* **1993**, *45*, 273-279.
- 63. Timasheff, S. N. Protein-solvent preferential interactions, protein hydration, and the modulation of biochemical reactions by solvent components. *Proc. Natl. Acad. Sci. U. S. A.* **2002**, *99*, 9721-9726.
- 64. Yang, Y.; Barker, S.; Chen, M. J.; Mayo, K. H. Effect of low molecular weight aliphatic alcohols and related compounds on Platelet Factor 4 subunit association. *J. Biol. Chem.* **1993**, 268, 9223-9229.
- 65. Wyman, J. Linked functions and reciprocal effects in hemoglobin: a second look. *Adv. Protein. Chem.* **1964**, *19*, 223-286.
- 66. Ahmad, F. Free energy changes in ribonuclease A denaturation. *J. Biol. Chem.* **1983**, 258, 11143-11146.
- 67. Biswas, B.; Muttathukattil, A. N.; Reddy, G.; Singh, P. C. Contrasting effects of guanidiniun chloride and urea on the activity and unfolding of lysozyme. *ACS Omega* **2018**, *3*, 14119-14216.
- 68. Dyson, H. J.; Wright, P. E. Peptide conformation and protein folding, *Curr. Opin. Struct. Biol.* **1993**, *3*, 60-65.
- 69. Sivaraman, T.; Kumar, T. K. S.; Yu, C. Destabilization of native tertiary structural interactions is linked to helix induction by 2,2,2-trifluoroethanol. *Int. J. Biol. Macromol.* **1996**, *19*, 235-239.

- 70. Grothe, H. L.; Little, M. R.; Cho, A. S.; Huang, A. J. W.; Yuan, C. Denaturation and solvent effect on the conformation and fibril formation of TGFBIp, *Mol. Vision.* **2009**, *15*, 2617-2626.
- 71. Sivaraman, T.; Kumar, T. K. S.; Hung, K. W.; and Yu, C. Influence of disulfide bonds on the induction of helical conformation in proteins. *J. Protein Chem.* **1999**, *18*, 481-488.
- 72. Buck, M.; Radford, S. E.; and Dobson, C. M. A partially folded state of hen egg-white lysozyme in trifluoroethanol: structural characterization and implication for protein folding. *Biochemistry* **1993**, *32*, 669-678.
- 73. Gast, K.; Zirwer, D.; Müller-Frohne, M.; Damaschun, G. Trifluoroethanol-induced conformational transitions of proteins: Insights gained from the differences between α -lactalbumin and ribonuclease A. *Protein Sci.* **1999**, *8*, 625-634.
- 74. Alexandrescu, A. T.; Ng, Y-L.; Dobson, C. M. Characterization of a trifluoroethanol-induced partially folded state of α-lactalbumin. *J. Mol.* Biol. **1994**, 235, 587-599.
- 75. Uversky, V. N.; Narizhneva, N. V.; Kirschstein, S. O.; Winter, S.; Löber, G. Conformational transitions provoked by organic solvents in β-lactoglobulin: can a molten globule like intermediate be induced by the decrease in dielectric constant. *Folding & Design.* **1997**, 2, 163-172.
- 76. Ohgushi, M.; and Wada, A. 'Molten globule state': a compact form of globular proteins with mobile side-chains. *FEBS Lett.* **1983**, *164*, 21-24.
- 77. Dolgikh, D. A.; Kolomiets, A. P.; Bolotina, I. A.; Ptitsyn, O. B. 'Molten-globule' state accumulates in carbonic anhydrase folding. FEBS Lett. **1984**, 165, 88-92.
- 78. Kuroda, Y.; Endo, S.; Nakamura, H. How a novel scientific concept was coined the "molten globule state". *Biomolecules* **2020**, *10*, 269.
- 79. Hoshino, M.; Hagihara, Y.; Yamada, D.; Kataoka, M.; Goto, Y. Trifluoroethanol induced conformational transition of hen egg-white lysozyme studied by small-angle X-ray scattering, *FEBS Lett.* **1997**, *416*, 72-76.
- 80. Bhuyan, A. K. Off-pathway status for the alkali molten globule of ferricytochrome *c. Biochemistry.* **2010**, *49*, 7764-7773.
- 81. Bhuyan, A. K. The off-pathway status of the alkali molten globule is unrelated to hememisligation and trans-pH effects: experiments with ferrocytochrome *c. Biochemistry* **2010**, *49*, 7774-7782.

- 82. Kjaergaard, M.; Teilum, K.; Poulsen, F. M. Conformational selection in the molten globule state of the nuclear coactivator binding domain of CBP. *Proc. Natl. Acad. Sci. U. S. A.* **2010**, *107*, 12535-12540.
- 83. Dyson, H. J.; Wright, P. E. Intrinsically unstructured proteins and their functions. *Nat. Rev. Mol. Cell. Biol.* **2005**, *6*, 197-208.
- 84. Mendes, L. F. S.; Basso, L. G. M.; Kumagai, P. S.; Fonseca-Maldonado, R.; Costa-Filho, A. J. Disorder-to-order transitions in the molten globule-like Golgi reassembly and stacking protein. *Biochim. Biophys. Acta.* **2018**, 1862,855-865.
- 85. Sánchez, I. E.; Kiefhaber, T. Evidence for sequential barriers and obligatory intermediates in apparent two-state protein folding. *J. Mol. Biol.* **2003**, *325*, 367-376.
- 86. Malhotra, P.; Udgaonkar, J. B. High-Energy intermediates in protein unfolding characterized by thiol labeling under nativelike conditions. *Biochemistry* **2014**, *53*, 3608-3620.
- 87. de Boer, J. H. *The dynamical character of adsorption*, 2nd ed. Oxford, UK: Clarendon Press. **1968**.
- 88. Hadži, S.; and Lah, J.The free energy folding penalty accompanying binding of intrinsically disordered α-helical motifs. *Protein Sci.* **2022**, *31*, e4370.

Publications

- Hossain, M.; Huda, N.; Bhuyan, A.K. A surprisingly simple three state Generic Process for Reversible Protein Denaturation by Trifluoroethanol. *Biophys. Chem.* 2022, 291, 106895
- Hossain, M.; Huda, N.; Bhuyan, A.K. A Three-State Mechanism for Trifluoroethanol Denaturation of an Intrinsically Disordered Protein (IDP). *J. Biochem.* 2023. (accepted for publication)
- 3. Huda, N.; **Hossain, M**.; Bhuyan, A.K. Complete observation of All Structural, Conformational, and Fibrillation Transitions of Monomeric Globular Proteins at Submiceller Sodium Dodecyl Concentrations. *Biopolymers* **2019**, *110*, e23255.
- 4. Ramesh,H.; Noorul, H.; Hossain,M.; Bhuyan, A. K. Food Additives Benzoic Acid and Its Methyl and Propyl Parahydroxy Derivatives Aggregate Proteins. *ACS Food Sci. Technol.* **2021**, *1*, 2162-2173.

Dynamics of some monohydric alcohols, and the effect of 2,2,2-trifluoroethanol on structure and folding of globular and intrinsically disordered proteins

by Mujahid Hossain

NIVERSITY OF HYDER

Central University P.O. HYDERABAL

Submission date: 27-Jul-2023 11:56AM (UTC+0530)

Submission ID: 2137457903

File name: Mujahid_Thesis-for-plagiarism-check.pdf (877.69K)

Word count: 16187 Character count: 85122 Dynamics of some monohydric alcohols, and the effect of 2,2,2-trifluoroethanol on structure and folding of globular and intrinsically disordered proteins

	ALITY REPORT	isoraci ca proteii				
3 SIMILA	3% ARITY INDEX	2% INTERNET SOURCES	33% PUBLICATIONS	1% STUDENT PAPERS		
PRIMAR	Y SOURCES					
1	Bhuyan generic denatu	d Hossain, Nooru . "A surprisingly process for reve ration by trifluor try, 2022	simple three-	state		
2	pubme Internet Sou	d.ncbi.nlm.nih.go	OV .	1%		
3	Abani K. Bhuyan. "Negative Thermal Expansion and Disorder-to-Order Collapse of an Intrinsically Disordered Protein under Marginally Denaturing Conditions", The Journal of Physical Chemistry B, 2022					
4	Submitted to University of Hyderabad, Hyderabad Student Paper					
5	WWW.re	searchgate.net		<1%		

Noorul Huda, Abani K. Bhuyan. "Mechanical Unfolding and Amorphous Aggregation of Protein in a Very Low DC Field", The Journal of Physical Chemistry B, 2023

<1%

Publication

Noorul Huda, Mujahid Hossain, Abani K.
Bhuyan. "Complete observation of all structural, conformational, and fibrillation transitions of monomeric globular proteins at submicellar sodium dodecyl sulfate concentrations", Biopolymers, 2019

<1%

Publication

Saikat Banerjee, Jonathan Furtado, Biman Bagchi. "Fluctuating micro-heterogeneity in water-tert-butyl alcohol mixtures and lambda-type divergence of the mean cluster size with phase transition-like multiple anomalies", The Journal of Chemical Physics, 2014

<1%

Publication

Kunihiro Kuwajima, Masahiro Mitani, Shintaro Sugai. "Characterization of the critical state in protein folding", Journal of Molecular Biology, 1989

<1%

Publication

Exclude quotes On Exclude matches < 14 words

Exclude bibliography On